Six1 is important for myoblast proliferation through direct regulation of Ccnd1

Ellias Horner

Thesis submitted to the
Faculty of Graduate and Postdoctoral Studies
In partial fulfillment of the requirements
For the MSc degree in Biochemistry

Department of Biochemistry, Microbiology and Immunology
Faculty of Medicine
University of Ottawa

Abstract

The transcription factor Six1 of the sine oculis homeobox family has been tied to skeletal muscle formation. Work completed thus far has allowed our research team to identify the precise mechanism by which Six1 regulates the expression of MyoD, a key myogenic gene, in muscle stem cells. Furthermore, loss-of-function of this protein, mediated by RNA interference, has implicated Six1 as essential towards normal myogenic differentiation. However, beyond Six1 and its involvement towards myogenesis, our data also suggests the transcription factor as a potential regulator of the cell cycle. Data from our lab shows that loss of Six1 expression significantly impairs primary myoblast proliferation and appears to impair satellite cell activation in response to muscle injury *in vivo*. Furthermore, loss of Six1 decreases the expression of key cell cycle genes. Combining functional genomics approaches such as ChIP-Seq and Gene Expression Profiling together with Gene Ontology Term Enrichment shows a significant representation for biological processes regarding the cell cycle and its regulation; these biological clusters contain a large subset of genes that are bound and modulated by Six1. In particular, Ccnd1 was found to display a similar expression pattern as Six1 in growing myoblasts and its expression was found to be directly controlled by Six1. Furthermore, Ccnd1 over-expression was sufficient to rescue the Six1-knockdown associated cell cycle phenotype. Together, these data suggest that in response to injury Six1 enhances the expression of the cell cycle gene Ccnd1 thus modulating myoblast proliferation for muscle regeneration.

Acknowledgements

Only one name is on the front page of this thesis, however none of this work would have been possible if not for the guidance, support, and patience of many people. My supervisor, Dr. Alexandre Blais, took me into his lab four years ago as an honour's student. Together with my student supervisor, Yubing, they taught me countless techniques and remained patient throughout. I cannot thank them enough.

I am appreciative of the other members of my lab who provided insightful conversations as well as various contributions to my project: Iman, Dabo, Alphonse, and John. Eventually moving on from my honour's project into a Master's degree I was given the opportunity to function as a mentor and teacher. I am appreciative of the work of my first two students, Mireille and Kathy, whom both helped with my project's many optimizations. A special thanks goes to my most recent honour's student, Daniel. He has been exemplary and has been an extreme help as we sought to develop a manuscript.

I am thankful for the funding provided by the uOBMRI and CNMD through the form of my STaR Scholarship which has been helpful this past year. I would also like to thank the members of the Skerjanc, Dilworth, and Brand labs, as well as the members of my thesis advisory committee for providing constructive criticisms on my results during meetings.

Finally, I would like to thank my parents, siblings, and my girlfriend, Shuhua for all the encouragement over the years. They were all understanding as I worked through numerous weekends and evenings and were unwavering in their support. Their love means so much to me and I hope I've made you all proud.

Table of Contents

List of Abbreviations

7-AAD	7-Aminoactinomycin D
AD	Activation Domain
ANOVA	Analysis of Variance
APC	Anaphase-Promoting Complex
ARF	Alternative Reading Frame
ATCC	American Type Culture Collection
ATP	Adenosine Triphosphate
BCA	Bicinchoninic Acid Assay
bFGF	Basic Fibroblast Growth Factor
bHGF	Basic Hepatocyte Growth Factor
bHLH	Basic Helix-Look-Helix
BMD	Becker Muscular Dystrophy
BOR	Branchio-oto-renal Syndrome
bp	Base Pairs
BrdU	Bromodeoxyuridine
BSA	Bovine Serum Albumin
CDK	Cyclin Dependent Kinase
CDKI	Cyclin Dependent Kinase Inhibitor
cDNA	Complementary Deoxyribonucleic Acid
ChIP	Chromatin Immunoprecipitation
ChIP-on-chip	Chromatin Immunoprecipitation followed by Microarray Hybridization
ChIP-Seq	Chromatin Immunoprecipitation followed by Sequencing
cRNA	Complementary Ribonucleic Acid
CTX	Cardiotoxin
Cy3	Cyanine 3 Dye
dach	Drosophila Dachshund
DAPI	4',6-diamidino-2-phenylindol
DES	Donor Equine Serum
DMD	Duchenne Muscular Dystrophy
DMEM	Dulbecco's Modified Eagle Medium
DMSO	Dimethyl Sulfoxide
DNA	Deoxyribonucleic Acid
dNTP	Deoxyribonucleotide Triphosphate
DSHB	The Developmental Studies Hybridoma Bank
EdU	5-ethynyl-2'-deoxyuridine
EGFP	Enhanced Green Fluorescent Protein
EtOH	Ethanol
eya	Drosophila Eyes Absent
FACS	Fluorescent Activated Cell Sorting
FBS	Fetal Bovine Serum

FDR	False Discovery Rate
FWER	Family-Wise Error Rate
GM	Growth Medium
GO	Gene Ontology
GSEA	Gene Set Enrichment Analysis
H3K27ac	Histone H3 Lysine 27 Acetylation
H3K27me3	Histone H3 Lysine 27 Trimethylation
H3K4me1	Histone H3 Lysine 4 Monomethylation
HCl	Hydrochloric Acid
HD	Homeodomain
HDAC	Histone Deacetylase
HRP	Horse Radish Peroxidase
IgG	Immunoglobulin G
kb	Kilobase
KD	Knock Down
KO	Knock Out
MB	Myoblast
MD	Muscular Dystrophy
MHC	Myosin Heavy Chain
miRNA	MicroRNA
MRF	Myogenic Regulatory Factors
mRNA	Messenger RNA
MSigDB	Molecular Signature Database
MT	Myotubes
Myog	Myogenin
NaCl	Sodium Chloride
NES	Normalized Enrichment Score
NS	Non-specific
nt	Nucleotides
NTP	Nucleotide Triphosphate
P/S	Penicillin and Streptomycin
Pax	Paired Homeobox
PBS	Phosphate Buffered Saline
PBST	Phosphate Buffered Saline with 0.1% Triton X-100
PBST-BSA	Phosphate Buffered Saline with 0.1% Triton X-100 and 3% BSA
PCR	Polymerase Chain Reaction
PEI	Polyethylenimine
pH3	Phosphorylation Histone H3
pRB	Retinoblastoma Protein
PVDF	Polyvinylidene Fluoride
qRT-PCR	Quantitative Reverse Transcription PCR

RNA	Ribonucleic Acid
RNAi	RNA Interference
RT-PCR	Reverse Transcription PCR
SD	Six Domain
SDS	Sodium Dodecyl Sulfate
SDS-PAGE	Sodium Dodecyl Sulfate Polyacrylamide Gel Electrophoresis
SEM	Standard Error over the Mean
siRNA	Small Interfering RNA
so	Drosophila Sine Oculis
SYBR	SYBR Green I Dye
TA	Tibialis Anterior
TBP	TATA Binding Protein
TF	Transcription Factor
TSS	Transcription Start Site
UTR	Untranslated Region
Xp21	X Chromosome Short-arm Position 21

List of Figures and Illustrations

List of Tables

1. Chapter 1 - Introduction

1.1. Muscles

There exist three encompassing forms of muscle tissue that account for close to half of a human's total body mass: cardiac, skeletal and smooth muscle. Smooth muscles are non-striated and responsible for involuntary movements and contractions in organs such as blood vessels, the gastrointestinal tract, bladder and other organs. Cardiac muscles are striated, involuntary muscles found exclusively in the heart composed of uni- and binucleated cells. Skeletal muscles are also striated but unique in so far as being multinucleated and responsible for voluntary movement. Skeletal muscles are composed of multiple clusters of muscle fascicles held together by connective tissue. Each muscle fascicle contains a bundle of long multinucleated muscle cells called myofibers: myofibers are individual muscle cells. Furthermore, each myofiber contains multiple myofibrils, the contractile apparatus of muscle cells. Myofibrils are composed of multiple sarcomeres which are the functional unit of the muscle. Sarcomeres are composed of thick and thin filaments including proteins such as actin, myosin, troponin and tropomyosin. Collectively, the filaments of the sarcomeres give skeletal muscle a striated appearance and when signaled will function to contract and allow movement (Reviewed in Frontera and Ochala, 2015). Skeletal muscles possess an extraordinary ability to rapidly respond to injury or stress and regenerate the damaged tissue. A large part of the regenerative capacity of muscle is due to muscle progenitor stem cells called satellite cells. These satellite cells function to proliferate, differentiate and fuse to repair a damaged muscle. The role and regulation of satellite cells are further detailed later.

Despite the massive regenerative capacity of muscle, there exist myopathies that ultimately slow and impair muscle regeneration.

1.2. Muscular Dystrophy and Sarcopenia

Muscular dystrophy encompasses a group of diseases afflicting skeletal muscle resulting in progressive muscle weakness, muscle wasting, degeneration, and tissue death. Two commonly inherited forms are Becker's and Duchenne's muscular dystrophy which arise respectively due to a partially functional form or complete loss of the dystrophin protein (reviewed in McNally and Pytel, 2007). The dystrophin gene is located at the Xp21 locus on the short arm of the X chromosome and is inherited recessively (Monaco et al., 1986). Dystrophin functions as a scaffold and shock-absorber during muscle contractions: dystrophin (with a complex of other proteins) links the contractile apparatus of the muscle fiber with the extracellular matrix of the basal lamina (reviewed in Nowak and Davies, 2004). Loss of dystrophin decreases the integrity of the muscle cell, decreases muscle stiffness and the cells are prone to tearing apart during muscle contractions. Muscular dystrophy being an X-linked recessive disease causes males to be more commonly afflicted. In the case of Duchenne's muscular dystrophy (DMD), boys are often required to use wheelchairs by age 12 due to limb muscle weakness and die in their 20s due to cardiac issues and respiratory failure: Becker's muscular dystrophy (BMD) is milder than Duchenne's due to the partially functional protein and the onset of symptoms are in the teenage years to early 20s (reviewed in Emery, 2002). In contrast, sarcopenia is not characterized as a disease but instead is progressive muscle wasting due to aging. It has been postulated that this muscle wasting in muscular dystrophy and sarcopenia is due to depletion of muscle progenitor stem cells

(satellite cells) as humans age (reviewed in Grounds, 1998; Fulle et al., 2004). Regardless, in the case of both muscular dystrophy and sarcopenia, successive rounds of injury may exhaust the satellite cell pool and consequently lead to impaired muscle repair after injury and muscle degeneration.

1.3. Cell Therapy as a Treatment for Muscular Dystrophy

Collectively, current research efforts for treatment strive to alleviate and slow the progression of the disease. Ongoing clinical research involve a multitude of approaches such as stem cell replacement therapy, gene therapy, exon-skipping and others techniques (reviewed in Cossu and Sampaolesi, 2004; Chamberlain, 2002). The therapeutic approach of utilizing stem cells in muscular dystrophy involves the isolation of satellite cells from a healthy donor, *in vitro* expansion of these cells and transplantation into the recipient dystrophic muscle. These injected cells will then differentiate and fuse to the damaged fiber in order to repair the injury. Early on, cell therapy appeared promising as the intramuscular injection of healthy muscle precursor cells into the muscle of dystrophic mice would render dystrophin positive fibers (Partridge et al, 1989). However, initial research to apply muscle stem cell therapy in human DMD patients revealed a number of shortcomings: Researchers noted poor engraftment of injected cells due to host immune rejection, poor survival, and migration of donor cells (reviewed in Tedesco and Cossu, 2012). For some of these roadblocks, researchers have already devised strategies. Immune rejection can be overcome by immunosuppression for use of allogeneic satellite cells or genetically manipulated autologous satellite cells. The isolation of a pure population of satellite cells using specific markers has helped improve the engraftment of intramuscular transplanted cells

(Montarras et al., 2005; Cerletti et al., 2008). Furthermore, the use of a soft, elastic hydrogel growth substrate during *in vitro* muscle stem cell expansion has proved to recapitulate similar self-renewal capacities observed *in vivo* (Gilbert et al., 2010). However, what remains to be addressed are methods to ensure sufficient material for transplantation as well as overcoming the transient effect of treatment: transplanted satellite cells will quickly differentiate in order to repair the injury, become depleted and repetitive injections will be required. For long-term therapeutic efficiency, a large expansion of satellite cells must be achieved in culture and the transplanted satellite cells must be able to repopulate the niche.

1.4. Embryonic Muscle Development

There exist two instances of myogenesis in mammals: embryonic myogenesis, which is the formation of muscle in the embryo; and adult myogenesis, the regeneration of muscle after injury, stress and growth. Although both processes of myogenesis share common transcription factors, there are numerous key differences. During embryogenesis, the majority of the bodies' skeletal muscles are derived from the somites of the mesoderm: the somites are bilateral segments that run along the head-to-tail axis on either side of the neural tube (reviewed in Buckingam et al., 2003). Each somite is composed of two components with the ventral component (the sclerotome) containing precursors for bone and cartilage and the dorsal component (the dermomyotome) containing precursors for skeletal muscle, skin and epithelium (reviewed in Buckingham and Relaix, 2007). The dermomyotome is further divided into regions based on anatomical positioning that yield specific musculature: the back musculature develops from the epaxial dermomyotome; the lateral trunk and limb muscles develop from

migration of myoblasts from the hypaxial dermomyotome. Myogenesis begins with the central, epaxial and hypaxial lips of the dermomyotome delaminating and folding to form the underlying myotome. The myotome represents the primitive muscle of the embryo consisting of committed myoblasts characterized by high levels of the myogenic regulatory factor MyoD (Sassoon et al., 1989). Along with the myogenic regulatory factor family (MRF), other transcription factor families have been implicated as critical towards embryonic muscle development including the Pax family and Six family (Tremblay et al., 1998; Relaix et al., 2005; Grifone et al., 2005; Laclef et al., 2003). Pax3 has been shown to be critical towards delamination, migration and proliferation; Six1 and Six4 have been shown to play roles in proliferation and differentiation; the MRFs MyoD, Myf5 and myogenin are critical for proliferation, determination and differentiation. Furthermore, during the various stages of myogenesis are other downstream and parallel factors such as c-Met, Lbx1, Mox2 and Mef2 (reviewed in Buckingam et al., 2003).

1.5. Satellite Cells and Adult Muscle Regeneration

Satellite cells are a population of adult muscle stem cells that play a key role during adult muscle regeneration and arise from the central and hypaxial dermomyotome during migration (Gros et al. 2005; Schienda et al. 2006). The term satellite cell was coined based on the localization of the cells: satellite cells are wedged between the basal lamina and sarcolemma of the myofiber (Mauro 1961). These myogenic progenitors are quiescent soon after birth and become activated in response to muscle growth or injury (reviewed in Buckingham et al., 2003). Upon activation, satellite cells possess multiple cellular fates: the cells can proliferate, differentiate, or return to quiescence. After

successive rounds of proliferation, activated satellite cells may differentiate and fuse to existing myofibers or fuse together to form new myofibers. Maintenance of the niche is essential to replenish the satellite cell pool and to ensure future regeneration. Furthermore, maintenance of the quiescent satellite cell pool is achieved through asymmetric division yielding one daughter cell that will undergo differentiation and another that will return to quiescence (Kuang et al., 2007).

1.6. Myoblast Proliferation and Differentiation

Adult myogenesis is tightly regulated and dependent on cell cycle progression in order to separate the events of proliferation and differentiation. In response to injury, satellite cells are activated and undergo massive proliferation in order to repair and repopulate the site of injury. Myoblasts cells are highly proliferative and are characterized by the expression of many genes involved with the cell cycle (Tomczak et al., 2004). The cell cycle is a highly regulated process involving a multitude of factors that are temporally controlled and dependent on various protein interactions. Some factors involved in regulating the cell cycle include the cyclins, cyclin dependent kinases, cyclin dependent kinase inhibitors, the pocket protein family and the E2F transcription factor family. Interactions between various cyclins and cyclin dependent kinases (CDK) allow for cell-cycle progression: Cyclin D with CDK4/6 for G1 entry; Cyclin E with CDK2 for G1/S transition; Cyclin A with CDK1/2 for S-phase progression and G2/M-phase transition; and Cyclin B with CDK1 for M-phase progression (reviewed in Vermeulen et al., 2003). These Cyclin-CDK interactions allow for downstream phosphorylation events such as the Cyclin D1-CDK4/6 targeted phosphorylation of the retinoblastoma pocket-protein pRb (Buchkovich et al., 1989;

Kato et al., 1993). In a hypophosphorylated state, pRb functions as an anti-proliferative factor through forming a complex with histone deacetylase (HDAC) and E2F-DP (E2F factor with its transcriptional dimerization partner) (Brehm et al., 1998). Consequently, hyperphosphorylation of pRb by Cyclin D1-CDK4/6 releases this complex, allowing E2F-DP targeted transcription of S-phase genes such as Cyclin E and Cyclin A (Buchkovich et al., 1989; Girling et al., 1993). However, once adequate proliferation has been achieved, proliferating myoblasts are eventually required to downregulate cell cycle genes and in turn upregulate genes critical towards myogenic differentiation (Blais et al., 2005, Liu et al., 2010). Cyclin dependent kinase inhibitors (CDKI) are employed to effectively stop cell cycle progression, allowing for quiescence and downstream differentiation (Andres and Walsh, 1996). Myoblasts ready to differentiate will upregulate the expression of myogenin and subsequently induce the expression of the CDKI p21 in order to allow cell cycle arrest. After both myogenin and p21 expression are induced, myoblasts will then begin to differentiate and fuse to form myotubes (Andres and Walsh, 1996). Furthermore, it was shown that pRb also plays a role in the myoblasts switch from proliferation to terminal differentiation and that pRb functions to prevent cell cycle re-entry of terminally differentiated muscle cells (Huh et al., 2004; Blais et al., 2007). Many cell cycle genes displayed the repressive mark H3K27me3 in arrested myoblasts and for some genes this appeared to be dependent on pRb expression (Blais et al., 2007). A summary on the life cycle of satellite cells during muscle regeneration and the contributing transcription factors is shown in Figure 1A.

1.7. Transcriptional Regulation of Skeletal Myogenesis

A number of transcription factor families have been implicated as important towards myogenesis in the embryo as well as during adult muscle regeneration including: the myogenic regulatory factors (MRFs), the paired homeobox (Pax) genes, and the sine oculis homeobox family (Six). A timeline of the expression patterns of these factors from embryonic progenitors to mature myotubes has been adapted from Bentzinger et al., 2012 and is shown in Figure 1B.

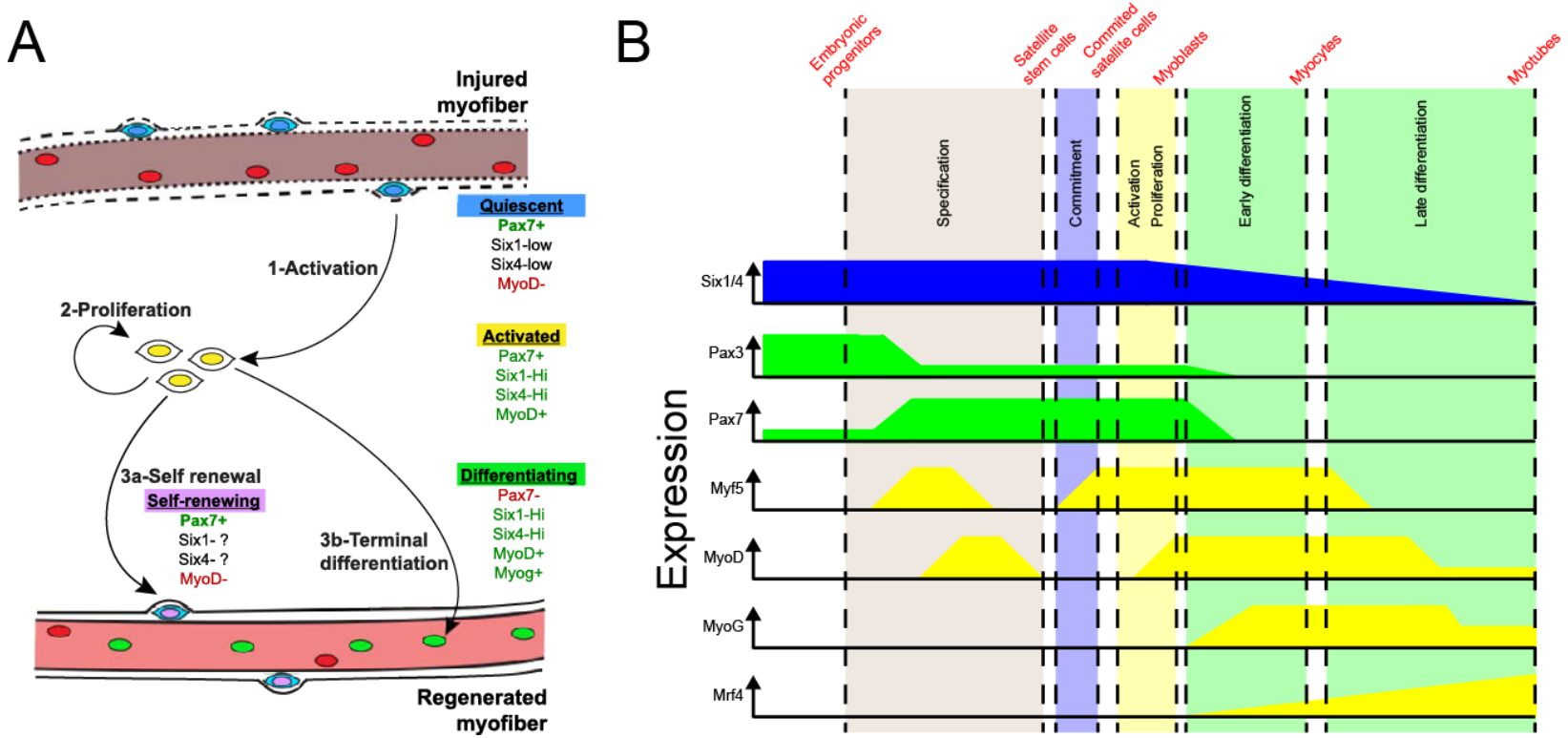

Figure 1: The Pax, Six and MRF families of transcription factors play critical roles in muscle development in the embryo and during adult muscle regeneration.

(A) In a healthy adult muscle fiber, satellite cells are quiescent. After injury, satellite cells undergo immense proliferation and can proceed towards two fates: return to quiescence in a process of self-renewal to maintain the satellite cell niche for future regeneration, or fuse into new myofibers and/or to existing fibers in a process of terminal differentiation. (B) A timeline for the expression of the Six, Pax, and MRF transcription factor families in the progression of the muscle lineage from embryonic precursors to adult muscle mass. This illustration has been adapted from the review by Bentzinger et al., 2012.

1.7.1. The Paired Homeobox Transcription Factors

The paired homeobox transcription factor family play key roles in the specification of various tissues during embryogenesis with roles of maintaining progenitor populations (reviewed in Buckingham and Relaix, 2007). There are nine members of the Pax family with roles for Pax3 and Pax7 identified in skeletal myogenesis. Pax3 has been shown to be critical towards myotome differentiation, delamination and myoblast migration: Pax3 mutants displayed unorganized dermomyotome and myotome structures leading to impaired trunk musculature formation as well as impaired hypaxial muscles arising from myogenic precursor migration (Tremblay et al., 1998). In the skeletal muscle lineage, Pax7 was identified as specifically expressed in satellite cells and proliferating myoblasts. Pax7 null mice demonstrate a severe reduction of satellite cells though Pax7 appears to be dispensable during embryonic muscle development (Seale et al., 2000). However, in Pax3/Pax7 double mutants, an aggravation of the previous Pax3 mutant phenotype is observed with prolonged apoptosis and only the early myotome formation suggesting complementary roles of Pax3 and Pax7 (Relaix et al., 2005). Outside of embryogenesis, Pax7 was shown to be required for the specification of satellite cells and essential towards satellite cell proliferation, expansion and differentiation during adult muscle regeneration: Pax7 deletion caused cell cycle arrest of satellite cells and myoblasts, impaired MRF expression, and a severe muscle regeneration deficit (Kuang et al., 2006, von Maltzahn et al., 2013). Over-expression of Pax7 has been shown to promote cell-cycle exit, prevent myogenic differentiation and promote the return of activated satellite cells to a state of quiescence (Olguin and Olwin, 2004). In a quiescent state, satellite cells express

high levels of Pax7 but low levels of Myf5 expression. Once activated in response to injury or growth, satellite cells can undergo asymmetric division and upregulate the expression of Myod and Myf5: Myod/Myf5 positive cells will commit to the myogenic lineage and repair the injury while MRF negative cells will maintain their self-renewing characteristics and replenish the satellite cell niche (Kuang et al., 2007).

1.7.2. The Myogenic Regulatory Factors (MRF)

MRFs are a family of basic helix-loop-helix (bHLH) proteins with critical roles in skeletal muscle development (reviewed in Berkes and Tapscott, 2005). The bHLH proteins of the MRF family consist of Myf5, MyoD, myogenin and MRF4 and are specifically expressed in skeletal muscle. MRFs are required to cooperate with another class of bHLH factors called E-proteins where they function as homo- or hetero-dimers through binding to a consensus E-box motif CANNTG (Blackwell and Weintraub, 1990). Together, MRFs and E-proteins coordinate muscle-specific gene expression in the developing embryo. The MRFs function as master transcriptional regulators of myogenesis and are so powerful that their forced expression in non-muscle cells upregulates the expression of myogenic genes causing a conversion to the myogenic lineage (Aurade et al., 1994; Braun et al., 1989; Braun et al., 1990; Weintraub et al., 1989; Wright et al., 1989). MyoD has been shown to be capable of regulating its own expression as well as the expression of myogenin (Thayer et al., 1989). In the absence of Myf5, MyoD and MRF4, skeletal muscle identity is compromised and fails to form (Kassar-Duchossoy et al., 2004). Mice mutants lacking either Myf5 or MyoD appear to develop normal skeletal musculature with only mild defects of the trunk musculature or the early limb buds, respectively, suggesting both genetic redundancy and distinct roles

for MyoD and Myf5 in embryogenesis (Rudnicki et al., 1992; Braun et al., 1992; Kabler et al., 1998). Mice lacking myogenin have poorly developed musculature due to impaired myogenic differentiation however myogenin has been shown to be dispensable for the formation of myoblasts (Hasty et al., 1993; Nabeshima et al., 1993). In adult muscles, satellite cells are a heterogeneous population based on Myf5 expression. Approximately 90% of adult satellite cells have previously expressed Myf5 with the remaining 10% having never expressed Myf5 (Kuang et al., 2007). Furthermore, Myf5 has been shown to be post-transcriptionally regulated by the microRNA-31. In quiescent satellites cells, miR-31 and Myf5 mRNA are sequestered into granules preventing Myf5 protein translation. Once activated, these granules will dissociate allowing for Myf5 translation and downstream myogenic differentiation (Crist et al., 2012). Previously it has been shown that MyoD is required for the expression of Cdc6, a factor essential for the initiation of DNA replication at the onset of S-phase. It was observed that MyoD was important for a quiescent satellite cells transition to proliferation and this effect was mediated through Cdc6 (Zhang et al., 2010).

1.8. Six Family of transcription factors

1.8.1. Characterization of the Six family of transcription factors

The sine oculis homeobox (Six) protein family was founded based on the characterization of mutants in the *sine oculis (so)* protein in *Drosophila melanogaster*. These loss-of-function *so* mutants have dramatic effects on the compound eye and adversely affect the entire visual system (Serikaku and O'Tousa, 1994). Additional members of the Six family were also identified in fruit flies: *optix* and *DSix4* (Seo et al., 1999). As the name suggests, *optix* plays a role in the developing eye, but *DSix4* instead

was determined to function in several mesoderm derivatives including somatic muscle and somatic cells of the gonads (Kirby et al., 2001). Since then, homologues of *so*, *optix* and *DSix4* have been identified in a wide range of organisms in the animal kingdom (reviewed in Kumar, 2009). In mammals there exist six homologues, Six1/2 (*so*), Six4/5 (*DSix4*) and Six3/6 (*optix*), with roles towards eye, kidney, thymus, male gonads and skeletal muscle development (Kawakami et al., 1996; Kobayashi et al., 2007; Fujimoto et al., 2013; Grifone et al., 2005). The Six family of transcription factors are characterized by their conserved Six and homeodomains which allow for protein interactions and DNA binding, respectively (Ohto et al., 1999; Zhu et al., 2002; Noyes et al., 2008). Through these domains, the Six factors have been shown to interact with the Eya co-activators and are able to bind to DNA directly as dimers to the consensus MEF3 motif (Ohto et al., 1999, Ikeda et al., 2002, Liu et al., 2012). The illustration of Six family transcription factors has been modified from Kawakami et al., 2000 and is shown in Figure 2.

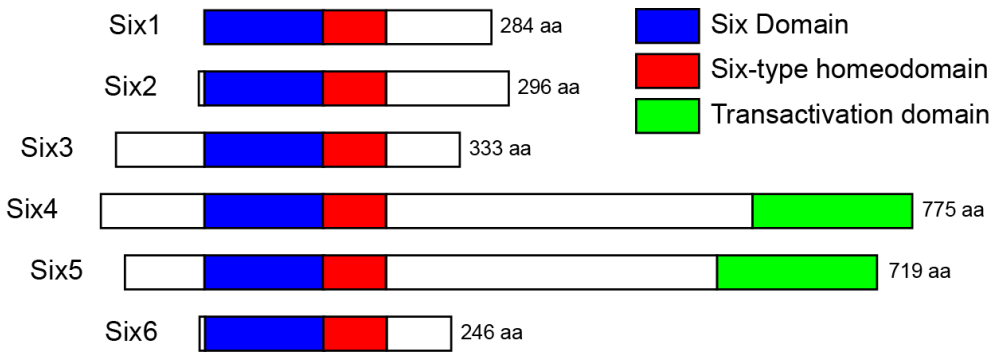

Figure 2: The Six family of transcription factors.

There are six members of the Six family of transcription factors in mammals and they are characterized by their Six domain and Six-type homeodomain. The Six domain allows for protein interactions and the homeodomain allows for binding to DNA through the consensus MEF3 motif. Six4 and Six5 have an additional transactivation domain. This illustration has been adapted and modified from Kawakami et al., 2000.

Mutations of several fly genes lead to compound eye defects. Other key members of the retinal development network in Drosophila include *eyes absent* (*eya)*, *dachshund*, *eyeless* and *twin of eyeless* (reviewed in Relaix and Buckingham, 1999). These gene products can then form multi-protein complexes and/or regulate each other's expression. Vertebrate homologues of the retinal development network exist in vertebrates: Six (*so*), Eya (*eya*), Dach (*dachshund*) and Pax (*eyeless* and *twin of eyeless*). Furthermore, in mammalian systems, this same gene network has been shown to be expressed during embryogenesis in the somites and to be involved in the control on development of multiple tissues and organs such as the kidneys and ears (reviewed in Relaix and Buckingham, 1999; Heanue et al., 1999, Xu et al., 1999). Six1, Pax3 and Pax7 knockout mice display muscle phenotypes, however Dach knockout mice do not (Laclef et al., 2003, Seale et al., 2000, Davis et al., 2001). Likewise, this network has been shown to be functional towards myogenesis, rather than eye development, in chickens (Heanue et al., 1999).

Of the Pax/Six/Eya/Dach proteins, biochemical interactions have been shown between Six/Eya and Eya/Dach through conserved domains (Ohto et al., 1999, Chen et al., 1997). In fact, the molecular interaction between Six and Eya promotes the nuclear localization of Eya from the cytoplasm allowing target gene activation (Kawakami et al., 2000; Ohto et al., 1999). Forced expression of *so* and *eya* can induce ectopic eyes in drosophila, though *eya* is more efficient in this process (Pignoni et al., 1997). Furthermore, over-expression of Six and Eya display synergistic activation of the MRF myogenin (Li et al., 2003). Interestingly, the forced expression of both Six1 and Eya1 has been shown to yield a conversion of slow-twitch muscle fibers toward a fast-twitch

glycolytic phenotype (Grifone et al., 2004). In a study of mammalian organogenesis, the phosphatase activity of Eya was demonstrated to functionally convert the Six1-Dach repressor complex to an activator through the recruitment of downstream co-activators (Li et al., 2003). The interactions between Six1 and Eya1 have a particular importance insofar that protein mutants preventing this interaction have been implicated in branchio-oto-renal syndrome in humans characterized by hearing impairment and renal abnormalities (Kochhar et al., 2008).

1.8.2. The roles of Six1 and Six4 in myogenesis

Of the Six family of transcription factors, a role in myogenesis has primarily been established for the homologues Six1 and Six4 which have been tied to skeletal muscle formation (Grifone et al., 2005). Knock-out (KO) studies of Six1 and/or Six4 in mice have been performed: Six1 null mice die at birth due to respiratory failure and show multiple organic developmental defects and delayed expression of MRFs in the limb buds while Six4 null mutants are viable and display no visible morphological abnormalities (Laclef et al., 2003, Ozaki et al., 2001). However, Six1/Six4 double KO mice show an aggravation of this previously reported phenotype in Six1 null mice: there is a greater decrease in MRF expression in the myotome, complete absence of limb muscles and severe muscle hypoplasia (Grifone et al., 2005). Furthermore, in a study in embryonic zebra fish, it was observed that both six1a and six1b were critical for the proliferation of Pax7 positive cells of the dermomyotome during embryonic development (Nord et al., 2013).

The previously reported role of Six1 and Six4 during muscle formation in embryogenesis has been well studied. However a role for Six1 and Six4 in adult muscle regeneration remains poorly understood, specifically in the proliferation of muscle satellite cells. Six1 and Six4 both regulate the expression of, and cooperate with, the members of the MRF family to activate gene expression during myogenic differentiation and the Six factor's function is essential to this process: Loss of either Six1, Six4 or both resulted in decreased myogenic fusion and differentiation in C2C12 myoblasts (Liu, Chu et al., 2010). Furthermore, it has been shown that Six1 directly regulates the expression of MyoD in muscle progenitor cells through binding of two MEF3 motifs in the Core Enhancer Region upstream of MyoD (Liu, Chakroun et al., 2013). Recently, it was shown that Six4, together with MyoD coordinates the expression of several genes critical for adult muscle regeneration. Furthermore, it was observed that Six4/Myod genome wide binding was correlated with the presence of the histone demethylase UTX, which is responsible for removing the repressive H3K27 trimethylation mark (Chakroun et al., 2015).

Six1 has been implicated with a role towards cell proliferation in myoblasts from ChIP-on-chip gene ontology showing significant enrichment of Six1 gene targets involved in the regulation of cell proliferation (Liu, Chu et al., 2010). However, overproduction of Six1 or Six4 was shown to interfere with primary myoblast proliferation as assessed by co-staining of Six1/4-EGFP and the proliferative marker Ki67 at 72-hours after infection; however loss of Six1 or Six4 mediated by siRNA showed no change in relative cell number 48-hours after transfection (Yajima et al., 2010). Similarly, overproduction of Six1 in a stable C2C12 myogenic cell line showed

delayed proliferative potential compared to an EGFP control (Wu et al., 2013). On the other hand, loss of Six1 expression or function in proliferating C2C12 myoblasts resulted in decreased proliferation as assessed by BrdU incorporation (Li et al., 2003). Recently, it was shown that Six1 is a critical regulator of satellite cell renewal and impaired Six1 expression *in vivo* resulted in a greater number of satellite cells 30 days after muscle injury. It was demonstrated that Six1 exerts this effect directly through the expression of the phosphatase Dusp6 (Le Grand et al., 2012). The phosphatase Dusp6 is a known negative regulator of ERK1/2 phosphorylation signaling (Maillet et al., 2008) and Dusp6 null mice possess the same increased satellite cell numbers after injury as the Six1 conditional knockout model (Le Grand et al., 2012).

With the previous studies of Six1 in adult muscle regeneration, some questions still remain due to the design of the experiments. Among the shortcomings of these studies are the use of immortalized C2C12 myoblasts with no replication in primary cells; timelines analyzing growth were too short; research was steered towards cell cycle exit as opposed to proliferation; and failure to investigate or propose a mechanism for the proliferation phenotype.

1.8.3. A role for Six1 in the development of other tissues

As mentioned previously, Six was initially identified to function in a network for retina development in drosophila (reviewed in Relaix and Buckingham, 1999). Later, Six was shown to be critical during mammalian embryogenesis in the control on development of multiple tissues and organs such as the head, retina, ear, nose, brain, kidney, and gonads (reviewed in Kumar et al., 2009). In particular, Six1 mutants in

humans have been implicated in branchio-oto-renal syndrome characterized by hearing loss and impaired kidney development and function (Ruf et al., 2004; Kochhar et al., 2008). Six1 deficient mice fail to develop kidneys and co-loss of Six4 impairs male gonad differentiation (Xu et al., 2003; Fujimoto et al., 2013). The importance of normal Six factor expression is further highlighted during the misregulation of Six1 in cancer and tumorigenesis of various tissues.

1.8.4. Six1 in Cancer

Outside of muscle cells, Six1 over-expression has been implicated in many different cancers playing roles in both the proliferation and metastasis of cancer. Numerous studies have identified and linked Six1 with breast cancer, rhabdomyosarcoma, colorectal cancer, pancreatic cancer and Wilm's tumours of the kidney (Reichenberger et al., 2005, Yu et al., 2006, Ono et al., 2012, Li et al., 2013, Wegert et al., 2015, Walz et al., 2015). Overexpression of Six1 was associated with circumvention of the G2 cell-cycle checkpoint in human breast cancer cells and implicated as a possible growth mechanism in breast carcinoma (Ford et al., 1998). Furthermore, Six1 overexpression in human breast cancer cells has been shown to increase cell proliferation and the expression of Cyclin A1 (Colleta et al., 2008). Another study of human breast cancer cells observed that Six1 protein expression fluctuates according to cell cycle progression and post-transcriptionally regulated in a similar pattern to Cyclin B1 (Christensen et al., 2007). It was shown that Six1 is degraded in the ubiquitin proteasome pathway and that this process is mediated by APC-Cdh1 through a protein interaction between Cdh1 and the N-terminal of Six1: the APC is involved in controlling the degradation of many important cell cycle regulators (e.g.

Cyclin A, Cyclin B) and the fact that Six1 is part of this list suggests that it might also be a cell cycle regulator (Christensen et al., 2007). In a mouse model of rhabdomyosarcoma, a pediatric cancer, Six1 was shown to drive the expression of key cell cycle genes such as Cyclin D1 and c-Myc. In the case of the former, Six1 was shown to bind to the Cyclin D1 promoter as well as drive its expression in a reporter assay (Yu et al., 2006). In pancreatic cancer cells, Six1 overexpression correlates with increased Cyclin D1 protein and mRNA expression. Furthermore, it was shown that knock-down of Six1 by siRNA in pancreatic cancer cells dramatically decreased proliferation of PANC-1 cells and this was phenocopied by Ccnd1 knock-down, suggesting that Six1 exerts its function on the cell cycle through Ccnd1 (Li et al., 2013). Interestingly, the phosphatase Eya1, which is often recruited by Six family members, has also been shown to regulate the cell cycle through its activity at the Cyclin D1 promoter in human breast cancer cells (Wu et al., 2013). Six1 has also been shown to correlate with increased proliferation without Six1 itself being overexpressed. In a screen of blastemal type Wilm's tumours, a mutation of Q177R of the homeodomain was identified as a culprit for high proliferative potential of these tumours (Wegert et al., 2015, Walz et al., 2015). The Six1-Q177R mutants generated an altered DNA binding profile compared to wild-type in which Wegert and colleagues postulate could induce subtle changes in Six1 target gene selection and/or expression.

1.9. Hypothesis and Aims

Ultimately, understanding the transcriptional regulation of myogenic precursors during adult muscle regeneration will provide important information that can be eventually exploited to allow for the development of novel treatment methods for

relevant diseases such as muscular dystrophy. One approach is stem cell based therapy. However, some important obstacles currently limit this therapeutic approach namely insufficient material for transplantation and the transient effect of treatment. For long-term therapeutic efficiency, a large expansion of satellite cells must be achieved in culture and the transplanted satellite cells must be able to repopulate the niche. In order to address this, it is proposed that during *in vitro* expansion, transcription factors important for proliferation must be highly expressed in order to maximize stem cell numbers for therapeutic use. However, in preparation for transplantation, the proliferative genes must be downregulated in favour of allowing satellite cell quiescence and self-renewal in order to favour repopulating the niche. Six1 is a highly appealing target for a number of reasons: Six1 expression has been shown to be pro-proliferative, critical for myogenic differentiation and important for satellite cell self-renewal (Figure 1). In order for the previous therapeutic method to be achieved and whether Six1 would be an appropriate target, a greater understanding of the molecular mode of action of Six1 is required.

Six1 is expressed at barely detectable levels in resting quiescent satellite cells, but its expression is rapidly induced following injury (Liu, Chakroun et al., 2013). Six1 protein and mRNA expression remain high through the proliferation and differentiation of myoblasts and drops markedly in mature, differentiated myotubes (Liu, Chu et al., 2010, Le Grand et al., 2012). Despite knowing the expression pattern of Six1 in proliferating myoblasts, little is known of the role of Six1 during proliferation. Furthermore, a link between Six1 and cellular proliferation is observed in numerous human cancers.

As such, at the onset of the project, it was hypothesized that **Six1 is a critical and positive regulator of cellular proliferation: In the muscle lineage, Six1 is responsible for normal satellite cell activation and myoblast proliferation in response to injury and stress. Furthermore, Six1 achieves this control on the cell cycle through direct regulation of Cyclin D1.**

Three questions were posed to help guide the project's research objectives: (1) What are the *in vivo* and *in vitro* phenotypes associated with Six1 impairment by siRNA? (2) What are the genome wide effects of Six1 knockdown in myoblast? (3) What are the mechanism(s) by which Six1 exerts its effect? All three of these questions were investigated with the following specific aims.

Specific Aim 1: To determine the effect of Six1 knock-down on myoblast proliferation *in vitro* and *in vivo*. To investigate *in vitro* and *in vivo* phenotypes, RNA interference was used to knock-down Six1 expression and investigate the effect on primary myoblasts maintained in growth medium (*in vitro*) and the effect of satellite cell activation in response to cardiotoxin injury (*in vivo*).

Specific Aim 2: Using functional genomics approaches, determine the global effects of Six1 knock-down in primary myoblast. In order to investigate the global impact of Six1 loss in myoblasts, techniques such as Gene Expression Profiling, qRT-PCR, ChIP-Seq, and Bioinformatic Analysis were utilized to query the genomic binding profile of Six1 and impact of Six1 loss-of-function.

Specific Aims 3: To determine the precise mechanism by which Six1 exerts its cell-cycle phenotype in myoblasts. To examine the mechanism, rescue assays were performed in order to restore the expression of Six1 cell-cycle targets in order to assess the importance of these targets during proliferation in the myogenic lineage.

2. Chapter 2 - Results

2.1. Six1 and Six4 protein and mRNA expression are effectively knocked down in C2C12 using siRNA

In order to study the role of Six during myoblast proliferation, consistent and reliable knock-down of Six1 and Six4 in myoblasts is required in order to study their roles from a loss of function approach. To accomplish this, Stealth siRNA duplexes and Lipofectamine RNAiMAX were tested and their usage was optimized for transfection efficiency. Tests of Stealth siRNA and Lipofectamine RNAiMAX first began in C2C12 myoblasts in order to ensure efficacy of the protocol with subsequent follow-up in primary myoblasts. Optimization was performed using BLOCK-iT Alexa Fluor Red Fluorescence in order to assess transfection efficiency across a multitude of Fluorescent siRNA and Lipofectamine RNAiMAX reagent concentrations (Figure 3). Numerous parameters were considered in selecting an optimal concentration: number of red cells, intensity of intracellular red fluorescence and cell survival. Increasing the amounts of lipofectamine, siRNA, or both correlated with increased number of red cells as well as the intensity of intracellular red fluorescence with the top three siRNA volumes at maximal lipofectamine amounts appearing to be quite similar. Across all conditions, the myoblasts appear healthy and achieved nearly identical confluency. It was determined that 1.0 µL of lipofectamine and 0.60 µL of RNAi would be appropriate for future transfections as these amounts provided an excellent balance between transfection efficiency and required reagent volumes. These volumes were set for 1.9cm² and scaled up accordingly by growth area (eg. a growth area of 9.5cm² received five-fold more transfection reagents: 5.0 µL of lipofectamine and 3.0 µL of RNAi). Having selected for

an optimal siRNA and Lipofectamine dosage, transfection was then tested with siRNA sequences specific to Six1, Six4 or a nonspecific control. Three duplexes for Six1 and four duplexes for Six4 were assessed for potency. C2C12 myoblasts were seeded and transfected and all tested siRNA duplexes are shown to be both reliable and robust in knocking down Six protein and mRNA as confirmed by western blot analysis and qRT-PCR (Figure 4; Figure 5). Furthermore, at various time points after siRNA transfection, decreased mRNA expression is observed as shortly as 24 hours after transfection and up to 72 hours after and protein loss is observed up to 96 hours after transfection (Figure 6).

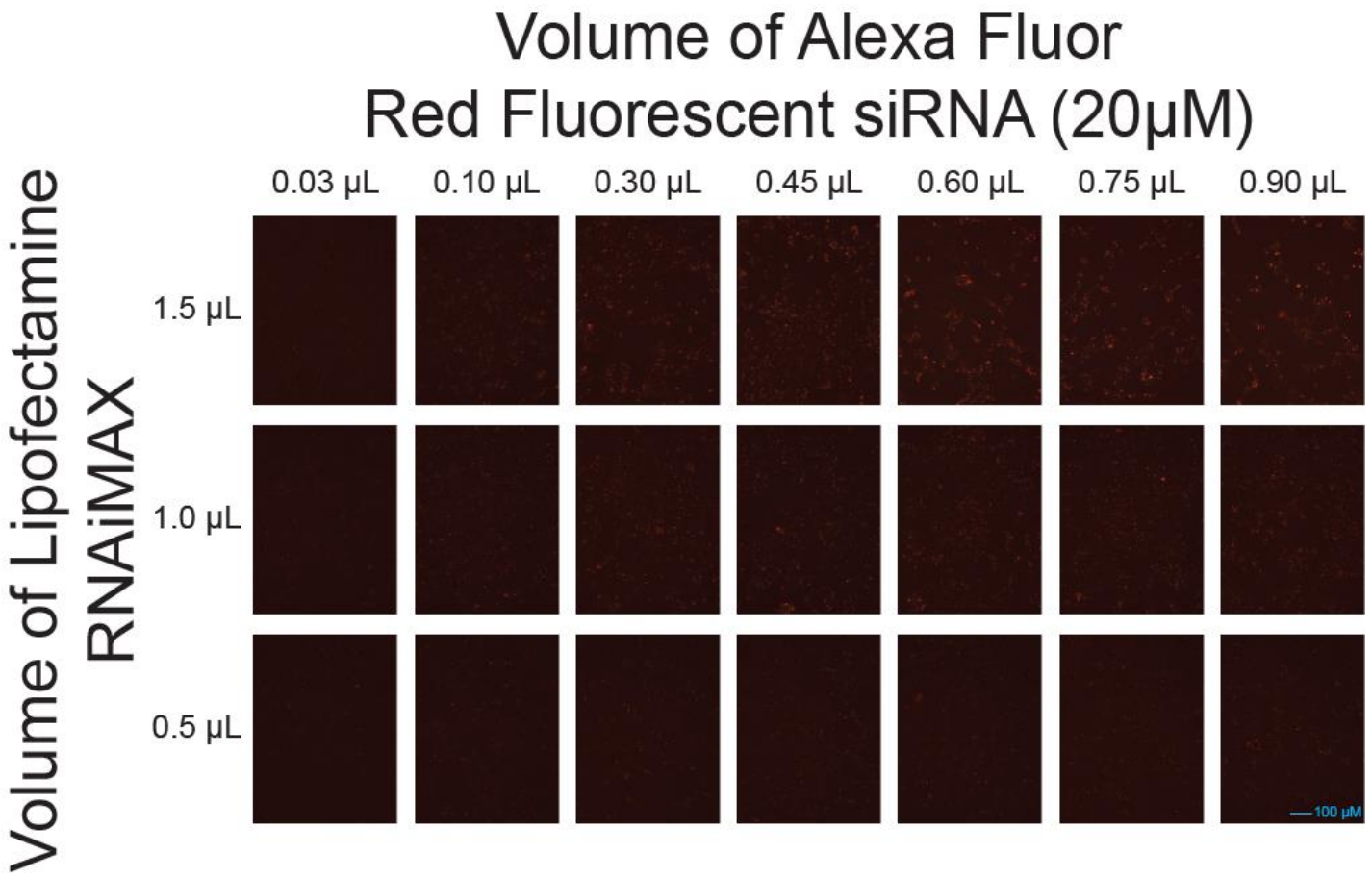

Figure 3: Optimization for stealth siRNA transfection in C2C12 myoblasts.

Increasing amounts of LipofectamineRNAiMAX and red fluorescent siRNA were utilized to assess transfection efficiency and effects on cell viability in C2C12 myoblasts. Representative microscopic fields for each transfection mix are shown 24 hours after transfection. Scale bar: 100 µM.

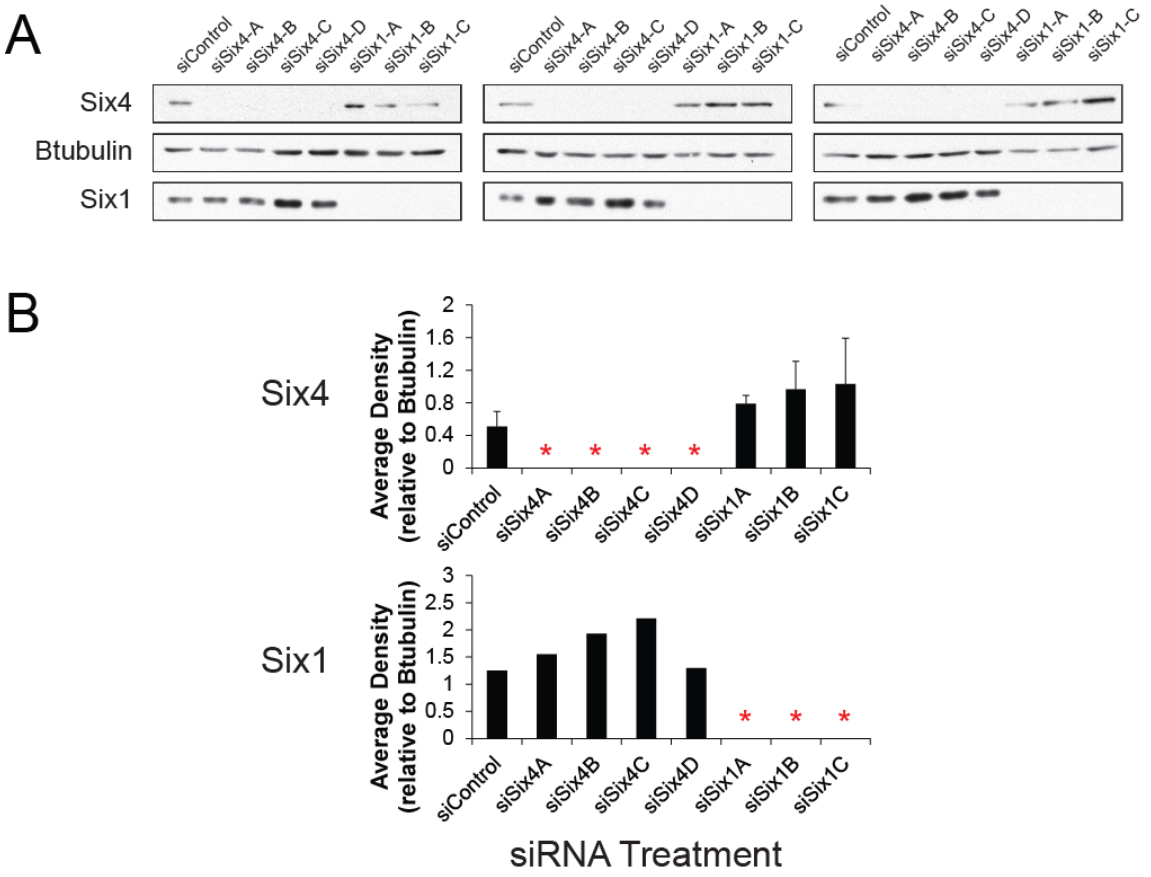

Figure 4: Six1 and Six4 protein are effectively knocked down in C2C12 myoblasts.

(A) Western blots illustrating the protein levels of Six1 and Six4 at 48 hours after treatment with various Six1, Six4 or control siRNA. (B) Western blot quantification of Six1 and Six4 by densitometry was normalized to the densitometry of B-tubulin. The data represent the average of 3 independent biological siRNA experiments. Error bars indicate the Standard Error over the Mean (SEM). * Represents statistically significant change by a two-tailed paired Student t-test relative to siControl (p-value ≤ 0.05).

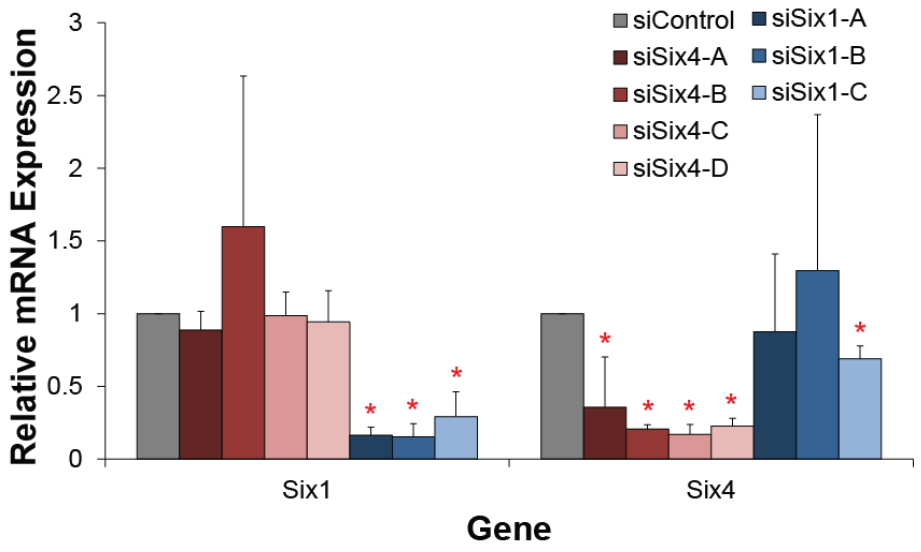

Figure 5: Six1 and Six4 mRNA are effectively knocked down in C2C12 myoblasts.

Levels of Six1 and Six4 mRNA were quantitated by real-time PCR (qRT-PCR). mRNA levels were normalized to Rps26. The data represent the average of 3 independent biological siRNA experiments. Error bars indicate the Standard Error over the Mean (SEM). * Represents statistically significant change by a two-tailed paired Student t-test relative to siControl (p-value ≤ 0.05).

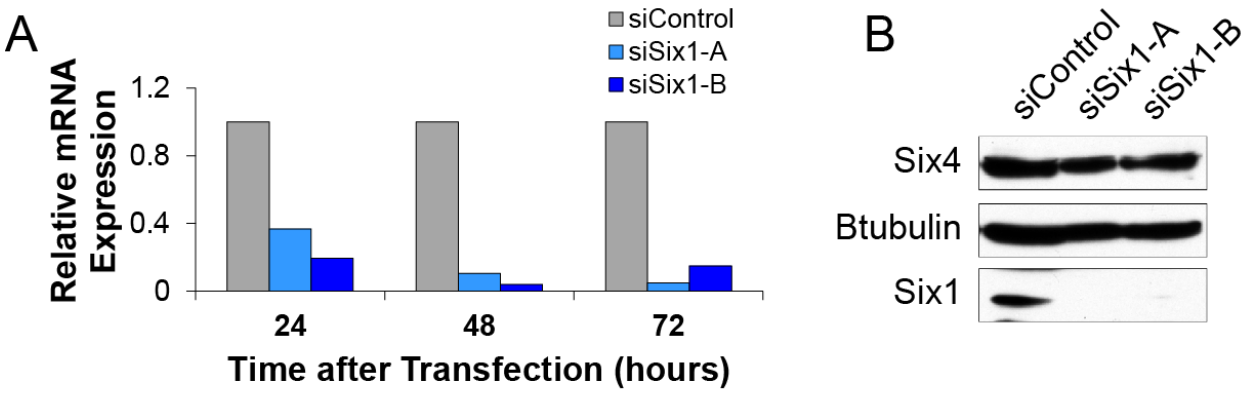

Figure 6: Six1 and Six4 protein and mRNA are effectively depleted after transfection in C2C12 myoblasts.

(A) Levels of Six1 mRNA were measured by qRT-PCR at 24, 48, and 72 hours after transfection. mRNA levels were normalized to Rps26. (B) Western blots illustrating the protein levels of Six1 and Six4 at 96 hours after treatment with Six1 specific siRNA. One independent biological siRNA experiment is shown.

2.2. Loss-of-function by siRNA impairs Six mRNA and protein expression in growing primary myoblasts

Having optimized a dosage and protocol for siRNA transfection using C2C12 myoblasts, it was next paramount to confirm the efficacy of this protocol in primary myoblasts. Cells were treated with siRNA and harvested for protein and mRNA to be analyzed by western blot and qRT-PCR, respectively. Consistent with the previous work in C2C12, significant impairment of Six1 mRNA and protein expression in growing primary myoblasts 48 hours after transfection is observed (Figure 7). Six1 and Six4 mRNA expression is reduced 60% relative to control and protein expression is undetectable in the knock-down samples. Furthermore, siRNA mediated knockdown is specific to their respective targets and there does not appear to be any compensation between Six1 and Six4.

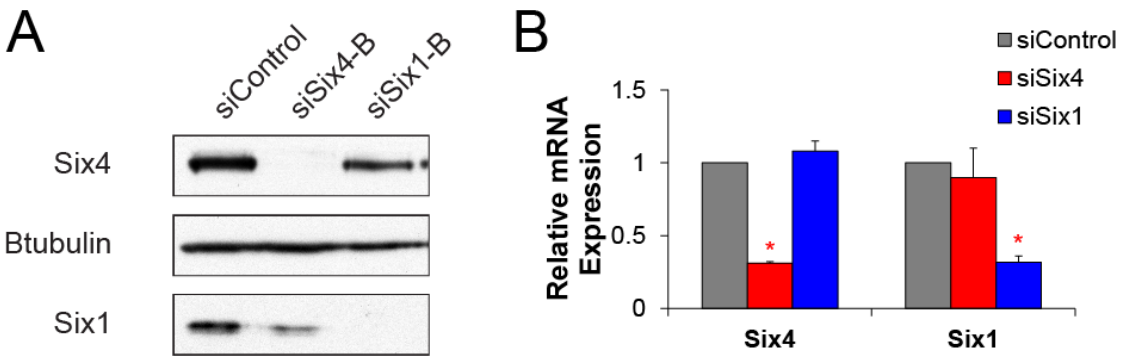

Figure 7: Six1 and Six4 protein and mRNA are effectively knocked down in primary myoblasts.

(A) Western blots illustrating the protein levels of Six1 and Six4 at 48 hours after treatment with siControl, siSix1 or siSix4. (B) Levels of Six1 and Six4 mRNA after siRNA treatment were measured by qRT-PCR. mRNA levels were normalized to a geometric mean of the control genes Rps26, Tbp and Rplp0. The data represent the average of 4 independent biological siRNA experiments. Error bars indicate the Standard Error over the Mean (SEM). * Represents statistically significant change by a two-tailed paired Student t-test relative to siControl (p-value ≤ 0.05).

2.3. Knockdown of Six1 in growing primary myoblasts significantly impairs proliferation

With consistent and robust knock-down of Six1 mRNA and proteins, the impact of their loss during primary myoblast proliferation was next examined. Cells were plated, transfected with siRNA and stained with crystal violet at multiple time points after transfection. Over a 96 hour time period following transfection, loss of Six1 results in significantly less cells (Figure 8). Interestingly, loss of Six4 has no effect on relative cell density. Similar experiments were also performed in C2C12 myoblasts and the same phenotype is observed (Figure 22).

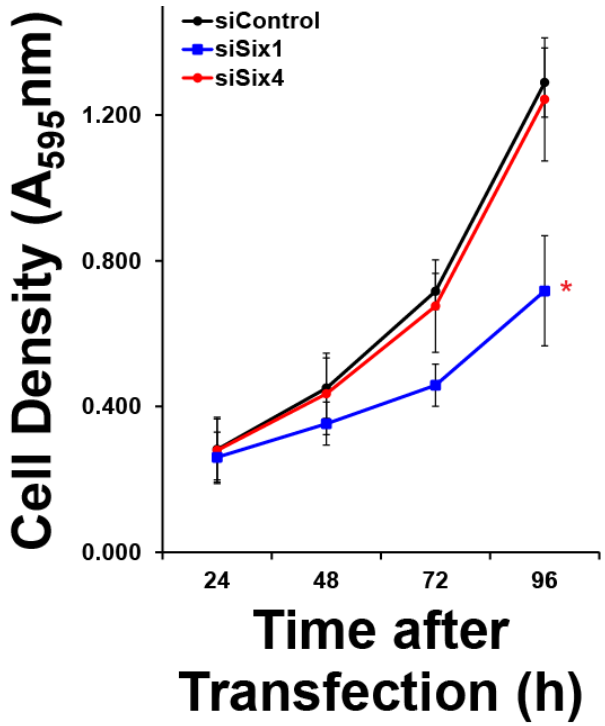

Figure 8: Loss of Six1 in growing primary myoblasts impairs proliferation.

Primary myoblasts were transfected with siRNA, harvested and stained with crystal violet at 24, 48, 72, and 96 hours after transfection. The data represent the average of 4 independent biological siRNA experiments. Error bars indicate the Standard Error over the Mean (SEM). * Represents statistically significant change by ANOVA analysis relative to siControl (p-value $\leq$ 0.05).

2.4. Loss of Six1 has inconsistent effects on cell cycle distribution with no effect on apoptosis in primary myoblasts

With the primary myoblasts demonstrating less growth potential in the Six1 knock-downs, flow cytometry was performed in order to assess the cell cycle distribution of proliferating primary myoblasts. Growing cells were pulsed with bromodeoxyuridine (BrdU) and counterstained with 7-amino-actinomycin D (7-AAD) to characterize the cell cycle positions (G0/1, S, and G2/M phase) after Six1 knock-down. Across the conditions of no transfection, siControl, siSix1-A and siSix1-B, there is absolutely no difference in the relative distribution of the cells. Furthermore, the relative number of apoptotic cells as determined by the sub-G1 population (less than 2N DNA) remains unchanged across all four conditions (Figure 9).

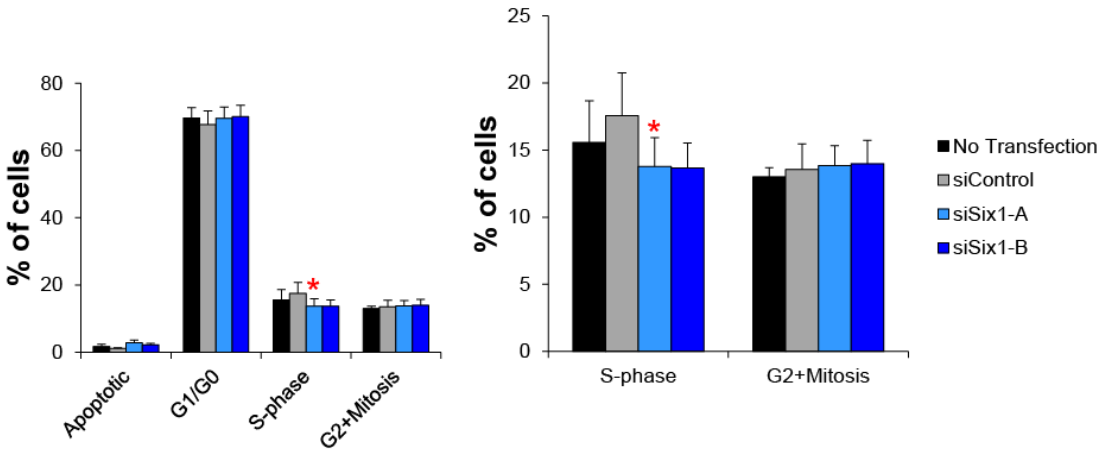

Figure 9: Knockdown of Six1 in primary myoblasts decreases the number of cells that proceed through S-phase.

Primary myoblasts were transfected with siRNA, pulsed with BrdU for one hour, harvested at 48 hours after transfection and prepared for analysis by flow cytometry. The data represent the average of 4 independent biological siRNA experiments. Error bars indicate the Standard Error over the Mean (SEM). * Represents statistically significant change by a two-tailed paired Student t-test relative to siControl (p-value ≤ 0.05).

2.5. Over-expression of Six1 resistant to siRNA is sufficient to rescue the cell cycle phenotype

In order to develop confidence in the Six1 phenotype, a simple rescue assay was performed in proliferating C2C12 myoblasts. Cell lines were generated to stably express luciferase (negative control) or Six1-res (a form of the Six1 mRNA that is insensitive to the siRNA duplex used to knock-down the endogenous Six1 mRNA). Next, a crystal violet staining protocol was employed to evaluate the proliferative potential of the cells. Over a 96 hour time period following transfection, the Six1-res cell line is effectively able to rescue the cell cycle phenotype (Figure 10). It is also interesting to note that the over-expression of Six1 yields increased proliferation as compared to the luciferase expressing cell-line in the siControl treated samples reinforcing the pro-proliferative effect of Six1.

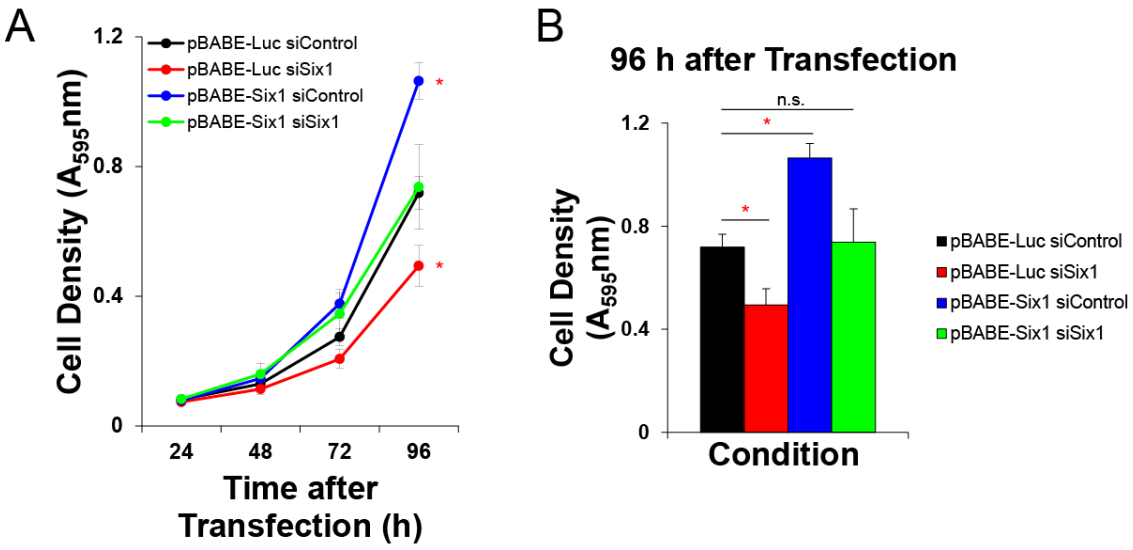

Figure 10: Over-expression of Six1 resistant to siRNA is sufficient to rescue the cell cycle phenotype.

(A) C2C12 myoblasts overexpressing luciferase (pBABE-Luc) or Six1 resistant to siRNA (pBABE-Six1-res) were transfected with siRNA, harvested and stained with crystal violet at 24, 48, 72, and 96 hours after transfection. (B) Cell densities of the siRNA treated cell lines at 96 hours after transfection are shown. The data represent the average of 4 independent biological siRNA experiments. Error bars indicate the Standard Error over the Mean (SEM). * Represents statistically significant change by ANOVA analysis (in Panel A) or two-tailed paired Student t-test (in Panel B) relative to pBABE-Luc siControl (p-value ≤ 0.05).

2.6. Intramuscular injection of Six1 siRNA impairs proliferation of satellite cells after injury in vivo

Having observed impaired proliferation following loss of Six1 expression in cells cultured *in vitro*, the effects *in vivo* were investigated. In order to achieve this, mice *tibialis anterior* (TA) muscles were injured with cardiotoxin and subsequently received two rounds of injections for siRNA specific to Six1 or a nonspecific control sequence. In order to assess the proliferative capacity of satellite cells, a double immunostaining was performed against the satellite cell specific marker Pax7 and the proliferative nuclear antigen Ki67. Whole muscle cross sections were quantified and it is observed that intramuscular injection of Six1 yields significantly less co-staining of Pax7 and Ki67

suggesting that less satellite cells are in a proliferative state (Figure 11, Table 1). It is also interesting to note that although there is a decrease in Ki67 positive satellite cells, there is no significant changes in the absolute number of satellite cells per cross section as determined by the total number of Pax7 positive cells (Table 1).

	Pax7 +ve & Ki67-high	Total Pax7 +ve cells	% Ki67-high Pax7 +ve cells
siControl	849	1425	59.59
siSix1	685	1373	49.90

Table 1: Quantification of in vivo immunostaining.

Muscle sections were quantified for the satellite cell specific marker Pax7 and the proliferative nuclear antigen Ki67 at four days after injury. The data represent the average of 3 mice.

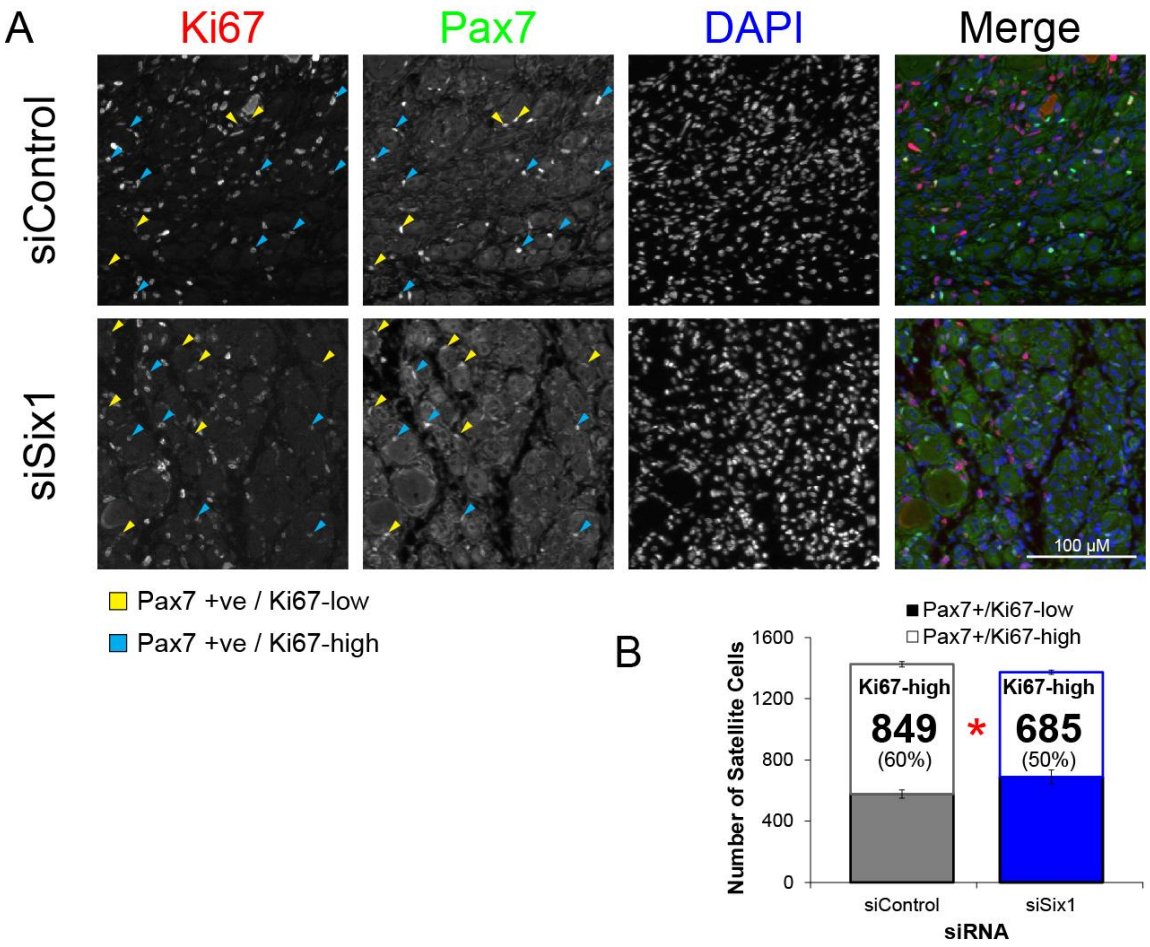

Figure 11: Intramuscular injection of Six1 siRNA impairs proliferation of satellite cells after injury *in vivo*.

(A) Representative microscopic fields with immunostaining for the satellite cell marker Pax7 (green) and the cell proliferation marker KI67 (red) on sections from regenerating muscles treated with siControl or siSix1. Yellow arrows point to KI67-low satellite cells and cyan arrows point to KI67-high satellite cells. (B) Summary for the quantification of immunostained paraffin muscle sections treated with siControl or siSix1. The data represent the average of 3 mice. Error bars indicate the Standard Error over the Mean (SEM). * Represents statistically significant change by a two-tailed paired Student t-test relative to siControl (p-value ≤ 0.05).

2.7. Gene expression profiling and bioinformatics analyses identify impaired cell cycle processes after Six1 knock-down

At this point, a proliferation related phenotype had been observed in two *in vitro* models and one *in vivo* model. Next the genomic binding profile of Six1 and impact of

Six1 loss-of-function was investigated. To accomplish this, techniques such as Gene Expression Profiling, qRT-PCR, ChIP-Seq, and bioinformatic analyses were utilized. RNA was extracted from primary myoblasts after transfection of Six1, Six4 or control sequence siRNA and prepared for gene expression microarray profiling on the Agilent SurePrint G3 technology platform. A pipeline was followed to cull missing, variable or poorly expressed probes. Following this cull, 37312 probes remain which underwent preprocessing by performing log2 transformation of probe expression values with subsequent quantile normalization. The overall data processing is shown in Figure 12.

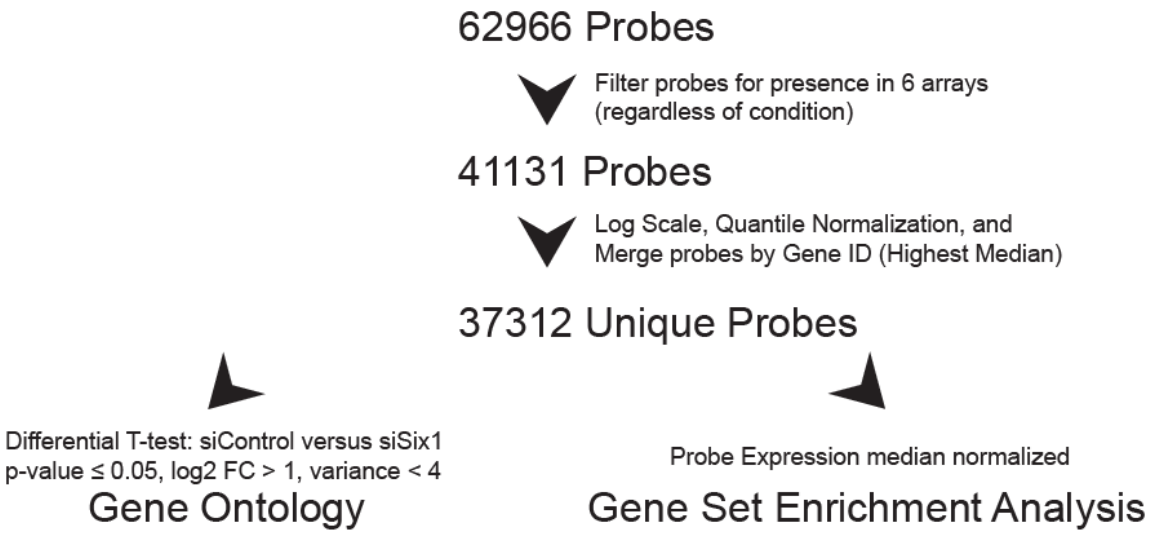

Figure 12: Data processing pipeline in the gene expression analysis.

Nearly 63,000 probes underwent data processing in preparation for gene ontology (GO) and gene set enrichment analysis (GSEA).

Gene Set Enrichment Analysis (GSEA) was performed using an input of all 37312 preprocessed probes that further had their expression median normalized across conditions. Results for the top five gene sets correlated to each condition are shown in (Table 2). A more comprehensive list is found in Table S3. Of particular interest are the cell cycle related gene sets which are enriched in siControl relative to siSix1: There is

greater expression of cell cycle related gene sets in siControl treated samples compared to siSix1 treated samples (Table 2). Upon closer examination of one of the gene sets (cell cycle processes) a few observations can be made (Figure 13). The positive enrichment score (ES) and normalized enrichment score (NES) indicates that the gene set cell cycle processes is enriched at the top of ranked list (positively correlated with the control condition) and this enrichment is even more pronounced when compared with the enrichment scores of all other permutations in the data set. The nominal p-value determines that the individual ES for the cell cycle processes gene set is significant. Furthermore, the small false discovery rate (FDR) q-value provides confidence that this indicates that it is unlikely to occur simply by chance.

	Rank	Gene Set Name	Size	ES	NES	NOM p-val	FDR q-val	FWER p-val
Decreased expression with siSix1	1	CELL CYCLE PROCESS	183	0.50	2.24	0.000	0.000	0.000
	2	RNA SPLICING	89	0.53	2.15	0.000	0.000	0.001
	3	M PHASE	107	0.50	2.10	0.000	0.002	0.008
	4	DNA DEPENDENT DNA REPLICATION	53	0.58	2.09	0.000	0.002	0.009
	5	CELL CYCLE PHASE	160	0.46	2.03	0.000	0.004	0.022
Increased expression with siSix1	1	REGULATION OF PROTEIN STABILITY	16	-0.63	-1.74	0.004	1.000	0.648
	2	REGULATION OF MAPKKK CASCADE	16	-0.64	-1.73	0.002	0.585	0.679
	3	RESPONSE TO DRUG	18	-0.59	-1.66	0.027	0.731	0.884
	4	DIGESTION	21	-0.54	-1.61	0.019	0.798	0.962
	5	GENERATION OF A SIGNAL INVOLVED IN CELL CELL SIGNALING	24	-0.51	-1.56	0.020	0.988	0.989

Table 2: GSEA Analysis of siControl versus siSix1.

Gene set enrichment analysis of the top 5 ranked gene sets correlated to siControl (red) and siSix1 (blue). A positive enrichment score indicates genes are expressed at higher levels in the control vs. the Six1 knock-down; a negative enrichment score indicates genes are expressed at higher levels in the Six1 knock-down vs. the control. A more complete list of siControl correlated gene sets can be found in Table S3. The enrichment score, normalized enrichment score, nominal p-value, false discovery rate q-value, and the family-wise error rate p-value are shown.

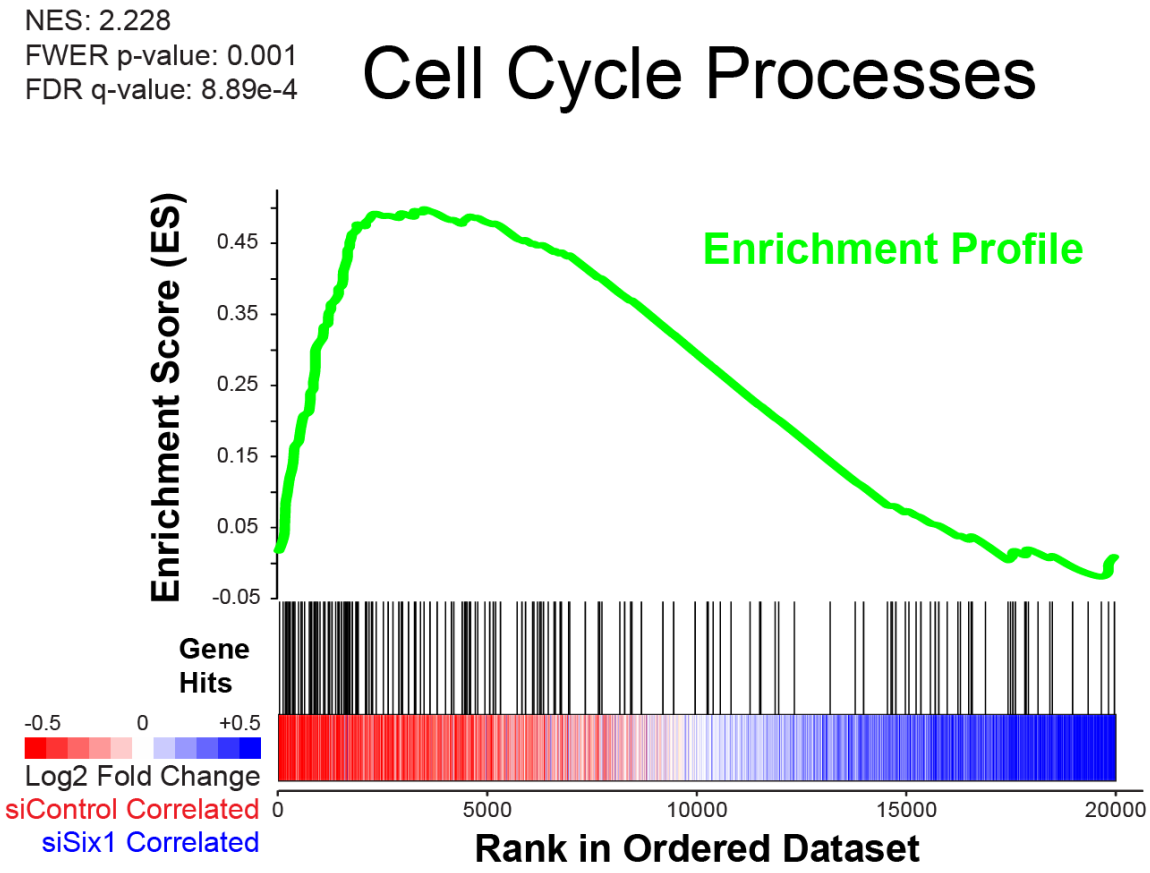

Figure 13: Gene set enrichment analysis identifies enrichment for cell cycle processes.

GSEA of the entire data set comparing siControl with siSix1 treatment. Cell cycle processes is the most enriched gene set among the siControl correlated analysis. For the full table, see Table S3. The normalized enrichment score (NES), false discovery rate (FDR), and familywise error rate (FWER) are shown.

2.8. Gene ontology identifies cell cycle impairment after Six1 knockdown

Having observed enrichment for cell cycle processes in the global analysis of the gene expression data, Gene Ontology analysis was pursued to help narrow down the list of candidates. In preparation for GO analysis, preprocessed probes were filtered based on differential expression between the control and Six1 knockdown with a *p-value*

cutoff of 0.05. To further ensure quality, probes were filtered to possess a minimum log2 fold-change of 1 and a maximum sample expression variance of 4 between replicates. This processing yields a group of 1301 significant and differentially expressed probes between the control and Six1 samples (Figure 14). Of these 1301 probes (corresponding to 756 unique genes), 596 probes (346 genes) are downregulated (Cluster #1) and 705 probes (410 genes) are upregulated (Cluster #2). Of particular interest with these two clusters is the fact that loss of Six4 largely has no effect on gene expression relative to the control (Figure 14). When gene ontology is performed on Cluster #1, significant enrichment for cell cycle and related terms is observed (Table 3). Among these lists of genes are various cell cycle regulators such as Ccna2, Ccnb1, Ccnd1, Cdk1, Foxm1, Mybl2, and Plk1. Furthermore, a number of these genes are predicted targets of Six1 from ChIP-Seq performed in primary myoblasts (Table 3).

Name	FDR B&H	Total Genes	With Six1 Peak
cell cycle	4.14E-41	121	68
cell division	4.14E-41	87	49
abnormal cell cycle	1.69E-05	22	9
Cell Cycle	1.74E-29	63	39
M Phase	7.05E-25	41	26
PLK1 signaling events	5.77E-16	17	10
Aurora B signaling	1.71E-12	14	10
FOXM1 transcription factor network	5.01E-06	9	7
RB in Cancer	1.30E-05	12	8

Table 3: Gene ontology analysis of Cluster #1.

Gene ontology was performed on Cluster #1. A subset of GO categories is shown in the table. For the full list, see Table S4. FDR B&H corresponds to the Benjamini-Hochberg false discovery rate. Total genes corresponds to the number of genes from Cluster #1 found in the GO category. With Six1 Peak identifies genes that are predicted targets of Six1 by ChIP-Seq.

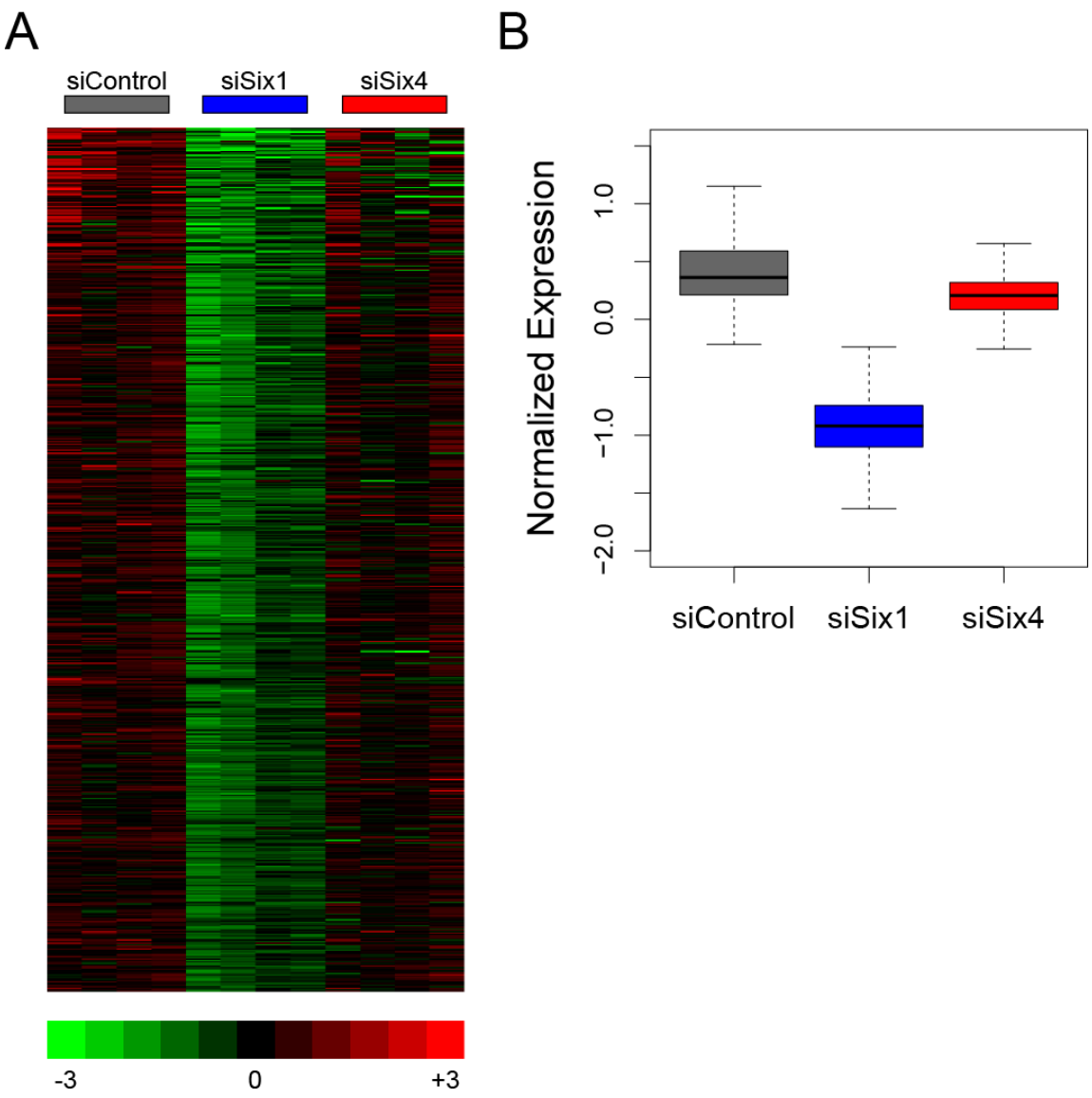

Figure 14: There is a cluster of genes that are downregulated after Six1 knockdown.

(A) Heatmap representing the expression levels of significantly downregulated probes after Six1 knockdown relative to the control. (B) Box Plot representing the average expression profile of 596 probes over 4 siRNA treatments in primary myoblasts. Whiskers represent 1.5 x inner quantile Range of the 1st and 3rd quantiles.

2.9. Validation of gene expression by qRT-PCR confirms downregulation of cell cycle genes

In order to confirm the results from gene expression profiling, qRT-PCR was performed on select genes that were annotated in the GSEA and GO analysis. Genes implicated as important during various phases of the cell cycle or towards satellite cell proliferation are downregulated exclusively in the Six1 siRNA treated samples (Figure 15). This impaired expression of cell cycle genes is further confirmed with another Six1 siRNA duplex (Figure 23).

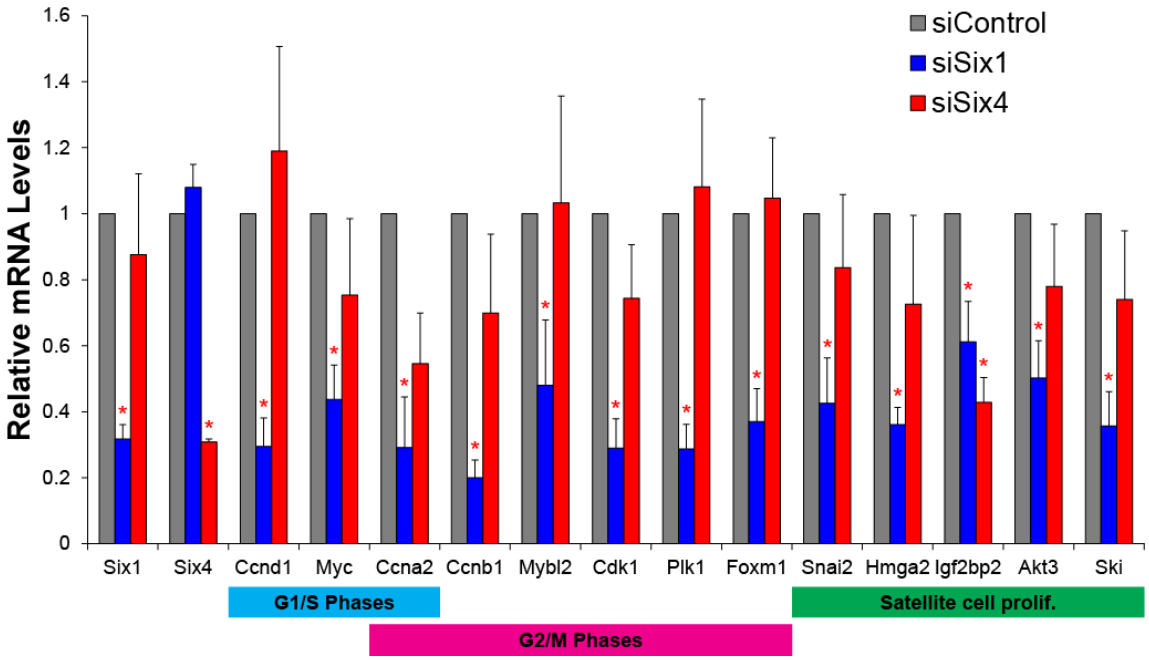

Figure 15: qRT-PCR confirms downregulation of cell cycle genes and genes involved in satellite cell proliferation after Six1 knockdown.

Levels of mRNA in primary myoblasts treated with siControl, siSix1, or siSix4 were quantified by real-time PCR (qRT-PCR) on a number of cell cycle regulators and satellite cell proliferation genes. mRNA levels were normalized to a geometric mean of the control genes Rps26, Tbp and Rplp0. The data represent the average of 4 independent biological siRNA experiments. Error bars indicate the Standard Error over the Mean (SEM). * Represents statistically significant change by a two-tailed paired Student t-test relative to siControl (p-value ≤ 0.05).

2.10. Cell cycle genes are directly bound by Six1 and downregulated by Six1 siRNA

Experiments next sought to identify a mechanism by which Six1 is exerting its cell cycle phenotype. In order to achieve this, gene expression data was crossed with ChIP-Seq data done on primary myoblasts and myotubes in which peaks are annotated to the single nearest gene within 10 kilobases (10kb). Referring to Table 3, it can be noted that of the 121 significantly downregulated cell cycle genes, 68 are predicted targets of Six1. Two predicted targets include c-Myc and Ccnd1 with Six1 binding upstream of the gene's TSS or in the 3' UTR, respectively (Figure 16). Interestingly, greater binding is observed in proliferating myoblasts compared to differentiated myotubes for both genes. This is in line with what is expected for Six1 and a role during proliferation. For comparison, the binding profile for the late differentiation marker Myl1 shows greater binding in differentiated myotubes. Six1 binding is validated by performing qChIP PCR: significant enrichment of Six1 at the c-Myc and Ccnd1 loci are observed (Figure 17).

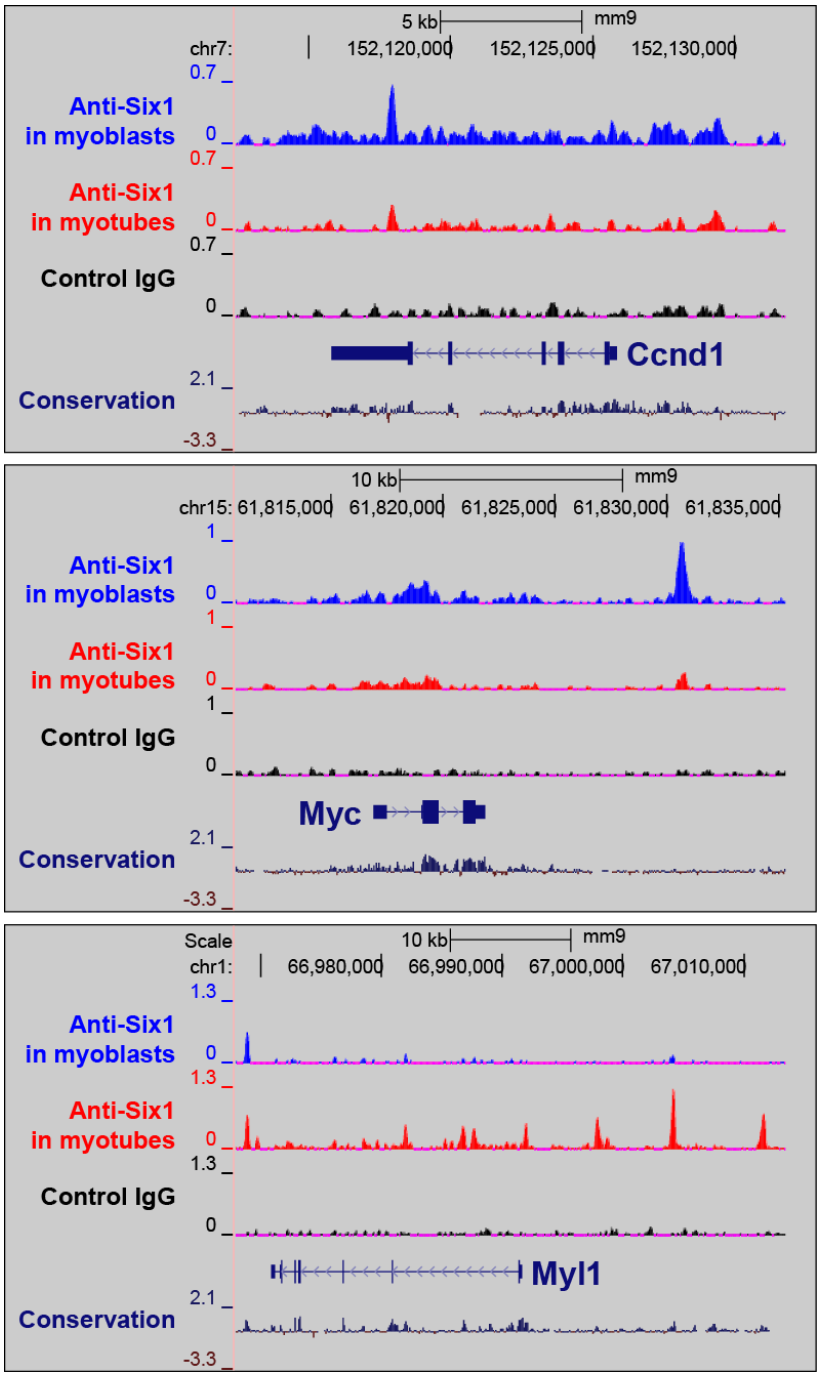

Figure 16: ChIP-sequencing (ChIP-seq) identifies Six1 binding of cell cycle regulators in primary myoblasts.

Peaks represent binding sites for Six1 in growing myoblasts (blue) and differentiated myotubes (red). The signal shown is the ChIP-seq read density smoothed over 25 bp and with signal in the input ChIP-seq sample subtracted. Myl1 ChIP-seq was included as a control. The ChIP-seq data was provided by another student in the lab.

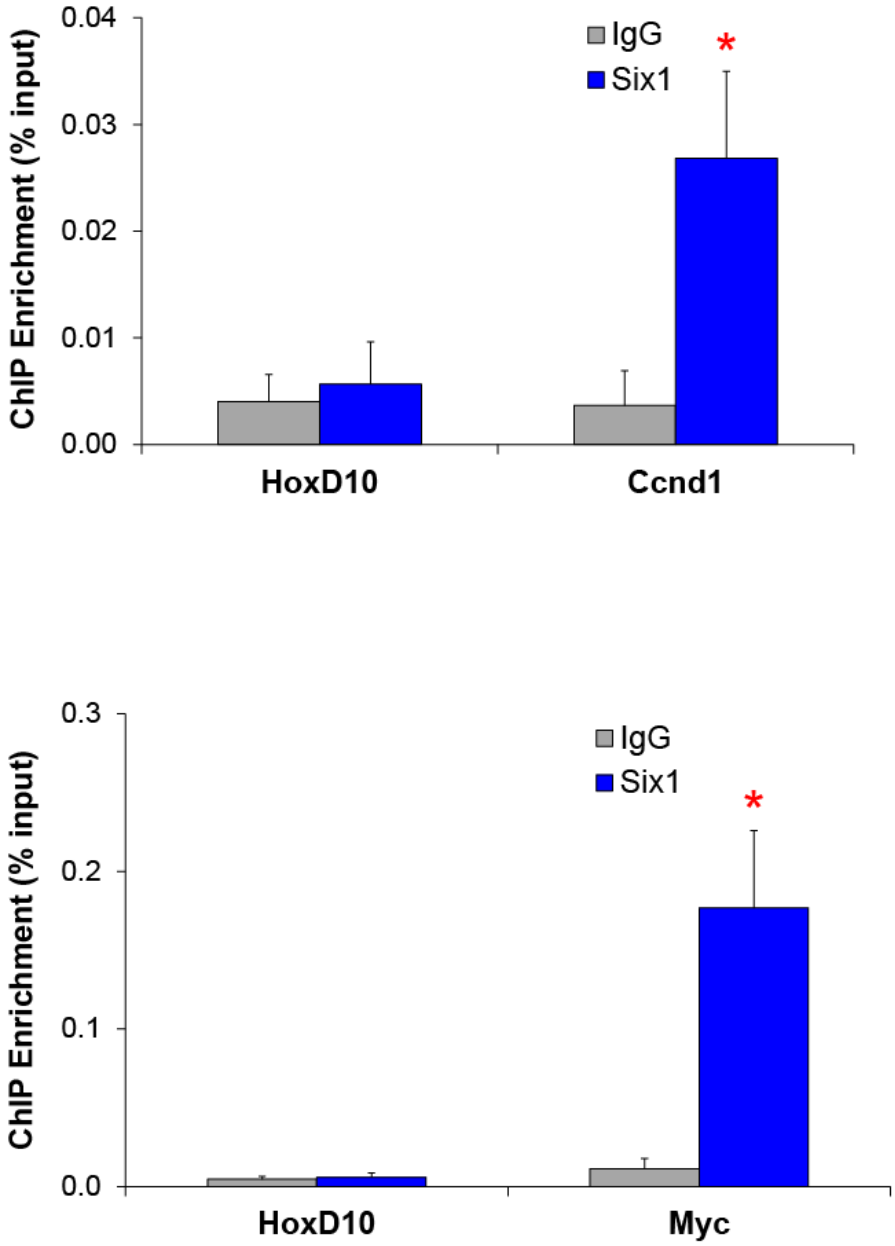

Figure 17: The Ccnd1 and Myc genes are bound by Six1.

C2C12 myoblasts were fixed, harvested for chromatin and ChIP was performed using Six1 or IgG antibodies. 10% of ChIP DNA input was quantified by real-time PCR. The HoxD10 locus was used as a negative control. The data represent the average of 3 independent biological chromatin immunoprecipitation experiments. Error bars indicate the Standard Error over the Mean (SEM). * Represents statistically significant change by a two-tailed paired Student t-test relative to siControl (p-value ≤ 0.05). The ChIP DNA was provided by another student in the lab.

2.11. Ccnd1 exhibits a similar protein expression pattern as Six1 during a time course of myoblast differentiation and is downregulated after Six1 knockdown

Having confirmed that downregulation of Six1 impaired Ccnd1 expression and that Six1 binds the Ccnd1 gene, it is critical to investigate the temporal protein expression of Ccnd1 during myogenic differentiation. Interestingly, both Six1 and Ccnd1 expression are highest in proliferating myoblasts (timepoints GM and T0) and begins to decrease after cells are induced to differentiate (timepoints T24 and T48) (Figure 18). Furthermore, loss of Six1 by two different siRNA duplexes effectively downregulates Ccnd1 protein expression in proliferating myoblasts (Figure 18)

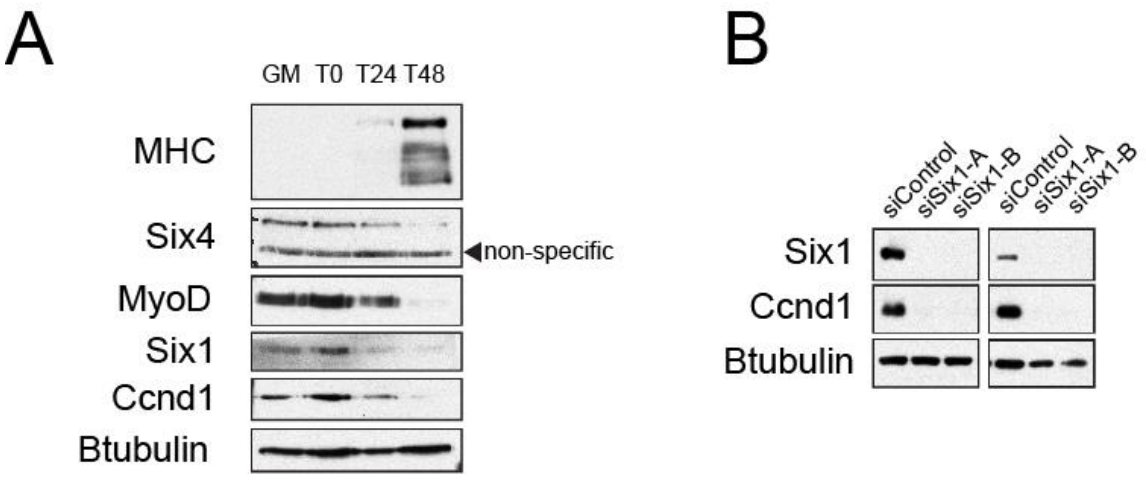

Figure 18: Ccnd1 exhibits a similar protein expression pattern as Six1 during a time course of myoblast differentiation and is downregulated after Six1 knockdown.

(A) Western blots illustrating the protein levels of myosin heavy chain (MHC), Six4, MyoD, Six1 and Ccnd1 at four time points during myogenic differentiation in primary myoblasts: Myoblasts (MB), 0h of differentiation (T0), 24h of differentiation (T24) and 48h of differentiation (T48). One representative time course experiment is shown. (B) Western blots illustrating the protein levels of Six1 and Ccnd1 after treatment with siControl, siSix1-A, or siSix1-B in primary myoblasts. Two independent biological siRNA experiments are shown.

2.12. The Six1 cell cycle phenotype can be rescued by Ccnd1 over-expression

A rescue assay was next performed in order to assess the ability of Ccnd1 to rescue the Six1 loss-of-function cell cycle phenotype. A C2C12 myoblast cell line stably expressing either luciferase or Ccnd1 was developed and the same previous crystal violet proliferation assay performed. Exogenous Ccnd1 is unaffected by the Six1 siRNA at 48 hours after transfection (Figure 19). In a timeline over 96 hours after siRNA transfection, the Ccnd1 expressing cell line was able to rescue the Six1 siRNA mediated cell cycle phenotype (Figure 20). Furthermore, it is observed that the cell line over-expressing Ccnd1 displayed significantly greater proliferation as compared to the luciferase expressing cell line.

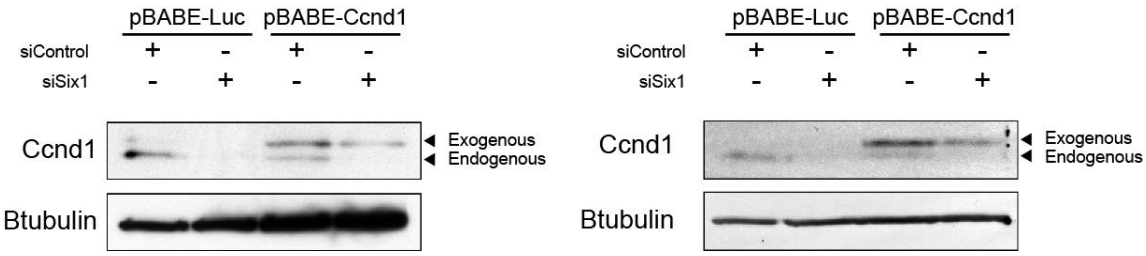

Figure 19: Endogenous, but not exogenous, Ccnd1 is affected by siSix1 treatment.

C2C12 myoblasts overexpressing luciferase (pBABE-Luc) or Ccnd1 (pBABE-Ccnd1) were transfected with siRNA and harvested for protein at 48 hours after transfection. Western blots illustrating the protein levels of exogenous and endogenous Ccnd1 after treatment with siControl or siSix1 from two independent biological siRNA experiments are shown.

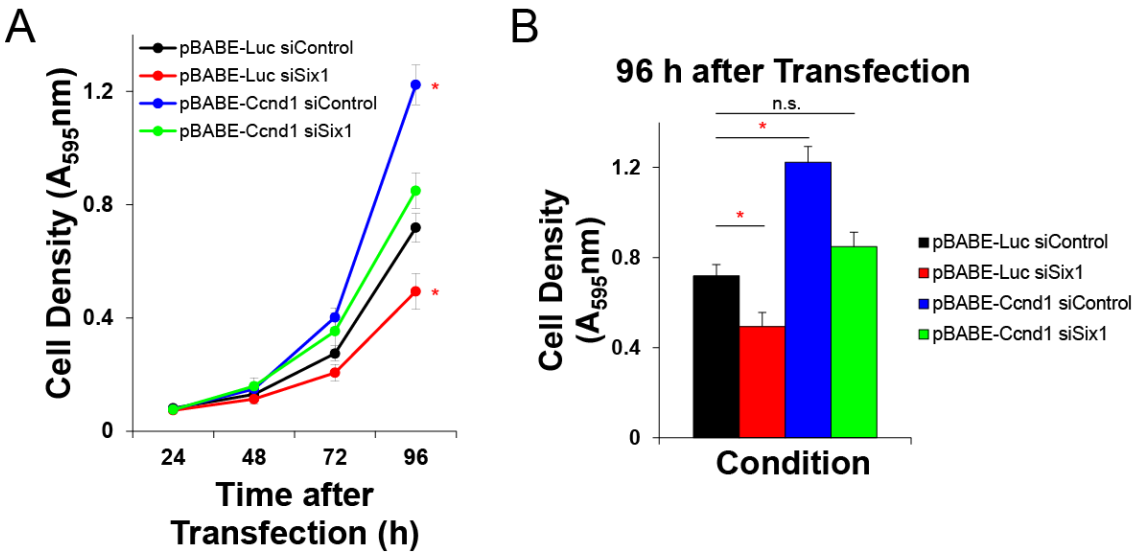

Figure 20: The Six1 cell cycle phenotype can be rescued by Ccnd1 over-expression.

(A) C2C12 myoblasts overexpressing luciferase (pBABE-Luc) or Ccnd1 (pBABE-Ccnd1) were transfected with siRNA, harvested and stained with crystal violet at 24, 48, 72, and 96 hours after transfection. (B) Cell densities of the siRNA treated cell lines at 96 hours after transfection are shown. The data represent the average of 4 independent biological siRNA experiments. Error bars indicate the Standard Error over the Mean (SEM). * Represents statistically significant change by ANOVA analysis (in Panel A) or two-tailed paired Student t-test (in Panel B) relative to pBABE-Luc siControl (p-value ≤ 0.05).

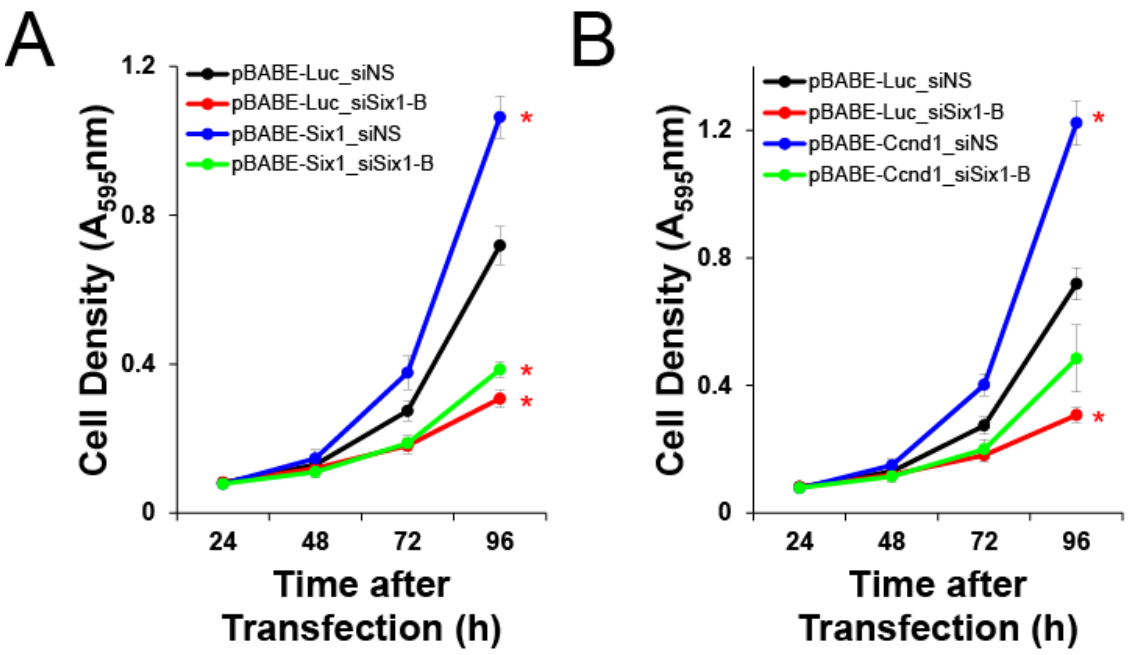

Figure 21: The siSix1-B duplex is not rescuable by Ccnd1 or Six1.

(A) C2C12 myoblasts overexpressing luciferase (pBABE-Luc), or Six1 resistant to siRNA (pBABE-Six1-res) were transfected with siSix1-B or siControl, harvested and stained with crystal violet at 24, 48, 72, and 96 hours after transfection. (B) C2C12 myoblasts overexpressing luciferase (pBABE-Luc), or Ccnd1 (pBABE-Ccnd1) were transfected with siSix1-B or siControl, harvested and stained with crystal violet at 24, 48, 72, and 96 hours after transfection. Error bars indicate the Standard Error over the Mean (SEM). * Represents statistically significant change by ANOVA analysis relative to pBABE-Luc siControl (p-value ≤ 0.05).

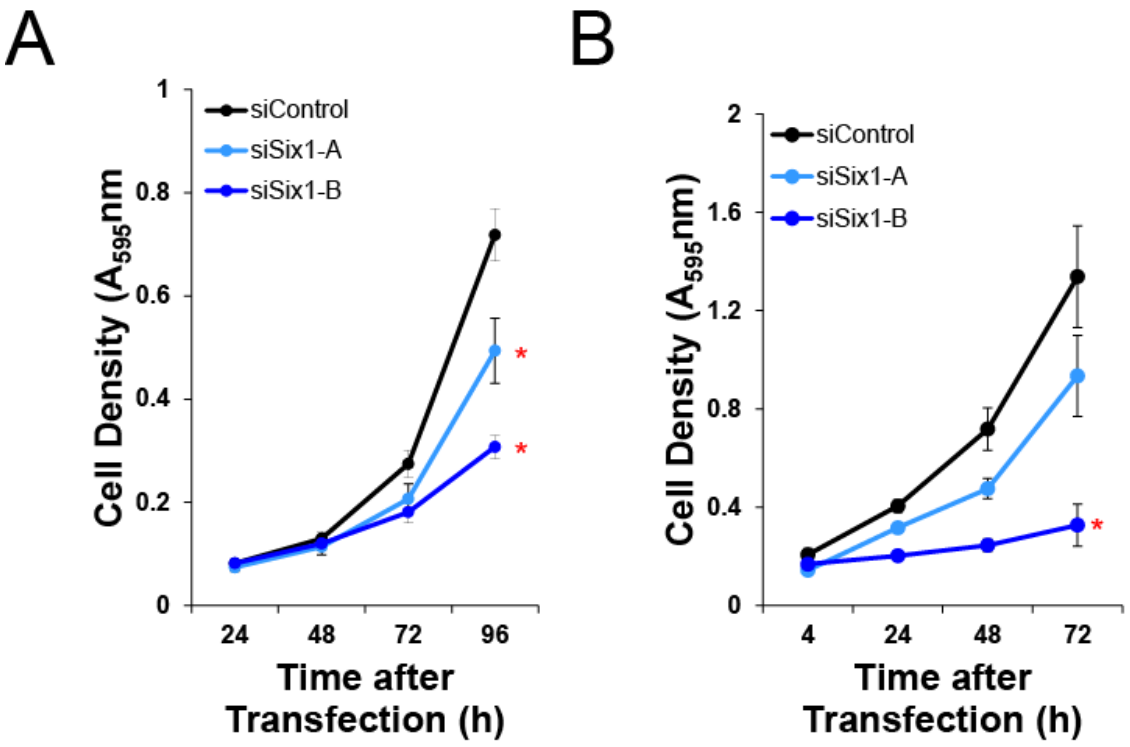

Figure 22: Loss of Six1 by siSix1-A or siSix1-B impairs proliferation.

(A) C2C12 myoblasts were transfected with siRNA, harvested and stained with crystal violet at 24, 48, 72, and 96 hours after transfection. (B) Primary myoblasts were transfected with siRNA, harvested and stained with crystal violet at 24, 48, 72, and 96 hours after transfection. The data represent the average of 4 independent biological siRNA experiments. Error bars indicate the Standard Error over the Mean (SEM). * Represents statistically significant change by ANOVA analysis relative to pBabe-Luc siControl (Panel A) or siControl (Panel B) ($p\text{-value} \leq 0.05$).

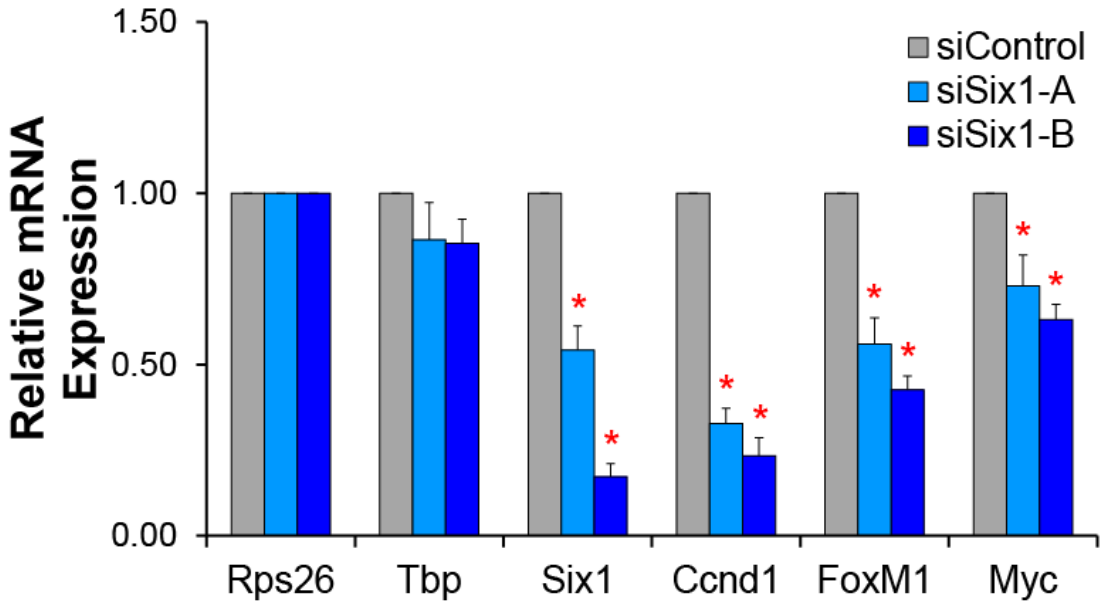

Figure 23: Validation of Six1 qRT-PCR results using two siSix1 duplexes.

Levels of mRNA in primary myoblasts treated with siControl, siSix1-A, or siSix1-B were quantified by real-time PCR (qRT-PCR) on select cell-cycle regulators. mRNA levels were normalized to Rps26 and Tbp was used to assess the quality of the Rps26 control gene. The data represent the average of 4 independent biological siRNA experiments. Error bars indicate the Standard Error over the Mean (SEM). * Represents statistically significant change by a two-tailed paired Student t-test relative to siControl (p-value ≤ 0.05).

3. Chapter 3 - Discussion

3.1. The pro-proliferative effects of Six1 in vitro

This study primarily uses an *in vitro* model in order to elucidate the role of Six1 in satellite cell proliferation and highlights Six1 as a positive regulator of the cell cycle in the myogenic lineage. Previously, others have shown that Six1 loss-of-function or expression in proliferating C2C12 myoblasts decreases the proliferative capacity of the cells as assessed by the incorporation of BrdU (Li et al., 2003). Similarly, the present study demonstrates in two different *in vitro* models with two different Six1 siRNA duplexes that downregulation of Six1 decreases cell density of proliferating myoblasts: The two siRNA duplexes targeting Six1, siSix1-A and siSix1-B, were utilized in primary myoblasts and C2C12 myoblasts. Initial experiments which knocked down the expression of Six1 resulted in decreased proliferation in primary myoblasts and this was similarly repeated in C2C12 myoblast cell lines. Furthermore, this decrease in cell density could not be explained by increased apoptosis as knockdown of Six1 had no significant effects on cell death as determined by flow cytometry. Additionally, the pro-proliferative effect of Six1 was apparent in a C2C12 cell-line stably overexpressing Six1. There was increased cell proliferation of Six1 over-expressing cells compared to luciferase-expressing in a timeline over 96 hours. Greater confidence in Six1 function as a pro-proliferative factor was achieved through the rescue assays in which over-expression of a version of Six1 resistant to siRNA treatments was able to effectively rescue the proliferation defect after Six1 knock-down.

Despite the promising results from the present study, issues have arisen. First, the results obtained with the two siRNA duplexes were not perfectly consistent. Both qRT-PCR validation and western analysis showed that knock-down of Six1 was comparable. In particular, when the myoblasts were treated with the siSix1-B duplex, the Six1-resistant cell line is incapable of rescuing the proliferation defect as was shown in Figure 21. This inability to rescue the treated myoblasts suggests that siSix1-B had off-target effects affecting cell-cycle proliferation. This is a further call for concern as early experiments, namely gene expression profiling and *in vivo* intramuscular siRNA injection, were performed using siSix1-B, exclusively. Therefore, in order to develop a more accurate reflection on the impact of Six1 downregulation on global gene expression, expression profiling must be repeated with the siSix1-A duplex. In spite of this, Six1 regulation of the cell cycle appears to be reliable: knockdown of Six1 mediated by either siRNA yields consistent down-regulation of cell cycle gene regulators and decreased proliferation as assessed by crystal violet assay and qRT-PCR in Figures 22 and 23. Furthermore, the pro-proliferative effects of Six1 are reinforced through the over-expression C2C12 myobast cell lines exhibiting increased proliferation.

Secondly, the findings of this study in primary myoblasts and C2C12 myoblasts confirm previous findings by other groups, but contradict others. For example, the study by Li and colleagues found that impaired Six1 expression or function in proliferating C2C12 myoblasts resulted in decreased proliferation (Li et al., 2003). Previous genome wide analysis of Six1 by ChIP-on-chip and gene expression profiling in C2C12 myoblast has hinted of a role for Six1 in the regulation of cell proliferation: Six1 predicted targets were enriched for proliferation (Liu et al., 2010). Furthermore, as

touched upon in the introduction, Six1 over-expression has been implicated in many different cancers playing roles in the proliferation of cancer cells such as in breast, rhabdomyosarcoma, colorectal, and pancreatic (Reichenberger et al., 2005, Yu et al., 2006, Ono et al., 2012, Li et al., 2013). In contrast, Yajima and colleagues found that knock-down of Six1 led to no significant changes in primary myoblast proliferation (Yajima et al., 2010). They showed that downregulation of Six1 mediated by siRNA had no effects on myoblast proliferation at 48 hours after transfection. It is critical to highlight the time of harvest of 48 hours. With the present study, a proliferative phenotype is not observed until 72 and 96 hours after transfection. Despite effective depletion of Six1 protein and mRNA expression 48 hours after transfection, this is not enough time for a discernable difference in cell density to be observed: the growth curves from the present work similarly show no significant difference in myoblast proliferation at 48 hours after transfection. Yajima and colleagues go on to show that transient over-expression of Six1 in primary myoblasts displayed decreased propensity to proliferate as determined by Ki67 and phosphorylated histone H3. This would suggest that Six1 possesses anti-proliferative properties. The Ki67 antigen marks cells in a proliferative state (outside of G0) and phospho-H3 marks cells in mitosis (Gerdes et al., 1984; Gurley et al., 1978). In both cases, less Ki67 or phospho-H3 staining in the Six1 over-expressing cells suggests decreased proliferation however it does not directly quantify cellular proliferation and whether the cells may be proliferating faster or slower. Ki67 and phospho-H3 staining function as a snapshot of the proliferative potential of the cells and suggests less proliferation but it does not provide information regarding any changes in proliferation rates.

At the same time, the phenotype observed by Yajima may not necessarily be a contradiction. Instead it may point to the importance of basal Six1 levels: imbalance or misregulation of Six1 may result in proliferative defects through unique pathways. Although the present study showed that stable over-expression of Six1 in C2C12 myoblasts yielded greater proliferation compared to the control, it is critical to note that primary myoblasts are different than C2C12 myoblasts. These differences are touched upon when analyzing the next paper that investigated a role for Six1 in myoblast proliferation. Furthermore, Yajima and colleagues utilized transient over-expression whereas the present study generated a stable cell line. There could be differences in the degree of over-expression as well as possible off-target effects due to the sequence of the transgene and viral components used.

This anti-proliferative effect associated with Six1 was similarly observed where it was shown that C2C12 myoblasts stably overexpressing Six1 displayed decreased proliferative potential determined by cell viability assays (Wu et al., 2013). First and foremost, Wu and colleagues evaluated the role of Six1 and proliferation exclusively in the immortalized C2C12 myoblast cell lineage. C2C12 myoblasts have a number of mutations making them different from primary myoblasts. In particular is the loss of p19ARF: a protein translated from the alternate reading frame of the INK4a/ARF locus. p19ARF functions to prevent cell cycle progression through blocking MDM2 mediated inhibition of the tumor suppressor p53 (Chin et al., 1998). Downstream, p53 induces p21CIP1 expression thereby causing cell cycle arrest through inhibition of the Cyclin D-dependent kinases Cdk4/6. It is also interesting to note that the other product of the INK4a/ARF locus, p16INK4a, functions to inhibit Cdk4/6 (Serrano et al., 1993). As

such, attempts to study cell cycle regulation and myoblast proliferation should not be performed exclusively in C2C12. Secondly, it is concerning with regards to how Wu and colleagues set out to evaluate the proliferation of cells. The authors indicate that 10,000 cells were seeded in wells of 96-well plate and assessed for proliferation using an MTT assay to measure cellular metabolic activity: rapidly dividing cells will generate greater MTT output. This is far too many cells for the provided growth area (0.32 cm^2). For comparison, the present study seeded 5,000 cells onto a growth area of 1.9 cm^2 and cells reached 100% confluence close to 96 hours after seeding. Cells seeded as described by Wu and colleagues are likely to achieve full confluence quickly, become growth impaired by contact inhibition, enter a state of quiescence and begin to differentiate. Additionally, Wu and colleagues fail to provide error bars, the effect is mild and there is no statistical test information provided suggesting the phenotype was not significant for the eight shown replicates.

To better investigate the effects of Six1 on proliferation rates and lengths of the cell cycle phases, BrdU and 7-AAD staining was performed in growing primary myoblasts and subsequently analyzed by flow cytometry. However, results appeared inconclusive. Knockdown by siSix1-A specifically decreased the number of myoblasts in S-phase at 48 hours after transfection, though knockdown by siSix1-B was near significant. This suggests that Six1 is important for proliferation through entry into S-phase. Furthermore, the previously observed effect in the crystal violet assays are unlikely to be a question of cell survival as the relative number of sub-G1 cells (apoptotic cells) remained consistent across all conditions. This effect of Six1 knockdown on S-phase entry of primary myoblasts is interesting though it does not

provide any information regarding proliferation rates. In order to better assess the effect of Six1 on proliferation rates, it would be possible to determine the length of time required for one cell division by performing a pulse-chase-pulse experiment. In such an experiment, siRNA treated cells would be pulsed with EdU for a short duration and rinsed of excess EdU. Following the EdU pulse, cells would be pulsed with BrdU at various time points after the initial EdU pulse. Cells would then be assessed for double EdU and BrdU staining and the minimum amount of time required for double EdU/BrdU stained cells would give an approximation of the time required for a cell to proceed through two rounds of S-phase, or two complete rounds of the cell-cycle. If Six1 downregulation increases the length of the cell cycle phases, the time required in order to observe double EdU/BrdU positive cells would be larger compared to the control. This is a strategy that has been used by other studies (Schorl and Sedivy, 2007; Weber et al., 2014).

3.2. The pro-proliferative effects of Six1 expression in vivo

This study continued by trying to determine if the pro-proliferative *in vitro* effects could also be observed *in vivo*. In fact, the intramuscular injection of Six1 siRNA results in a decreased number of satellite cells expressing high levels of the proliferation marker Ki67 four days after injury. This protocol had been adapted from a study in which Pax3/7BP siRNA was delivered *in vivo* in order to assess the proliferation potential of myogenic precursor cells at postnatal day 12 (Diao et al., 2012). After three siRNA injections at postnatal days 6, 8 and 10, Diao and colleagues observed a 40% reduction in Pax7 mRNA. The same protocol has also been utilized to examine the effects of Six4 siRNA intramuscular injection four days after injury (Chakroun et al.,

2015). The present study observed that Six1 siRNA injected mice showed no differences in the absolute number of satellite cells though there was a 10% decrease in the number of Ki67 highly expressing satellite cells. This decreased Ki67 expression suggests decreased proliferative potential of satellite cells after injury. However, it is a bit paradoxical that there are less Ki67 positive cells without a decrease in the total number of satellite cells. It is possible that harvesting the muscles 4 days after injury is too early to see a change in the number of satellite cells. Though this is a modest effect, it can possibly be explained by the limitations of the experiment. Intramuscular injection of siRNA provides unknown efficiency, which could be low siRNA uptake by the satellite cells thus providing a less robust phenotype: the same protocol only yielded a 20% reduction in Six4 mRNA expression across all cells from a mouse muscle lysate (Chakroun et al., 2015). If greater efficiency of Six1 knock-down in satellite cells could be achieved or if satellite cells could be isolated from conditional Six1 knock-out mice, a more profound effect may be observed.

Initially, experiments were run to assess the efficacy of an intramuscular siRNA injection protocol; what is the proportion of satellite cells receiving the siRNA after injection? Three assays were performed with negative or inconclusive results. All three assays involved the intramuscular injection of a red-fluorescent siRNA control into an injured TA muscle of a mouse. The first assay utilized immunofluorescence and microscopic imaging in order to assess red-fluorescence uptake in satellite cells however no fluorescence signal beyond background signal was detected in the red channel. The second and third assays were instead repeated in the TA muscles of zsGreen-Pax7 mice, genetically modified mice in which satellite cells (Pax7 positive cells) would express a

green fluorescence marker (Bosnakovski et al., 2008). Four days after injury, mice TA muscles were isolated, digested, and processed by either flow cytometry or mounted for fluorescent microscopic analysis. In both cases, signal from the green channel was so strong that it spilled over into the red channel making quantification impossible. In order to tackle the question of siRNA knockdown efficiency in satellite cells, cell sorting can be performed to isolate satellite cells for analysis of Six1 mRNA expression by qRT-PCR. However, this would not answer the question of how many cells have taken up the siRNA; single-cell qRT-PCR would be required. To truly determine siRNA uptake through intramuscular injection, a more sensitive method to detect the injected siRNA must be performed. For example, biotinylated siRNA combined with streptavidin may provide adequate signal amplification in order to be detected by microscopy.

Previously, it was shown that Six1 expression in satellite cells is required for normal muscle regeneration: loss of Six1 resulted in smaller myofibers after injury (Le Grand et al., 2012). However, Le Grand and colleagues go on to state that Six1 gene disruption had no effect on satellite cell proliferation, though it is important to note the differences of the experimental timelines. In the present study, Six1 expression was targeted following muscle injury whereas Le Grand and colleagues elicit no injury prior to Six1 gene disruption. The muscle injury leads to the activation and cell cycle entry of satellite cells as well as to upregulate the expression of Six1 (Liu et al., 2013). This suggests that Six1 plays a role in the proliferative response after satellite cell activation. Le Grand and colleagues do go on to disrupt Six1 expression after injury; however with key differences from the present study. They impaired Six1 expression starting at 7 days after injury and they examined the effects on satellite cells 30 days after injury. It has

been shown that the proliferation of satellite cells peaks at 4 days after injury and begins to decrease by 7 days after injury; 30 days after injury, the majority of satellite cells have returned to a state of quiescence (Liu et al., 2013, Shea et al., 2011). As such, this assay provides insight to a role for Six1 in satellite cell return to quiescence instead of satellite cell proliferation. The various elements of evidence obtained in the present study suggests that Six1 downregulation immediately after injury impairs satellite cell proliferation and Le Grand and colleagues data show that loss of Six1 once satellite cells have completed their intense bout of proliferation prevents their return to quiescence. Therefore, Six1 would play multiple roles during regeneration. In the early phase, Six1 is needed for satellite cell proliferation (this work). In the later phases, Six1 would instead be needed for the return of satellite cells to quiescence (the work of Le Grand and colleagues)

3.3. A role for Six1 in the transcriptional regulation of the cell cycle

Previous genome wide analysis of Six1 by ChIP-on-chip and gene expression profiling in C2C12 myoblast has revealed that there may be a role for Six1 in the regulation of cell proliferation (Liu et al., 2010). C2C12 myoblasts provide an excellent model for the study of myogenesis, however their mutation causing immortality becomes concerning with studies regarding cellular proliferation. In the present study, gene expression profiling performed on primary myoblasts revealed that Six1 knock-down is associated with the downregulation of numerous cell cycle regulators. Both the clustering combined with functional gene ontology and the GSEA analysis indicate that knockdown of Six1 is associated with decreased expression of numerous cell cycle genes including Ccna2, Ccnb1, Ccnd1, Cdk1, Foxm1, Mybl2, and Plk1. Furthermore,

Six1 ChIP-Seq performed by another student in the lab has demonstrated that a number of these cell cycle genes are directly bound by Six1. Gene expression analysis performed in primary myoblasts as opposed to immortalized C2C12 myoblasts provide a more relevant data set that is more directly transferable to clinical applications. Regardless, the combination of the genomic data from C2C12 myoblasts and the present data provides greater confidence in a link between Six1 and the regulation of the cell cycle in adult muscle precursor cells.

3.4. Six1 regulates Ccnd1 expression

Six1 may regulate the expression of many genes that can control cell proliferation. One gene that stands out as an interesting target for Six1-mediated cell cycle regulation is Ccnd1. Six1 and Ccnd1 have previously been linked in numerous cancers: in mouse rhabdomyosarcoma, Six1 binds the Ccnd1 proximal gene promoter and drives its expression (Yu et al., 2006); in human pancreatic cancer, downregulation of either Six1 or Ccnd1 decreased proliferation to the same extent (Li et al., 2013). Furthermore, roles for Ccnd1 in myoblasts have been reported. Effective downregulation of Ccnd1 by Brm is required for myoblast arrest prior to myogenic differentiation (Albini et al., 2015). Pitx2 increases myoblast proliferation by down-regulating a group of microRNAs that target Ccnd1 (Lozano-Velasco et al., 2015). Furthermore, Pitx2 in complex with HuR functions to stabilize Ccnd1 mRNA during myoblast proliferation and this stabilization is impaired by Akt2 mediated phosphorylation of Pitx2 prior to myoblast differentiation (Gherzi et al., 2010). Together, these studies suggest that Ccnd1 has a role in myoblast proliferation which is in opposition to an established role of Ccnd3 in myoblast differentiation (Cenciarelli et al., 1999; Gurung et al., 2012). As

such, the previously reported connection of Six1 and Ccnd1 together with the pro-proliferative role of Ccnd1 in myoblasts labels Ccnd1 as a highly appealing candidate for further study.

The timeline of myogenic differentiation demonstrates a temporal overlap in the expression of Six1 and Ccnd1 suggesting parallel roles during myogenesis. Specifically, Six1 and Ccnd1 expression are highest in growing cells and low in differentiating cells. Furthermore, it appears that Six1 functions upstream of Ccnd1 as Six1 binds the Ccnd1 gene and the downregulation of Six1 results in decreased Ccnd1 mRNA and protein expression. Most interestingly, rescue of Ccnd1 expression after Six1 knockdown is sufficient to rescue the cell cycle phenotype. Furthermore, over-expression of Ccnd1 is capable of eliciting increased cell proliferation. However, similar to the issues during Six1 rescue after Six1 knockdown, Ccnd1 expression is incapable of rescuing the siSix1-B knockdown. Again, this suggests that the siSix1-B RNA duplex has off-target effects, and that probably at least one off-target mRNA codes for a positive regulator of the cell cycle. Regardless, the rescue of siSix1-A by either Six1 or Ccnd1 expression suggest that Ccnd1 may be the limiting factor in the Six1/Ccnd1/cell cycle pathway during myoblast proliferation. It would be interesting to investigate if greater over-expression of Ccnd1 could further increase myoblast proliferation.

Although Six1 binding is observed in the 3' UTR of the Ccnd1 gene, it is not known if Six1 is serving any function here. Furthermore, analysis of a multitude of ChIP-Seq datasets (not shown) reveals that this region of the Ccnd1 gene bound by Six1 is not accompanied by features of gene regulatory regions, such as high histone methylation or acetylation, binding of RNA polymerase II, or binding by the

transcriptional co-activator p300 (Asp et al., Blum et al., 2012). Perhaps more interesting is a locus 173 kb upstream of the Ccnd1 promoter. This region is enriched in histone marks associated with enhancers: H3K27ac, H3K4me1; similarly this region is bound by RNA polymerase II, the acetyltransferase p300, the transcription factor c-Jun along with Six1 and MyoD (Blum et al., 2012; Encode Project Consortium, 2012). Furthermore, these transcriptional marks were greater in growing myoblasts compared to differentiated myotubes. Preliminary qChIP data suggests this genomic locus is enriched for Six1.

In the case of both the Ccnd1 3' UTR locus and the 173 kb enhancer, to evaluate Six1 transcriptional activity from these loci would require a transcriptional activity assay. Cloning these loci upstream of the reporter gene luciferase would yield information regarding the transcriptional output of these putative gene regulatory elements. Two approaches can be taken to examine the activity of Six1 on such reporter constructs at these loci. First, Six1 downregulation by siRNA-mediated knock-down would reveal if Six1 expression is required for reporter gene transcription. Second, mutation of the Six1 binding sites within the reporter constructs would tell us if the direct binding of Six1 on these genomic elements is needed for transcription.

To further cement the role of Ccnd1 during myoblast proliferation, it would also be prudent to impair Ccnd1 expression by siRNA and observe the effects on the cell cycle. It is predicted that knockdown of Ccnd1 would phenocopy the Six1 siRNA phenotype, however this may not necessarily be the case. On one hand, Ccnd1 knockdown may not be as robust as Six1 knockdown because Six1 appears to regulate the expression of other cell cycle genes thus the downregulation of Ccnd1 alone may

yield a milder effect on myoblast proliferation. However, it is also possible that Ccnd1 knockdown may yield an even greater phenotype than Six1 downregulation. If Ccnd1 is the limiting factor in the Six1 mediated cell cycle phenotype, its direct impairment by siRNA could result in a more robust arrest in myoblast proliferation. Finally, *in vivo* analysis of Ccnd1 expression after Six1 downregulation in satellite cells would be important in order to demonstrate the consistency of Six1 mediated regulation of Ccnd1 within satellite cells in the context of regeneration in the TA muscle. Similarly, repeat assays involving the intramuscular injection of Ccnd1 specific siRNA after injury would be important to demonstrate the role of Ccnd1 during satellite cell proliferation.

3.5. Extending the Six1-Ccnd1 link to clinical applications

In the introduction, it was proposed that Six1 is a highly appealing target for the long-term therapeutic efficiency of stem cell therapy in DMD due to its varied roles during the life cycle of myogenic precursor cells. As it now stands, stem cell therapy is limited by insufficient material for transplantation (the challenge to grow enough cells *in vitro* for transplantation) and the transient effect of treatment (the challenge to prevent the premature differentiation of satellite cells immediately after transplantation). To overcome this, a large expansion of satellite cells must be achieved in culture and the transplanted satellite cells must be able avoid differentiation and instead return to quiescence to repopulate the stem cell niche. The genetic manipulation of Six1 may very well be capable of addressing both of these concerns. The present study has demonstrated the pro-proliferative effect of Six1 expression in proliferating myoblasts *in vitro* and this effect mediated through the regulation of the cell-cycle regulator Ccnd1. Isolated donor cells can be forced to overexpress Six1 thereby maximizing stem cell

numbers for therapeutic use. However, prior to transplantation, Six1 expression must be decreased in order to favour self-renewal as the loss of Six1 expression in satellite cells has shown to increase niche occupancy and the absolute number of satellite cells after injury (Le Grand et al., 2012). This last step is critical in order to ensure the transplanted cells are readily available for future regeneration. Overall, Six1 is an exciting target for the enhancement of DMD cell therapy, but a still greater understanding of Six1's mode of action is required in order to extend this biochemical knowledge towards clinical applications.

4. Chapter 4 - Materials and Methods

4.1. Animal Work (in vivo mice)

36-52 days old female C56BL/6 underwent muscle injury of the tibialis anterior by Cardiotoxin (Latoxin cat: L8102) injection and subsequently received two rounds of siRNA injection: first injection 6 hours after injury, second injection 48 hours after injury. Injection mix contained a pool of 3 µL siRNA, Lipofectamine RNAiMAX, and Opti-Mem. 96 hours after injury, mice were sacrificed by cervical dislocation and tibialis anterior muscles were isolated.

4.2. Immunostaining on Paraffin Sections

4.2.1. Muscle Tissue Processing and Sectioning:

Extracted TA muscles were fixed in cold PBS-2%PFA for 30 minutes at 4C on a rocker. Following fixation, muscles were rinsed 2x5 minutes in cold PBS and subsequently quenched 2x10 minutes with 0.25M glycine in PBS on ice on a rocker. The TA muscles were then transferred into 70%EtOH and sent to Pathology department for paraffin embedding. Paraffin blocks were trimmed on microtome cutting cross-sections at 4 microns near the centre of the muscle. The slides were baked overnight at 37°C and then deparaffinized with 3x10 minutes Xylene, 2x5 minutes 100% EtOH, 1 minute 95% EtOH, 1 minute 80%EtOH, 1 minute 70% EtOH, then distilled water.

4.2.2. Antigen Retrieval:

Slides were immersed in pre-warmed jars of 10mM Citrate Buffer-0.05%Tween 20 pH 6.0 in a water-bath between 95°C and 98.5°C for 20 minutes. Slides were then cooled (still in buffer) outside the water bath for 20 minutes.

4.2.3. Slide Preparation – Permeabilization/Blocking:

Circles were drawn around muscle sections with hydrophobic pen and sections were rinsed with PBS-0.1%Triton for 3 quick washes. Sections were permeabilized with PBS-0.5%Triton for 10 minutes at room temperature with 3 quick washes with PBS-0.1% triton. Finally, sections were blocked with PBS-0.1%Triton-3%BSA-5%Goat Serum for 1 hour at room temperature (or overnight at 4°C).

4.2.4. Antibody staining:

Sections were incubated with Primary Antibody (Pax7b from DSHB – 1:100, Ki67 from Abcam – 1:50 dilutions) in PBS-0.1%Triton-3%BSA-5%Goat Serum for 1 hour at room temperature. Sections were rinsed with PBS-0.1%Triton for 3 quick washes, then 3x5 minute washes. Next, sections were incubated with Secondary Antibody in PBS-0.1%Triton-3%BSA-5%Goat Serum for 30 minutes at room temperature and subsequently rinsed with PBS-0.1%Triton for 3 quick washes, then 3x5 minute washes.

4.2.5. Slide Post-Processing/Mounting:

Sections were rinsed with PBS, then water, then 70%EtOH and incubated with 0.3% Sudan Black-70% EtOH for 10 minutes to reduce fat-tissue auto fluorescence. Sections were rinsed with PBS until no precipitate from the Sudan Black step was observed then rinsed with water. Antifade-DAPI reagent was applied and cover slips

mounted. Sections were cured for 24 hours horizontally at room temperature prior to taking pictures.

4.3. Cell Culture Work

20-24 week old female C57BL/6 mice were sacrificed by cervical dislocation and both sets of gastrocnemius, quadriceps, and tibialis anterior muscles were isolated and placed in PBS on ice. Muscle fragments were pulled apart longitudinally using tweezers, pooled and transferred to a freshly prepared collegenase solution for digestion at 37°C over 2-2.5 hours. The 0.2% Collegenase I (Sigma) in DMEM (ATCC) with Dispase II (Roche) added at a final concentration of 0.625 μg/mL was sterilized by syringe filtration prior to mice sacrifice. Muscle fragments were triturated every 20 minutes by 10mL pipette and until the muscle fibres completely dissociated. Digested muscle were passed through a 0.75μm nylon mesh filter (BD Falcon) to remove undigested connective tissue. Cells were then rinsed twice with DMEM and then resuspended in plating medium: 89% DMEM, 10% donor equine serum (DES, HyClone), 10 units Penicillin/Streptomycin (P/S, Gibco) and 5 ng/mL bFGF (Peprotech). Cells were pre-plated twice on 10 cm plastic dishes (Corning) to remove fast-attaching fibroblasts. Non-adhering cells were then transferred to Matrigel (BD Biosciences) treated plastic dishes and allowed to adhere and grow for 48 hours. Following this, cells were passaged and switched to primary growth medium (pGM): 69% DMEM, 20% Fetal Bovine Serum (FBS, HyClone), 10% DES, 10 units P/S, 2 ng/mL HGF (Peprotech) and 10 ng/mL bFGF (Peprotech). Medium is changed daily past this point. To induce differentiation, cells approaching confluence were switched to

differentiation medium (DMEM supplemented with 10% horse serum and 1% Penicillin/Streptomycin).

The C2C12 murine myoblast cell line was obtained from the American Type Culture Collection (ATCC). Cells were grown in growth medium (GM): DMEM supplemented with 10% FBS, 1% Glutamine stock solution and 1% Penicillin/Streptomycin.

The Phoenix Eco packaging cells (modified 293T cells) were obtained from. Cells were grown in growth medium (GM): DMEM supplemented with 10% FBS, 1% Glutamine stock solution and 1% Penicillin/Streptomycin.

4.4. Lipofectamine and siRNA Transfections

Transfections were performed using Stealth siRNA technology (Invitrogen) and Lipofectamine RNAiMAX (Invitrogen). siRNA duplexes were suspended and diluted as described by the manufacturer to a final concentration of 20 μM. siRNA sequences are available in Table S5. For a 6 well-plate, 3 μL of siRNA was suspended in 100 μL OptiMEM (Invitrogen) and 5 μL Lipofectamine was suspended in a separate 100 μL OptiMEM. The Lipofectamine mix was added to the siRNA mix and incubated at room temperature for five minutes. Following the incubation, 200 μL of the Lipofectamine-siRNA mix was added dropwise to adherent cells in 2 mL growth medium.

4.5. Polyethyleneimine (PEI) Plasmid Transfections

For a 10 cm dish, 10.5 μg of DNA was mixed with 32.5 μL 1.5M NaCl and topped up to 325 μL with serum free media (unsupplemented DMEM). In a separate

tube, 116 µL 1µg/µL PEI (Polysciences) was mixed with 32.5 µL NaCl and 176.5 µL serum free media (scaled up for each DNA tube) and incubated for 5 minutes at room temperature (RT). The appropriate volume of PEI mix was added to each DNA tube and incubated for 20 minutes at RT. During this incubation, cells are refed with 20 mL GM. The PEI-DNA mix was added to the cells dropwise and incubated for 24 hours.

4.6. RNA Extraction

RNA was extracted from cells using TRIzol Reagent (Invitrogen). Cells were rinsed twice with PBS and lysed with 500 µL of TRIzol. Cell lysates were transferred to Eppendorf tubes and allowed to incubate at room temperature for five minutes. Following incubation, 100 µL of chloroform was added to lysates and samples were vortexed for 15 seconds and incubated at room temperature for three minutes. The samples were centrifuged at 12000g for 15 minutes at 4°C. Following spin-down, three phases are observed: aqueous phase, interphase, and organic phase. The aqueous phase contains RNA and is transferred to a new tube. The interphase and organic phases contain DNA and protein, respectively, and are put aside for protein extraction. The RNA was precipitated from solution by adding 250 µL of isopropanol, vortexed for 10 seconds and allow to incubate for 10 minutes at room temperature. Following this, samples were centrifuged at 12000g at 4°C for 10 minutes. Pellets were washed twice with 70% ethanol with centrifuge performed between washes at 7500g for five minutes at 4°C. RNA pellet was resolubilized in 20 to 30 µL of DEPC-treated water.

4.7. Protein Extraction

Interphase and organic phases of TRIzol extract undergo further processing for protein extraction. 300 µL of 100% ethanol is added to the organic and interphase and mixed by gentle inversion five times. Samples were incubated for three minutes at room temperature and centrifuged at 2000g for five minutes at 4°C. Supernatant was transferred to a new tube and supplemented with 1.5 mL of 100% isopropanol. Samples were then vortexed, incubated for 20 minutes at room temperature, and then centrifuged at 12000g for five minutes at 4°C. Pellets were washed three times and rocked for 30 minutes at room temperature with 1.5 mL guanidine-ethanol: 28.5g guanidine-HCl in 950 mL ethanol and 50 mL water. Pellets were then washed twice with 1.5 mL 100% ethanol and rocked for 5 minutes at room temperature. Between all washes, pellets were centrifuged at 7500g for 5 minutes at 4°C. Protein pellet was resolubilized in 100 µL urea-SDS buffer: 6M urea, 1% SDS, 20mM Tris pH 6.8. Protein was allowed to resolubilize for a minimum of 10 hours.

4.8. Retrovirus Preparation and Infections

4.8.1. Cloning:

Protein coding sequences corresponding to luciferase, Six1, or Ccnd1 were cloned with an HA-tag and amplified by PCR on a PX2 thermal cycler. Primers used are described in the Appendix in Table S5. Following PCR, products were ran on 1% agarose gel and cleaned up using a DNA Gel Extraction Kit (Axygen). After gel clean-up, samples were digested for ligation into pBabe-puro using FastDigest enzymes (ThermoFisher). Ligation was carried out for 1 hour at room temperature using T4 DNA Ligase (ThermoFisher) and transformed into DH5alpa competent cells (Invitrogen) and plated overnight at 37°C. Mini-preps were performed on EZ-10 Spin Columns

(BioBasic) and subsequently digested to screen for positive colonies prior to sequencing. Positive colonies were selected, re-transformed and amplified for large preps performed on EndoFree Plasmid Kits (Qiagen).

4.8.2. Retrovirus Preparation:

pBABE-puro vectors expressing luciferase, Six1 or Ccnd1 were transfected into Phoenix-Eco retroviral packaging cells by the PEI transfection method. 24 hours after transfection, the Phoenix cells were refed with growth medium and virus containing media was collected at 48, 60, and 72 hours post-transfection. Virus supernatants were then filtered through a 0.2 µM PVDF low-protein membrane and aliquot for freezing at -80°C or for immediate infection.

4.8.3. Retroviral Infection:

Infection mix was prepared combing 1mL virus supernatant with 1mL GM and 4 uL Polybrene. The entirety of the mix was added to C2C12 myoblasts. 48 hours after transfection, cells were split and maintained in growth medium supplemented with 2 µg/ml puromycin. Cells were selected for 48-72 hours and then maintained in 0.5 µg/ml puromycin.

4.9. Protein Quantification Assay

Protein concentration was quantified using Pierce BCA Protein Assay Kit (Thermo Scientific). Provided bovine serum albumin (BSA) was diluted to 0, 250, 500, 100 and 2000 ng/µL in water as a standard curve. Samples were done in duplicate and points of the standard curve were done in triplicate using a 96-well plate (Corning). The reaction was performed as follows: 2 µL of sample was mixed with 8 µL water whereas

2 µL of each standard was mixed with 6 µL water and 2 µL urea-sds buffer. BCA reagent A and B were mixed at a ratio of 50:1 and 160 µL of the mix was added to each sample or standard. The plate was incubated for 30 minutes at 37°C and quantified by spectrophotometer reading at 562 nm.

4.10. Western Blot Analysis

15 to 20 µg of protein were loaded on a 10% SDS-PAGE as previously described. The proteins were transferred from the SDS-PAGE to a polyvinylidene fluoride (PVDF) membrane (Millipore) following an established protocol. Detection of the proteins were accomplished using conjugated horseradish peroxidase (HRP) coupled with a mouse or rabbit specific antibody. HRP presence was detected using a homemade revelation kit. The four components included 90 mM coumaric acid dissolved in DMSO, 250 mM 3-aminophtalyhydraize free azide (luminol) dissolved in DMSO, hydrogen peroxide and 0.1 M Tris pH 8.5. 5 mL of Tris was mixed with 3 µL of hydrogen peroxide and a separate 5 mL of Tris was mixed with 25 µL coumaric acid and 50 µL luminol. Each mix was agitated separately, combined and incubated with membranes for 30 seconds. Antibodies used and dilutions can be found in Table S6.

4.11. Crystal violet growth assay

Cells were transfected with siRNA and split into four 24-well plates 24 hours after transfection. Cells were seeded at 15,000 cells per well in duplicate and harvested at 4, 24, 48 and 72 hours after the split. At time of harvest, cells were rinsed twice with 1X PBS and fixed at room temperature for 10 minutes with formalin. Cells were again rinsed with PBS then stained with 0.01% crystal violet (w/v) dissolved in water for 10

minutes. Cells were rinsed with water and allowed to dry for five minutes and then resuspended in 0.1% SDS and quantified by spectrophotometer reading at 595 nm.

4.12. BrdU and Flow Cytometry

At 47 hours after transfection, primary myoblasts were pulsed with BrdU for 1 hour and harvested according to manufacturer's protocol for the BD Pharmingen FITC BrdU Flow Kit. Cells were fixed, permeabilized, and stained according to the manufacturer's protocol. Cells were analyzed by flow on the Cyan ADP9 Analyzer and data was extracted using Kaluza Flow Cytometry Analysis software.

4.13. RT-PCR

Reverse transcription PCR (RT-PCR) was performed on 1000 ng RNA using the SuperScript First-Strand Synthesis System (Invitrogen). PCR reactions were performed on a thermocycler. RNA in a total volume of 5 µL was mixed with 1 µL of 10 mM dNTP, 1 µL of random hexamers, and 3 µL of water. Samples were incubated at 65C for five minutes and immediately transferred to ice for two minutes. Added to the samples were 9µL of buffer mix: 2 µL of 10X reaction buffer, 4 µL of 25 mM $MgCl_2$, 2 µL of 0.1 M DTT, 0.5 µL of RNase OUT (50 units/µL) and 0.5 µL of water. Samples were incubated at 25°C for two minutes and then supplemented with 0.5 µL of SuperScript II (50 units/µL) or 0.5 µL of water (no RT control) and incubated sequentially at 25°C for 10 minutes, 42°C for 50 minutes, 70°C for 15 minutes. Following this, 0.5 µL of RNase H was added and samples were incubated at 37°C for 20 minutes. Samples were topped up with 30 µL 10mM Tris pH 8 and stored at -20°C

4.14. qPCR and qChIP

Quantitative PCR (qPCR) was performed on the Mx3000P platform and MxPro software (Stratagene) using a SYBR green quantification strategy. The components for a 10 µL reaction are as follows: 2 µL of sample cDNA diluted 1:10 in 10 mM Tris pH 8, 1 µL 5 µM primer pair (Operon), 1 µL 10X Buffer (Qiagen), 1 µL of 1.5% Trixton X-100 (Fisher), 0.2 µL of 10 mM dNTP (Fisher), 0.3 µL of 3 µM ROX Reference Dye (Invitrogen), 0.05 µL of SYBR Green diluted 1:500 in DMSO (Invitrogen), 0.04 µL of HotStart TAQ (Qiagen) and 4.41 µL of water. Standard curves and samples were performed in duplicate. Quantitative ChIP PCR was performed using the same quantification strategy and recipe with small differences. 1 µL of sample DNA was used and 5.41 µL of water (everything else the same). Standard curves ranged from 10% to 0.01% DNA input. Oligonucleotide primer sequences are provided in appendix Table S5. GEOMEAN normalization was performed using multiple control genes (Rps26, Rplp0, Tbp).

4.15. Gene Expression Profiling

4.15.1. Forward and reverse transcription:

One-color microarray-based gene expression analysis was performed using the Agilent Low Input Quick Amp Labeling Kit with 100 ng starting RNA according to the manufacturers protocol. An RNA Spike-In Kit was used wherein 2 µL of 1:10,000 Spike Mix was mixed with 1.5 µL starting RNA. 1.8 µL of T7 Primer Mix was added to the RNA: 0.8 µL of T7 primer and 1 µL of nuclease free water. The primer and template were denatured for 10 minutes in a 65°C water bath and immediately transferred to ice for five minutes. 4.7 µL of freshly prepared cDNA Master Mix was added to each sample tube: 2 µL of 5X First Strand Buffer, 1 µL of 0.1 M DTT, 0.5 µL of 10 mM

dNTP and 1.2 µL of Affinity Script RNase Block Mix. The samples were incubated in a 40°C water bath for 2 hours and transferred to a 70°C water bath for 15 minutes to stop the reaction. Sample tubes were then transferred to ice for five minutes. 6 µL of freshly prepared Transcription Master Mix was added to each sample tube: 0.75 µL nuclease free water, 3.2 µL of 5X Transcription Buffer, 0.6 µL of 0.1M DTT, 1 µL of NTP mix, 0.21 µL of T7 RNA Polymerase Blend and 0.24 µL of Cyanine 3-CTP. The samples were incubated in a 40°C water bath for 2 hours protected from light.

4.15.2. cRNA Clean-up:

Labeled/amplified RNA were purified using the RNeasy Mini Kit (Agilent) according to the manufacturer's protocol. 84 µL of nuclease-free water was added to each cRNA sample (16 µL) along with 350 µL Buffer RLT and 250 µL of 100% ethanol and mixed thoroughly by pipetting. The total 700 µL sample was transferred to an RNeasy Mini Spin Column and spin using table top centrifuge at 4°C for 30 seconds at 13,000g. The flow-through and collection tube were discarded. Using a fresh collection tube, cRNA was washed two times with 500 µL Buffer RPE (containing ethanol) with spins at 4°C for 30 seconds at 13,000g. The flow-through were discarded after both washes. A final spin at 4°C for 30 seconds at 13,000g was performed to remove any remaining traces of Buffer RPE. Using a new collection tube, cRNA was eluted by adding 30 µL of RNase-Free water directly onto the RNeasy filter membrane. After 60 seconds, the samples were centrifuged a final time at 4°C for 30 seconds at 13,000 rpm. The yield and specific activity of cRNA were quantified using the NanoDrop ND-1000 UV-VIS Spectrophotometer version 3.2.1. Specific activity is defined as the pmol Cy3 per µg cRNA.

4.15.3. Hybridization:

In order to prepare samples for hybridization, 600 ng of Cy3 labeled cRNA was combined with 5 µL of 10X Gene Expression Blocking Agent and 1 µL 25X Fragmentation Buffer up to a final volume of 25 µL with nuclease free water. The fragmentation reaction was incubated at 60C for 30 minutes and immediately transferred to ice for one minute. In order to stop the fragmentation reaction, 25 µL of 2X Hi-RPM Hybridization Buffer was added. Samples were mixed well by careful pipetting to avoid introducing bubbles. From the 50 µL of hybridization sample prepared, 40 µL was loaded into each gasket well of an 8-pack Agilent SureHyb chamber base. The Agilent SurePrint G3 8x60K mouse platform array was assembled into a clamp assembly chamber and incubated in a hybridization oven pre-warmed to 65C and set to rotate at 10g for 17 hours.

4.15.4. Microarray Washing and Scanning:

Microarrays were washed using Gene Expression Wash Buffer 1 and 2 supplemented with 0.005% Triton X-102 (Wash Buffer 2 was warmed at 37°C overnight). Washes and disassembly were performed in slide-rack staining dishes. The microarray-gasket sandwich were disassembled in Wash Buffer 1, washed in Wash Buffer 1 at room temperature for one minute and subsequently washed in Wash Buffer 2 at elevated temperature for one minute. Microarray slides were transferred to slide holders and analyzed using the Agilent G4900DA SureScan Microarray Scanner System.

4.16. Bioinformatics Analysis

4.16.1. Agilent Feature Extraction 11.5.1.1

Scanned microarray images were processed for analysis with Agilent Feature Extraction using default parameters. Extraction set configuration utilized Grid Name "028005_D_F_20131202" and Protocol Name "GE1_1105_Oct12".

4.16.2. Perl Script Filtering

Exported gene expression data reports were processed and filtered using a Perl Script to cull missing or absent probes based user input settings. Probes which were not expressed in 50% of the arrays regardless of condition were culled. Furthermore, Perl scripting annotated probe IDs using Gene Expression Omnibus (GEO) annotation file "028005_D_GEO_20131202" and combined replicate data into a tabular data file ready to be imported to Expander 7 for analysis.

4.16.3. Expander 7

Combined tabular expression data was imported into Expander 7 and had a baseline of 5.0 set for missing values. Expression data underwent preprocessing: expression values were log2 transformed, quantile normalized and probes were merged by Gene ID. Preprocessed data was exported for Gene Set Enrichment Analysis (GSEA) or further processed to filter probes by differential ttest. Probes were filtered with a p-value cut off of 0.05 with no multiple tests correction.

4.16.4. Gene Set Enrichment Analysis:

Preprocessed gene expression data were median normalized and imported into Gene Set Enrichment Analysis (GSEA) software package (Mootha et al., 2003; Subramanian et al., 2005).

Data from the microarrays were loaded and run with the following paramaters: (1) Number of permutations: 1000, (2) Permutation type: gene_set, (3) Enrichment statistic: weighted, (4) Metric for ranking genes: Signal2Noise, (5) Collapsing mode for probe sets => 1 gene: Median_of_probes. Phenotype labels compared siControl with siSix1 and siControl with siSix4. The entire molecular signature database (MsigDB) version 4.0 was used in the GSEA analysis.

4.16.5. ToppFun Gene Ontology:

Differentially regulated probe sets (down-regulated or up-regulated) were imported into the ToppFun component of the ToppGene Suite. Entry type setting used was HGNC Symbol. Calculations were made across all available features with a p-value cut-off of 0.05 FDR corrected and set gene limits of $1 \leq n \leq 2000$.

4.16.6. JavaTreeView v1:

Data was median normalized and imported into JavaTreeview in order to generate heatmaps using default settings.

References

An integrated encyclopedia of DNA elements in the human genome. Nature. 2012 Sep 6;489(7414):57-74.

Abou-Khalil R, Brack AS. Muscle stem cells and reversible quiescence: the role of sprouty. Cell Cycle. 2010 Jul 1;9(13):2575-80.

Albini S, Coutinho Toto P, Dall'Agnese A, Malecova B, Cenciarelli C, et al. Brahma is required for cell cycle arrest and late muscle gene expression during skeletal myogenesis. EMBO Rep. 2015 Aug;16(8):1037-50.

Andrés V, Walsh K. Myogenin expression, cell cycle withdrawal, and phenotypic differentiation are temporally separable events that precede cell fusion upon myogenesis. J Cell Biol. 1996 Feb;132(4):657-66.

Auradé F, Pinset C, Chafey P, Gros F, Montarras D. Myf5, MyoD, myogenin and MRF4 myogenic derivatives of the embryonic mesenchymal cell line C3H10T1/2 exhibit the same adult muscle phenotype. Differentiation. 1994 Feb;55(3):185-92.

Bentzinger CF, Wang YX, Rudnicki MA. Building muscle: molecular regulation of myogenesis. Cold Spring Harb Perspect Biol. 2012 Feb 1;4(2).

Berkes CA, Tapscott SJ. MyoD and the transcriptional control of myogenesis. Semin Cell Dev Biol. 2005 Aug-Oct;16(4-5):585-95.

Blackwell TK, Weintraub H. Differences and similarities in DNA-binding preferences of MyoD and E2A protein complexes revealed by binding site selection. Science. 1990 Nov 23;250(4984):1104-10. PubMed PMID: 2174572.

Blais A, van Oevelen CJ, Margueron R, Acosta-Alvear D, Dynlacht BD. Retinoblastoma tumor suppressor protein-dependent methylation of histone H3 lysine 27 is associated with irreversible cell cycle exit. J Cell Biol. 2007 Dec 31;179(7):1399-412.

Blais A, Tsikitis M, Acosta-Alvear D, Sharan R, Kluger Y, et al. An initial blueprint for myogenic differentiation. Genes Dev. 2005 Mar 1;19(5):553-69.

Blum R, Vethantham V, Bowman C, Rudnicki M, Dynlacht BD. Genome-wide identification of enhancers in skeletal muscle: the role of MyoD1. Genes Dev. 2012 Dec 15;26(24):2763-79.

Bosnakovski D, Xu Z, Li W, Thet S, Cleaver O, et al. Prospective isolation of skeletal muscle stem cells with a Pax7 reporter. Stem Cells. 2008 Dec;26(12):3194-204.

Braun T, Buschhausen-Denker G, Bober E, Tannich E, Arnold HH. A novel human muscle factor related to but distinct from MyoD1 induces myogenic conversion in 10T1/2 fibroblasts. EMBO J. 1989 Mar;8(3):701-9.

Braun T, Winter B, Bober E, Arnold HH. Transcriptional activation domain of the muscle-specific gene-regulatory protein myf5. Nature. 1990 Aug 16;346(6285):663-5.

Brehm A, Miska EA, McCance DJ, Reid JL, Bannister AJ, et al. Retinoblastoma protein recruits histone deacetylase to repress transcription. Nature. 1998 Feb 5;391(6667):597-601.

Buchkovich K, Duffy LA, Harlow E. The retinoblastoma protein is phosphorylated during specific phases of the cell cycle. Cell. 1989 Sep 22;58(6):1097-105.

Buckingham M, Bajard L, Chang T, Daubas P, Hadchouel J, et al. The formation of skeletal muscle: from somite to limb. J Anat. 2003 Jan;202(1):59-68.

Buckingham M, Relaix F. The role of Pax genes in the development of tissues and organs: Pax3 and Pax7 regulate muscle progenitor cell functions. Annu Rev Cell Dev Biol. 2007;23:645-73.

Cao Y, Yao Z, Sarkar D, Lawrence M, Sanchez GJ, et al. Genome-wide MyoD binding in skeletal muscle cells: a potential for broad cellular reprogramming. Dev Cell. 2010 Apr 20;18(4):662-74.

Cenciarelli C, De Santa F, Puri PL, Mattei E, Ricci L, et al. Critical role played by cyclin D3 in the MyoD-mediated arrest of cell cycle during myoblast differentiation. Mol Cell Biol. 1999 Jul;19(7):5203-17.

Cerletti M, Jurga S, Witczak CA, Hirshman MF, Shadrach JL, et al. Highly efficient, functional engraftment of skeletal muscle stem cells in dystrophic muscles. Cell. 2008 Jul 11;134(1):37-47.

Chakroun I, Yang D, Girgis J, Gunasekharan A, Phenix H, et al. Genome-wide association between Six4, MyoD and the histone demethylase Utx during myogenesis. FASEB J. 2015 Jul 30.

Chamberlain JS. Gene therapy of muscular dystrophy. Hum Mol Genet. 2002 Oct 1;11(20):2355-62.

Chen JC, Goldhamer DJ. The core enhancer is essential for proper timing of MyoD activation in limb buds and branchial arches. Dev Biol. 2004 Jan 15;265(2):502-12.

Chen R, Amoui M, Zhang Z, Mardon G. Dachshund and eyes absent proteins form a complex and function synergistically to induce ectopic eye development in Drosophila. Cell. 1997 Dec 26;91(7):893-903.

Chin L, Pomerantz J, DePinho RA. The INK4a/ARF tumor suppressor: one gene--two products--two pathways. Trends Biochem Sci. 1998 Aug;23(8):291-6.

Christensen KL, Brennan JD, Aldridge CS, Ford HL. Cell cycle regulation of the human Six1 homeoprotein is mediated by APC(Cdh1). Oncogene. 2007 May 17;26(23):3406-14.

Coletta RD, Christensen KL, Micalizzi DS, Jedlicka P, Varella-Garcia M, et al. Six1 overexpression in mammary cells induces genomic instability and is sufficient for malignant transformation. Cancer Res. 2008 Apr 1;68(7):2204-13.

Cossu G, Sampaolesi M. New therapies for muscular dystrophy: cautious optimism. Trends Mol Med. 2004 Oct;10(10):516-20.

Crist CG, Montarras D, Buckingham M. Muscle satellite cells are primed for myogenesis but maintain quiescence with sequestration of Myf5 mRNA targeted by microRNA-31 in mRNP granules. Cell Stem Cell. 2012 Jul 6;11(1):118-26.

Davis RJ, Shen W, Sandler YI, Amoui M, Purcell P, et al. Dach1 mutant mice bear no gross abnormalities in eye, limb, and brain development and exhibit postnatal lethality. Mol Cell Biol. 2001 Mar;21(5):1484-90.

Diao Y, Guo X, Li Y, Sun K, Lu L, et al. Pax3/7BP is a Pax7- and Pax3-binding protein that regulates the proliferation of muscle precursor cells by an epigenetic mechanism. Cell Stem Cell. 2012 Aug 3;11(2):231-41.

Dietrich S, Abou-Rebyeh F, Brohmann H, Bladt F, Sonnenberg-Riethmacher E, et al. The role of SF/HGF and c-Met in the development of skeletal muscle. Development. 1999 Apr;126(8):1621-9.

Emery AE. The muscular dystrophies. Lancet. 2002 Feb 23;359(9307):687-95.

Ford HL, Kabingu EN, Bump EA, Mutter GL, Pardee AB. Abrogation of the G2 cell cycle checkpoint associated with overexpression of HSIX1: a possible mechanism of breast carcinogenesis. Proc Natl Acad Sci U S A. 1998 Oct 13;95(21):12608-13.

Fujimoto Y, Tanaka SS, Yamaguchi YL, Kobayashi H, Kuroki S, et al. Homeoproteins Six1 and Six4 regulate male sex determination and mouse gonadal development. Dev Cell. 2013 Aug 26;26(4):416-30.

Fukada S, Higuchi S, Segawa M, Koda K, Yamamoto Y, et al. Purification and cell-surface marker characterization of quiescent satellite cells from murine skeletal muscle by a novel monoclonal antibody. Exp Cell Res. 2004 Jun 10;296(2):245-55.

Fulle S, Protasi F, Di Tano G, Pietrangelo T, Beltramin A, et al. The contribution of reactive oxygen species to sarcopenia and muscle ageing. Exp Gerontol. 2004 Jan;39(1):17-24.

Gherzi R, Trabucchi M, Ponassi M, Gallouzi IE, Rosenfeld MG, et al. Akt2-mediated phosphorylation of Pitx2 controls Ccnd1 mRNA decay during muscle cell differentiation. Cell Death Differ. 2010 Jun;17(6):975-83.

Girling R, Partridge JF, Bandara LR, Burden N, Totty NF, et al. A new component of the transcription factor DRTF1/E2F. Nature. 1993 Sep 30;365(6445):468.

Grifone R, Demignon J, Houbron C, Souil E, Niro C, et al. Six1 and Six4 homeoproteins are required for Pax3 and Mrf expression during myogenesis in the mouse embryo. Development. 2005 May;132(9):2235-49.

Grifone R, Laclef C, Spitz F, Lopez S, Demignon J, et al. Six1 and Eya1 expression can reprogram adult muscle from the slow-twitch phenotype into the fast-twitch phenotype. Mol Cell Biol. 2004 Jul;24(14):6253-67.

Gros J, Manceau M, Thomé V, Marcelle C. A common somitic origin for embryonic muscle progenitors and satellite cells. Nature. 2005 Jun 16;435(7044):954-8.

Grounds MD. Age-associated changes in the response of skeletal muscle cells to exercise and regeneration. Ann N Y Acad Sci. 1998 Nov 20;854:78-91.

Gurung R, Parnaik VK. Cyclin D3 promotes myogenic differentiation and Pax7 transcription. J Cell Biochem. 2012 Jan;113(1):209-19.

Hasty P, Bradley A, Morris JH, Edmondson DG, Venuti JM, et al. Muscle deficiency and neonatal death in mice with a targeted mutation in the myogenin gene. Nature. 1993 Aug 5;364(6437):501-6.

Heanue TA, Reshef R, Davis RJ, Mardon G, Oliver G, et al. Synergistic regulation of vertebrate muscle development by Dach2, Eya2, and Six1, homologs of genes required for Drosophila eye formation. Genes Dev. 1999 Dec 15;13(24):3231-43.

Huh MS, Parker MH, Scimè A, Parks R, Rudnicki MA. Rb is required for progression through myogenic differentiation but not maintenance of terminal differentiation. J Cell Biol. 2004 Sep 13;166(6):865-76.

Ikeda K, Watanabe Y, Ohto H, Kawakami K. Molecular interaction and synergistic activation of a promoter by Six, Eya, and Dach proteins mediated through CREB binding protein. Mol Cell Biol. 2002 Oct;22(19):6759-66.

Kablar B, Asakura A, Krastel K, Ying C, May LL, et al. MyoD and Myf-5 define the specification of musculature of distinct embryonic origin. Biochem Cell Biol. 1998;76(6):1079-91.

Kassar-Duchossoy L, Gayraud-Morel B, Gomès D, Rocancourt D, Buckingham M, et al. Mrf4 determines skeletal muscle identity in Myf5:Myod double-mutant mice. Nature. 2004 Sep 23;431(7007):466-71.

Kato J, Matsushime H, Hiebert SW, Ewen ME, Sherr CJ. Direct binding of cyclin D to the retinoblastoma gene product (pRb) and pRb phosphorylation by the cyclin D-dependent kinase CDK4. Genes Dev. 1993 Mar;7(3):331-42.

Kawakami K, Sato S, Ozaki H, Ikeda K. Six family genes--structure and function as transcription factors and their roles in development. Bioessays. 2000 Jul;22(7):616-26.

Kawakami K, Ohto H, Takizawa T, Saito T. Identification and expression of six family genes in mouse retina. FEBS Lett. 1996 Sep 16;393(2-3):259-63.

Kirby RJ, Hamilton GM, Finnegan DJ, Johnson KJ, Jarman AP. Drosophila homolog of the myotonic dystrophy-associated gene, SIX5, is required for muscle and gonad development. Curr Biol. 2001 Jul 10;11(13):1044-9.

Kobayashi H, Kawakami K, Asashima M, Nishinakamura R. Six1 and Six4 are essential for Gdnf expression in the metanephric mesenchyme and ureteric bud formation, while Six1 deficiency alone causes mesonephric-tubule defects. Mech Dev. 2007 Apr;124(4):290-303.

Kochhar A, Orten DJ, Sorensen JL, Fischer SM, Cremers CW, et al. SIX1 mutation screening in 247 branchio-oto-renal syndrome families: a recurrent missense mutation associated with BOR. Hum Mutat. 2008 Apr;29(4):565.

Kuang S, Kuroda K, Le Grand F, Rudnicki MA. Asymmetric self-renewal and commitment of satellite stem cells in muscle. Cell. 2007 Jun 1;129(5):999-1010.

Kuang S, Chargé SB, Seale P, Huh M, Rudnicki MA. Distinct roles for Pax7 and Pax3 in adult regenerative myogenesis. J Cell Biol. 2006 Jan 2;172(1):103-13.

Kucharczuk KL, Love CM, Dougherty NM, Goldhamer DJ. Fine-scale transgenic mapping of the MyoD core enhancer: MyoD is regulated by distinct but overlapping mechanisms in myotomal and non-myotomal muscle lineages. Development. 1999 May;126(9):1957-65.

Kumar JP. The sine oculis homeobox (SIX) family of transcription factors as regulators of development and disease. Cell Mol Life Sci. 2009 Feb;66(4):565-83.

Laclef C, Hamard G, Demignon J, Souil E, Houbron C, et al. Altered myogenesis in Six1-deficient mice. Development. 2003 May;130(10):2239-52.

Le Grand F, Grifone R, Mourikis P, Houbron C, Gigaud C, et al. Six1 regulates stem cell repair potential and self-renewal during skeletal muscle regeneration. J Cell Biol. 2012 Sep 3;198(5):815-32.

Li X, Oghi KA, Zhang J, Krones A, Bush KT, et al. Eya protein phosphatase activity regulates Six1-Dach-Eya transcriptional effects in mammalian organogenesis. Nature. 2003 Nov 20;426(6964):247-54.

Li Z, Tian T, Lv F, Chang Y, Wang X, et al. Six1 promotes proliferation of pancreatic cancer cells via upregulation of cyclin D1 expression. PLoS One. 2013;8(3):e59203.

Liu Y, Chu A, Chakroun I, Islam U, Blais A. Cooperation between myogenic regulatory factors and SIX family transcription factors is important for myoblast differentiation. Nucleic Acids Res. 2010 Nov;38(20):6857-71.

Liu Y, Chakroun I, Yang D, Horner E, Liang J, et al. Six1 regulates MyoD expression in adult muscle progenitor cells. PLoS One. 2013;8(6):e67762.

Liu Y, Nandi S, Martel A, Antoun A, Ioshikhes I, et al. Discovery, optimization and validation of an optimal DNA-binding sequence for the Six1 homeodomain transcription factor. Nucleic Acids Res. 2012 Sep 1;40(17):8227-39.

Maillet M, Purcell NH, Sargent MA, York AJ, Bueno OF, et al. DUSP6 (MKP3) null mice show enhanced ERK1/2 phosphorylation at baseline and increased myocyte proliferation in the heart affecting disease susceptibility. J Biol Chem. 2008 Nov 7;283(45):31246-55.

MAURO A. Satellite cell of skeletal muscle fibers. J Biophys Biochem Cytol. 1961 Feb;9:493-5.

McNally EM, Pytel P. Muscle diseases: the muscular dystrophies. Annu Rev Pathol. 2007;2:87-109.

Monaco AP, Neve RL, Colletti-Feener C, Bertelson CJ, Kurnit DM, et al. Isolation of candidate cDNAs for portions of the Duchenne muscular dystrophy gene. Nature. 1986 Oct 16-22;323(6089):646-50.

Montarras D, Morgan J, Collins C, Relaix F, Zaffran S, et al. Direct isolation of satellite cells for skeletal muscle regeneration. Science. 2005 Sep 23;309(5743):2064-7.

Nabeshima Y, Hanaoka K, Hayasaka M, Esumi E, Li S, et al. Myogenin gene disruption results in perinatal lethality because of severe muscle defect. Nature. 1993 Aug 5;364(6437):532-5.

Nord H, Nygård Skalman L, von Hofsten J. Six1 regulates proliferation of Pax7-positive muscle progenitors in zebrafish. J Cell Sci. 2013 Apr 15;126(Pt 8):1868-80.

Nowak KJ, Davies KE. Duchenne muscular dystrophy and dystrophin: pathogenesis and opportunities for treatment. EMBO Rep. 2004 Sep;5(9):872-6.

Noyes MB, Christensen RG, Wakabayashi A, Stormo GD, Brodsky MH, et al. Analysis of homeodomain specificities allows the family-wide prediction of preferred recognition sites. Cell. 2008 Jun 27;133(7):1277-89.

Ohto H, Kamada S, Tago K, Tominaga SI, Ozaki H, et al. Cooperation of six and eya in activation of their target genes through nuclear translocation of Eya. Mol Cell Biol. 1999 Oct;19(10):6815-24.

Olguin HC, Olwin BB. Pax-7 up-regulation inhibits myogenesis and cell cycle progression in satellite cells: a potential mechanism for self-renewal. Dev Biol. 2004 Nov 15;275(2):375-88.

Ono H, Imoto I, Kozaki K, Tsuda H, Matsui T, et al. SIX1 promotes epithelial-mesenchymal transition in colorectal cancer through ZEB1 activation. Oncogene. 2012 Nov 22;31(47):4923-34.

Ozaki H, Watanabe Y, Takahashi K, Kitamura K, Tanaka A, et al. Six4, a putative myogenin gene regulator, is not essential for mouse embryonal development. Mol Cell Biol. 2001 May;21(10):3343-50.

Pignoni F, Hu B, Zavitz KH, Xiao J, Garrity PA, et al. The eye-specification proteins So and Eya form a complex and regulate multiple steps in Drosophila eye development. Cell. 1997 Dec 26;91(7):881-91.

Reichenberger KJ, Coletta RD, Schulte AP, Varella-Garcia M, Ford HL. Gene amplification is a mechanism of Six1 overexpression in breast cancer. Cancer Res. 2005 Apr 1;65(7):2668-75.

Relaix F, Rocancourt D, Mansouri A, Buckingham M. A Pax3/Pax7-dependent population of skeletal muscle progenitor cells. Nature. 2005 Jun 16;435(7044):948-53.

Relaix F, Buckingham M. From insect eye to vertebrate muscle: redeployment of a regulatory network. Genes Dev. 1999 Dec 15;13(24):3171-8.

Rudnicki MA, Braun T, Hinuma S, Jaenisch R. Inactivation of MyoD in mice leads to up-regulation of the myogenic HLH gene Myf-5 and results in apparently normal muscle development. Cell. 1992 Oct 30;71(3):383-90.

Ruf RG, Xu PX, Silvius D, Otto EA, Beekmann F, et al. SIX1 mutations cause branchio-oto-renal syndrome by disruption of EYA1-SIX1-DNA complexes. Proc Natl Acad Sci U S A. 2004 May 25;101(21):8090-5.

Sassoon D, Lyons G, Wright WE, Lin V, Lassar A, et al. Expression of two myogenic regulatory factors myogenin and MyoD1 during mouse embryogenesis. Nature. 1989 Sep 28;341(6240):303-7.

Schienda J, Engleka KA, Jun S, Hansen MS, Epstein JA, et al. Somitic origin of limb muscle satellite and side population cells. Proc Natl Acad Sci U S A. 2006 Jan 24;103(4):945-50.

Schorl C, Sedivy JM. Analysis of cell cycle phases and progression in cultured mammalian cells. Methods. 2007 Feb;41(2):143-50.

Seale P, Sabourin LA, Girgis-Gabardo A, Mansouri A, Gruss P, et al. Pax7 is required for the specification of myogenic satellite cells. Cell. 2000 Sep 15;102(6):777-86.

Seo HC, Curtiss J, Mlodzik M, Fjose A. Six class homeobox genes in drosophila belong to three distinct families and are involved in head development. Mech Dev. 1999 May;83(1-2):127-39.

Serikaku MA, O'Tousa JE. sine oculis is a homeobox gene required for Drosophila visual system development. Genetics. 1994 Dec;138(4):1137-50.

Serrano M, Hannon GJ, Beach D. A new regulatory motif in cell-cycle control causing specific inhibition of cyclin D/CDK4. Nature. 1993 Dec 16;366(6456):704-7.

Shea KL, Xiang W, LaPorta VS, Licht JD, Keller C, et al. Sprouty1 regulates reversible quiescence of a self-renewing adult muscle stem cell pool during regeneration. Cell Stem Cell. 2010 Feb 5;6(2):117-29.

Spitz F, Demignon J, Porteu A, Kahn A, Concordet JP, et al. Expression of myogenin during embryogenesis is controlled by Six/sine oculis homeoproteins through a conserved MEF3 binding site. Proc Natl Acad Sci U S A. 1998 Nov 24;95(24):14220-5.

Tedesco FS, Cossu G. Stem cell therapies for muscle disorders. Curr Opin Neurol. 2012 Oct;25(5):597-603.

Thayer MJ, Tapscott SJ, Davis RL, Wright WE, Lassar AB, et al. Positive autoregulation of the myogenic determination gene MyoD1. Cell. 1989 Jul 28;58(2):241-8.

Tomczak KK, Marinescu VD, Ramoni MF, Sanoudou D, Montanaro F, et al. Expression profiling and identification of novel genes involved in myogenic differentiation. FASEB J. 2004 Feb;18(2):403-5.

Tremblay P, Dietrich S, Mericskay M, Schubert FR, Li Z, et al. A crucial role for Pax3 in the development of the hypaxial musculature and the long-range migration of muscle precursors. Dev Biol. 1998 Nov 1;203(1):49-61.

Vermeulen K, Van Bockstaele DR, Berneman ZN. The cell cycle: a review of regulation, deregulation and therapeutic targets in cancer. Cell Prolif. 2003 Jun;36(3):131-49.

von Maltzahn J, Jones AE, Parks RJ, Rudnicki MA. Pax7 is critical for the normal function of satellite cells in adult skeletal muscle. Proc Natl Acad Sci U S A. 2013 Oct 8;110(41):16474-9.

Walz AL, Ooms A, Gadd S, Gerhard DS, Smith MA, et al. Recurrent DGCR8, DROSHA, and SIX homeodomain mutations in favorable histology Wilms tumors. Cancer Cell. 2015 Feb 9;27(2):286-97.

Weber TS, Jaehnert I, Schichor C, Or-Guil M, Carneiro J. Quantifying the length and variance of the eukaryotic cell cycle phases by a stochastic model and dual nucleoside pulse labelling. PLoS Comput Biol. 2014 Jul;10(7):e1003616.

Wegert J, Ishaque N, Vardapour R, Geörg C, Gu Z, et al. Mutations in the SIX1/2 pathway and the DROSHA/DGCR8 miRNA microprocessor complex underlie high-risk blastemal type Wilms tumors. Cancer Cell. 2015 Feb 9;27(2):298-311.

Weintraub H, Tapscott SJ, Davis RL, Thayer MJ, Adam MA, et al. Activation of muscle-specific genes in pigment, nerve, fat, liver, and fibroblast cell lines by forced expression of MyoD. Proc Natl Acad Sci U S A. 1989 Jul;86(14):5434-8.

Wright WE, Sassoon DA, Lin VK. Myogenin, a factor regulating myogenesis, has a domain homologous to MyoD. Cell. 1989 Feb 24;56(4):607-17.

Wu W, Ren Z, Zhang L, Liu Y, Li H, et al. Overexpression of Six1 gene suppresses proliferation and enhances expression of fast-type muscle genes in C2C12 myoblasts. Mol Cell Biochem. 2013 Aug;380(1-2):23-32.

Xu PX, Adams J, Peters H, Brown MC, Heaney S, et al. Eya1-deficient mice lack ears and kidneys and show abnormal apoptosis of organ primordia. Nat Genet. 1999 Sep;23(1):113-7.

Xu PX, Zheng W, Huang L, Maire P, Laclef C, et al. Six1 is required for the early organogenesis of mammalian kidney. Development. 2003 Jul;130(14):3085-94.

Yajima H, Motohashi N, Ono Y, Sato S, Ikeda K, et al. Six family genes control the proliferation and differentiation of muscle satellite cells. Exp Cell Res. 2010 Oct 15;316(17):2932-44.

Yu Y, Davicioni E, Triche TJ, Merlino G. The homeoprotein six1 transcriptionally activates multiple protumorigenic genes but requires ezrin to promote metastasis. Cancer Res. 2006 Feb 15;66(4):1982-9.

Zhang K, Sha J, Harter ML. Activation of Cdc6 by MyoD is associated with the expansion of quiescent myogenic satellite cells. J Cell Biol. 2010 Jan 11;188(1):39-48.

Zhu CC, Dyer MA, Uchikawa M, Kondoh H, Lagutin OV, et al. Six3-mediated auto repression and eye development requires its interaction with members of the Groucho-related family of co-repressors. Development. 2002 Jun;129(12):2835-49.

Appendices

Table S1: Probe list of Cluster #1

Probes categorized into Cluster #1 are listed in the following table. Agilent probe ID, Genebank accession number, gene symbol, the average log2 expression values are shown. The probes are sorted by pvalue comparing siNS with siSix1. Probes with no gene symbol are denoted with --.

Table S1: Cluster 1

Agilent ID	GB Accession	Gene Symbol	siNS	siSix1	siSix4	pvalue
A_55_P2068414	XR_141112	Gm19924	8.21	7.19	7.89	0.000
A_55_P2097840	--	--	10.32	8.94	10.07	0.000
A_52_P151320	NM_025566	Tnfaip8l1	10.19	9.19	10.30	0.000
A_55_P1992421	NM_008253	Hmgb3	13.31	12.18	13.23	0.000
A_51_P324410	NM_016862	Vti1a	10.96	9.52	10.87	0.000
A_52_P325527	NM_010103	Edil3	8.57	6.21	8.65	0.000
A_30_P01030682	--	--	4.69	2.85	4.33	0.000
A_51_P422540	NM_028829	Paqr8	7.19	6.11	7.16	0.000
A_52_P201551	NM_173437	Nav1	10.52	9.18	10.54	0.000
A_55_P2129944	XM_003945486	LOC100861614	6.68	5.38	6.49	0.000
A_55_P2042487	NM_009468	Dpysl3	15.82	14.77	16.35	0.000
A_51_P461504	NM_007908	Eef2k	8.59	7.42	8.57	0.000
A_55_P1965939	AK014019	3110007F17Rik	5.84	4.74	5.85	0.000
A_51_P353008	NM_010799	Minpp1	10.97	9.80	11.00	0.000
A_51_P348325	NM_027740	Poc1b	10.10	9.04	10.30	0.000
A_52_P964651	NM_001080708	Fam65c	6.05	4.85	5.27	0.000
A_52_P432919	NM_031874	Rab3d	8.31	7.01	8.45	0.000
A_51_P228171	NM_025495	Cenpp	10.26	9.14	9.68	0.000
A_52_P550147	AJ584850	Sned1	10.03	8.96	10.03	0.000
A_55_P2014555	NM_001080926	Lrp8	8.37	7.15	8.24	0.000
A_52_P8685	NM_020588	Tmem183a	11.27	9.74	10.88	0.000
A_51_P175205	NM_001114334	Rps6kb1	9.58	8.56	9.04	0.000
A_52_P510107	NM_172527	Nudt15	6.98	5.76	6.75	0.000
A_55_P2000280	NM_001170786	Mthfd1l	10.88	9.86	11.16	0.000
A_51_P312336	NM_028122	Slc14a1	8.97	7.67	9.20	0.000
A_52_P226348	AK089514	--	10.57	9.44	9.84	0.000
A_66_P100853	BC147161	--	17.86	16.48	17.83	0.000
A_55_P2149575	NM_001082975	Sdr39u1	8.50	7.39	8.47	0.000
A_55_P1960145	NM_001271484	Clip4	8.34	7.19	7.63	0.000
A_51_P158388	NM_198164	Cdk19	9.24	7.65	9.01	0.000
A_52_P522372	NM_175503	Aard	5.95	3.90	5.11	0.000
A_55_P2027136	NM_013548	Hist1h3f	9.31	8.26	9.47	0.000

Table S1: Cluster 1						
Agilent ID	**GB Accession**	**Gene Symbol**	**siNS**	**siSix1**	**siSix4**	**pvalue**
A_30_P01019709	--	--	8.08	6.75	7.03	0.000
A_55_P2051322	NM_025994	Efhd2	11.20	10.16	11.46	0.000
A_55_P1956734	--	--	10.70	9.63	10.60	0.000
A_55_P2142033	NM_001271484	Clip4	7.90	6.59	7.04	0.000
A_55_P2068260	NM_145073	Hist1h3g	8.70	7.51	8.76	0.000
A_55_P1957080	--	--	8.82	7.22	8.65	0.000
A_55_P2015137	NM_001033330	Frmpd4	5.60	3.16	4.34	0.000
A_30_P01021855	--	--	7.74	6.14	7.72	0.000
A_66_P106789	--	--	12.80	11.25	12.73	0.000
A_55_P2109505	--	--	15.62	14.33	15.71	0.000
A_55_P2084631	NM_178184	Hist1h2an	17.42	16.32	17.47	0.000
A_55_P1956718	NM_028238	Rab38	8.13	6.54	8.33	0.000
A_55_P1980292	NM_011221	Purb	13.49	12.46	12.58	0.000
A_55_P2024530	NM_009174	Siah2	10.03	8.82	10.28	0.000
A_30_P01025480	--	--	7.81	6.75	6.90	0.000
A_65_P10865	NM_029825	Scfd1	11.68	10.27	11.71	0.000
A_55_P1953172	NM_008238	Foxn1	6.33	4.68	5.93	0.000
A_51_P359983	NM_144529	Arhgap17	11.12	9.94	11.09	0.001
A_51_P133562	NM_007618	Serpina6	7.35	5.64	6.54	0.001
A_55_P2305010	XR_035383	A730089K16Rik	6.33	4.47	5.78	0.001
A_55_P2038489	--	--	9.80	8.08	9.11	0.001
A_51_P457528	NM_007630	Ccnb2	13.51	12.09	13.55	0.001
A_55_P1987964	NM_001013816	Gm5622	6.62	3.79	5.79	0.001
A_55_P2028655	NM_175090	Slc31a1	12.01	10.61	12.24	0.001
A_51_P259861	NM_021554	Mettl9	13.26	11.88	13.28	0.001
A_55_P2004801	NM_001040435	Tacc3	13.84	12.55	13.82	0.001
A_52_P469502	NM_028176	Cda	7.34	6.13	7.63	0.001
A_55_P1982733	NM_001271585	Dnajc5	10.71	9.67	10.56	0.001
A_55_P2004248	NM_133237	Apcdd1	8.72	7.20	8.63	0.001
A_30_P01020717	--	--	7.56	6.54	7.68	0.001
A_55_P1996583	NM_025598	Ppdpf	12.73	11.49	12.79	0.001
A_52_P260696	NM_007488	Arnt2	8.58	7.52	8.45	0.001
A_55_P2068663	NM_019641	Stmn1	16.19	15.04	15.91	0.001
A_30_P01031282	--	--	7.63	6.24	7.24	0.001
A_55_P1987331	NM_001205322	Prl3d1	9.62	8.45	8.32	0.001
A_55_P1958246	NM_001198984	Tcof1	12.77	11.70	12.68	0.001
A_52_P21550	NM_173442	Gcnt1	10.64	9.25	10.97	0.001
A_55_P2045007	NM_001252643	Hrh1	7.57	6.22	7.21	0.001
A_66_P138584	NM_029797	Mnd1	9.51	8.50	9.46	0.001

Table S1: Cluster 1						
Agilent ID	**GB Accession**	**Gene Symbol**	**siNS**	**siSix1**	**siSix4**	**pvalue**
A_30_P01020734	--	--	7.76	6.74	7.08	0.001
A_51_P149422	NM_022422	Gng13	7.31	6.05	7.62	0.001
A_51_P270949	NM_020034	Hist1h1b	13.57	12.08	13.55	0.001
A_51_P324287	NM_024245	Kif23	11.28	9.66	11.11	0.001
A_55_P2150831	NM_009867	Cdh4	5.63	4.41	6.76	0.001
A_55_P2096035	NM_001252347	Rundc3a	5.84	4.56	5.95	0.001
A_55_P2039439	NM_031868	Ppp1ca	16.45	15.40	16.64	0.001
A_51_P122740	NM_028123	Slc37a3	10.67	9.61	10.83	0.001
A_55_P2105873	NM_001135001	Ppp2r5c	10.56	9.51	10.87	0.001
A_30_P01023499	--	--	7.71	6.53	7.26	0.001
A_52_P354823	NM_008320	Irf8	5.63	4.03	4.54	0.001
A_55_P1993807	NM_001031664	Nudt10	9.36	7.79	8.63	0.001
A_51_P171965	NM_026503	1110058L19Rik	11.93	10.89	11.92	0.001
A_55_P2008417	NM_029797	Mnd1	10.46	9.42	10.59	0.001
A_55_P2028496	--	--	14.52	13.25	14.55	0.001
A_55_P2099961	NM_178186	Hist1h2ag	17.98	16.81	17.97	0.001
A_51_P341349	NM_024433	Mtap	11.76	10.67	11.87	0.001
A_55_P2059947	--	--	8.14	6.40	7.30	0.001
A_51_P225224	NM_019564	Htra1	11.68	10.47	12.34	0.001
A_51_P234864	NM_178639	Sfxn5	7.50	6.42	7.94	0.001
A_55_P2053057	NM_028614	Ppp2r1b	8.12	6.99	7.47	0.001
A_30_P01033504	--	--	8.15	7.12	8.11	0.001
A_55_P2003576	NM_001141977	Tpx2	8.64	7.61	8.54	0.001
A_55_P2112355	--	--	13.95	12.55	13.75	0.001
A_55_P2157814	NM_146041	Gmds	11.62	10.25	11.74	0.001
A_52_P24631	NM_018745	Azin1	11.31	10.27	11.29	0.001
A_55_P2036417	NM_001111140	Lrrc10b	5.07	3.09	4.36	0.001
A_55_P2063336	NM_134041	4930427A07Rik	11.92	10.55	12.15	0.001
A_30_P01028731	--	--	6.62	5.47	6.59	0.001
A_55_P2090519	NM_025598	Ppdpf	14.27	13.04	14.38	0.001
A_55_P2108773	NM_134041	4930427A07Rik	10.93	9.37	11.14	0.001
A_66_P109562	XM_890719	Gm12271	11.92	10.70	11.80	0.001
A_30_P01029383	--	--	8.52	7.30	8.50	0.001
A_65_P20249	NM_008855	Prkcb	12.19	10.69	12.26	0.001
A_52_P206861	NM_173780	Klf8	8.64	7.32	8.66	0.001
A_55_P2082186	--	--	14.83	13.80	15.16	0.002
A_52_P330540	NM_025642	Mis18a	10.82	9.56	10.89	0.002
A_55_P1993789	NM_016957	Hmgn2	14.87	13.53	14.98	0.002
A_30_P01021830	--	--	6.47	5.41	6.06	0.002

Table S1: Cluster 1						
Agilent ID	**GB Accession**	**Gene Symbol**	**siNS**	**siSix1**	**siSix4**	**pvalue**
A_55_P1966169	BC091753	Ppdpf	14.24	13.02	14.46	0.002
A_30_P01031572	--	--	12.95	11.56	12.88	0.002
A_55_P2004046	BC052527	--	7.65	6.02	7.32	0.002
A_51_P354706	NM_010094	Lefty1	7.01	5.89	7.43	0.002
A_55_P2160253	AK020160	6720475J19Rik	9.84	8.60	9.50	0.002
A_52_P76355	NM_001145676	2210408I21Rik	5.57	4.45	5.36	0.002
A_55_P2083949	AK129238	Scfd1	7.54	6.51	7.55	0.002
A_51_P378298	NM_026976	Faim3	5.63	3.92	5.18	0.002
A_51_P151586	NM_010353	Gsg2	9.42	8.08	9.26	0.002
A_55_P2023772	NM_025626	Fam107b	11.43	10.14	11.31	0.002
A_55_P1992368	NM_194347	AY358078	6.15	3.48	5.08	0.002
A_52_P252258	NM_013871	Mapk12	10.29	9.15	9.67	0.002
A_51_P455897	NM_144526	Fam64a	12.26	10.29	11.82	0.002
A_30_P01028837	--	--	8.95	7.64	8.95	0.002
A_55_P1997581	--	--	8.94	7.64	8.47	0.002
A_52_P488427	NM_144520	Sec14l2	9.66	8.64	9.85	0.002
A_30_P01025383	--	--	6.76	5.18	6.60	0.002
A_55_P2051400	NM_172155	Prl3d2	8.64	6.63	6.36	0.002
A_55_P2081656	--	--	10.86	9.29	10.73	0.002
A_55_P2008639	--	--	14.74	13.72	14.60	0.002
A_55_P1967291	NM_144818	Ncaph	12.99	11.45	12.97	0.002
A_55_P2136289	BC057871	Ripk4	5.40	4.23	6.20	0.002
A_51_P233727	NM_023893	Sapcd1	5.86	4.29	5.61	0.002
A_52_P251450	NM_016675	Cldn2	7.27	4.82	5.91	0.002
A_52_P350537	NM_181409	Mtmr11	8.78	7.73	8.84	0.002
A_30_P01024879	--	--	8.09	6.94	8.27	0.002
A_55_P2088601	NM_010180	Fbln1	7.54	6.25	7.84	0.002
A_51_P433091	NM_011221	Purb	15.36	14.15	14.52	0.002
A_55_P2019293	--	--	8.44	6.40	7.40	0.002
A_51_P429903	NM_010883	Ndp	8.35	6.75	7.91	0.002
A_55_P2085905	NM_008486	Anpep	10.69	9.50	9.16	0.002
A_52_P117313	NM_018745	Azin1	7.52	6.48	7.54	0.002
A_55_P2038747	NM_178642	Ano1	11.13	9.26	11.38	0.002
A_51_P376445	NM_008818	Rhox5	7.14	6.08	6.28	0.003
A_51_P267508	NM_025563	2010012O05Rik	9.66	8.55	9.40	0.003
A_55_P2019294	--	--	7.53	6.05	7.04	0.003
A_51_P472217	NM_001081085	Sapcd2	11.63	10.24	11.49	0.003
A_52_P46419	NM_001038018	Grk6	10.86	9.65	10.92	0.003
A_55_P2121364	NM_172552	Tdg	9.17	8.09	8.95	0.003

Table S1: Cluster 1						
Agilent ID	**GB Accession**	**Gene Symbol**	**siNS**	**siSix1**	**siSix4**	**pvalue**
A_51_P133137	NM_009004	Kif20a	12.74	11.22	12.74	0.003
A_55_P2002019	--	--	7.62	5.84	6.90	0.003
A_55_P2000958	NM_001082975	Sdr39u1	10.85	9.56	11.04	0.003
A_55_P2004037	XM_993996	3110040M04Rik	4.73	3.35	3.92	0.003
A_51_P205106	NM_010801	Mlf1	8.96	7.89	9.36	0.003
A_51_P318510	NM_008985	Ptprn	11.58	10.45	10.82	0.003
A_52_P64687	NM_025451	Camk2n1	9.07	7.79	9.00	0.003
A_55_P2011436	AK030082	Gm11223	16.18	15.17	15.78	0.003
A_55_P1990066	--	--	10.77	9.02	10.40	0.003
A_55_P2041753	NM_133704	Sec22a	4.89	3.87	4.84	0.003
A_52_P502771	NM_001039556	Rad54b	9.83	8.51	9.56	0.003
A_51_P369200	NM_028109	Tpx2	12.49	10.95	12.17	0.003
A_55_P2179793	--	--	10.60	9.44	10.44	0.003
A_55_P2144132	--	--	6.77	4.97	5.91	0.003
A_55_P2158011	NM_026412	Knstrn	10.84	9.45	10.71	0.003
A_52_P80965	NM_175400	Sephs1	7.66	6.62	8.04	0.003
A_52_P432904	NM_001003919	Ddx11	8.35	6.96	8.17	0.003
A_55_P1978201	NM_016692	Incenp	14.25	13.00	14.18	0.003
A_55_P2096558	NM_172891	Styk1	6.33	5.17	6.16	0.003
A_55_P2020188	--	--	7.67	6.61	7.49	0.003
A_51_P210143	NM_001005510	Syne2	9.12	7.56	9.06	0.003
A_55_P2099910	NR_015602	F730043M19Rik	5.62	4.61	5.11	0.003
A_55_P2031949	NM_177235	Bend6	9.90	8.81	10.26	0.003
A_55_P2135769	XM_003945535	LOC101056136	8.49	6.37	7.69	0.003
A_66_P128963	NM_010006	Cyp2d9	5.20	4.20	4.96	0.004
A_55_P1979863	NM_001005510	Syne2	10.74	9.15	10.74	0.004
A_55_P2002018	--	--	8.46	6.27	7.56	0.004
A_55_P2148744	--	--	13.41	12.36	13.03	0.004
A_51_P223709	NM_080850	Pask	10.92	9.74	10.68	0.004
A_51_P273556	NM_027975	Fam83d	9.40	7.55	9.24	0.004
A_52_P151393	NM_198860	Fam211b	6.15	5.00	6.48	0.004
A_55_P1985236	XM_904838	LOC666692	5.29	3.51	4.13	0.004
A_55_P2031887	XM_907662	LOC633282	6.17	3.50	5.00	0.004
A_65_P14325	NM_001286647	Atl2	7.23	6.15	7.19	0.004
A_66_P105175	NM_009738	Bche	8.50	7.29	8.59	0.004
A_55_P2127659	NM_023858	Mtmr2	9.52	8.48	9.38	0.004
A_30_P01028947	--	--	6.08	4.98	6.59	0.004
A_55_P2057040	NM_001159662	Ppp1r16b	5.37	2.97	4.58	0.004
A_30_P01023551	--	--	6.07	4.66	5.91	0.004

Table S1: Cluster 1						
Agilent ID	**GB Accession**	**Gene Symbol**	**siNS**	**siSix1**	**siSix4**	**pvalue**
A_55_P2062255	NM_001042699	Syne3	10.97	9.68	10.68	0.004
A_30_P01026907	--	--	4.73	3.40	4.12	0.004
A_55_P2043862	NM_019641	Stmn1	14.95	13.77	14.72	0.004
A_55_P2032498	NM_027420	2610034B18Rik	10.38	9.36	10.80	0.004
A_51_P510891	NM_007423	Afp	6.05	4.50	4.65	0.004
A_51_P264769	NM_016779	Dmp1	8.33	7.08	7.74	0.004
A_51_P481920	NM_009828	Ccna2	12.71	11.14	12.49	0.004
A_55_P2086811	NM_001013817	Sp140	9.36	8.32	9.35	0.004
A_55_P2011490	XM_003945350	--	13.23	12.14	13.26	0.004
A_55_P2000943	NM_020610	Nrip3	6.34	3.73	6.66	0.004
A_55_P2143131	NM_025637	Rwdd3	4.41	3.37	4.14	0.004
A_51_P344566	NM_011121	Plk1	14.57	13.12	14.47	0.004
A_51_P481398	NM_010615	Kif11	9.28	7.62	9.14	0.004
A_55_P2091916	--	--	7.53	5.38	6.66	0.004
A_51_P157953	NM_026138	Soga3	7.77	6.65	7.93	0.004
A_55_P2024366	NM_183024	Raver2	9.24	8.05	8.73	0.004
A_55_P2037111	NM_009391	Ran	13.18	12.09	13.35	0.004
A_51_P421538	NM_178877	Slc9b2	7.17	5.94	7.35	0.004
A_55_P1973178	NM_027999	Haus5	11.15	10.07	11.06	0.004
A_55_P2037023	NM_001177795	Rgs20	5.22	3.13	5.17	0.004
A_55_P2042486	NM_001136086	Dpysl3	9.74	8.72	10.23	0.004
A_55_P2164534	NM_029766	Dtl	10.97	9.66	10.93	0.004
A_55_P2178036	NM_007618	Serpina6	5.32	3.87	5.31	0.005
A_55_P2146249	--	--	14.68	13.64	14.97	0.005
A_51_P518621	NM_013550	Hist1h3a	7.22	6.04	7.48	0.005
A_52_P628067	NM_013538	Cdca3	12.84	11.44	12.61	0.005
A_30_P01028400	--	--	6.82	5.67	7.03	0.005
A_52_P229959	NM_019942	Sept6	9.10	7.64	8.33	0.005
A_51_P145220	NM_008691	Nefm	10.55	8.86	9.20	0.005
A_55_P2002757	NM_008528	Blnk	10.29	9.06	9.51	0.005
A_30_P01030211	--	--	6.49	5.40	6.52	0.005
A_51_P202074	NM_146171	Ncapd2	13.92	12.75	13.57	0.005
A_52_P274028	NM_025965	Ssr1	9.17	7.96	9.52	0.005
A_55_P2028054	NM_016692	Incenp	14.56	13.28	14.39	0.005
A_55_P2060269	NR_073362	1700091H14Rik	7.37	5.50	6.69	0.005
A_55_P2079912	--	--	10.10	9.04	10.12	0.005
A_51_P253732	NM_134437	Il17rd	9.60	8.34	9.43	0.005
A_55_P2181334	NM_176921	6030419C18Rik	7.28	6.04	7.06	0.005
A_55_P2082310	NM_001081346	Rtkn2	6.12	5.09	5.12	0.005

Table S1: Cluster 1						
Agilent ID	**GB Accession**	**Gene Symbol**	**siNS**	**siSix1**	**siSix4**	**pvalue**
A_55_P2151832	--	--	6.09	3.37	5.13	0.005
A_55_P2117903	NM_023377	Stard5	8.11	7.08	8.52	0.005
A_66_P114695	NM_009860	Cdc25c	8.68	7.08	8.71	0.005
A_51_P208361	NM_021299	Ak3	12.00	10.81	12.04	0.005
A_55_P2039324	NM_007634	Ccnf	12.64	11.43	12.47	0.005
A_55_P2043627	NM_001081120	Fam89a	8.97	7.58	7.52	0.005
A_55_P1956418	NM_001082483	Efr3b	9.44	8.05	9.48	0.005
A_51_P155152	NM_020332	Ank	12.81	11.55	13.03	0.005
A_55_P2019359	XM_984157	Gm10375	6.62	5.55	6.36	0.005
A_55_P2071626	NM_001163793	C530008M17Rik	9.04	6.99	8.43	0.005
A_30_P01024209	--	--	5.48	4.39	5.34	0.005
A_52_P657123	XM_003945586	LOC101056031	11.56	10.34	11.55	0.005
A_51_P297679	NM_008225	Hcls1	7.97	6.59	7.64	0.006
A_55_P1953341	NM_026323	Wfdc2	7.45	6.34	9.00	0.006
A_55_P2073035	NR_073362	1700091H14Rik	7.64	5.28	6.69	0.006
A_52_P496956	NM_053178	Acsbg1	10.93	8.88	9.67	0.006
A_55_P2069221	NM_175563	Prr11	9.41	8.13	9.37	0.006
A_51_P269792	NM_009014	Rad51b	7.54	6.42	7.05	0.006
A_66_P121459	NM_007681	Cenpa	13.02	11.66	12.88	0.006
A_52_P515057	NM_172685	Slc25a24	13.91	12.90	13.35	0.006
A_55_P2076048	NM_023284	Nuf2	10.89	9.37	10.99	0.006
A_55_P1965050	NM_025415	Cks2	11.74	10.62	11.48	0.006
A_51_P330213	NM_024184	Asf1b	12.60	11.45	12.78	0.006
A_55_P2164609	AK134945	Gm960	5.75	4.46	5.06	0.006
A_51_P240453	NM_133851	Nusap1	10.63	9.40	10.56	0.006
A_55_P2084158	--	--	8.14	7.03	8.03	0.006
A_55_P2361547	AK011855	2610201A13Rik	10.53	9.41	10.75	0.006
A_55_P1996946	NM_023223	Cdc20	14.33	13.24	14.25	0.006
A_55_P2100997	NM_001253705	Wibg	5.05	3.91	4.33	0.006
A_51_P124647	AK018169	Anapc15	7.49	6.46	7.77	0.006
A_30_P01019123	--	--	11.84	10.34	11.77	0.006
A_55_P2140383	NM_025642	Mis18a	10.91	9.89	11.01	0.006
A_55_P2175356	AK164297	Uros	7.40	6.37	6.81	0.006
A_30_P01029085	--	--	5.54	3.95	5.73	0.006
A_55_P1956507	--	--	5.35	4.28	5.14	0.006
A_55_P1964078	--	--	13.37	12.28	13.45	0.006
A_55_P1993106	--	--	8.12	6.89	7.46	0.007
A_52_P836852	NM_013698	Txk	4.59	3.35	4.64	0.007
A_30_P01030451	--	--	5.90	4.19	6.06	0.007

Table S1: Cluster 1						
Agilent ID	**GB Accession**	**Gene Symbol**	**siNS**	**siSix1**	**siSix4**	**pvalue**
A_52_P498208	NM_178183	Hist1h2ak	14.89	13.52	15.01	0.007
A_55_P1990067	--	--	13.77	12.56	13.79	0.007
A_55_P1953713	NM_013481	Bop1	13.65	12.64	13.66	0.007
A_30_P01023831	--	--	9.33	8.02	8.81	0.007
A_52_P526852	NM_026067	Eri1	9.12	7.98	9.35	0.007
A_51_P258281	NM_010253	Gal	15.59	14.24	14.37	0.007
A_55_P2020461	NM_016957	Hmgn2	11.53	10.48	11.65	0.007
A_30_P01032393	--	--	6.63	5.15	6.47	0.007
A_51_P339934	NM_010910	Nefl	11.42	8.18	9.81	0.007
A_52_P190647	NM_016662	Mxd3	8.33	6.62	7.20	0.007
A_51_P513530	NM_017407	Spag5	11.42	9.99	11.44	0.007
A_55_P2187034	--	--	13.51	12.32	13.15	0.007
A_55_P2089035	AK165879	Pole	7.68	6.49	6.97	0.007
A_55_P2109782	NM_007677	Psg17	6.87	5.84	6.32	0.007
A_52_P648601	NM_029352	Dusp9	10.18	9.14	9.76	0.007
A_55_P2167984	--	Mmd	13.39	12.33	13.23	0.007
A_55_P2183652	NR_030721	Foxd2os	8.85	7.83	8.20	0.007
A_52_P965502	NM_025965	Ssr1	9.16	7.97	9.41	0.007
A_30_P01033054	--	--	12.51	10.99	12.24	0.007
A_66_P121590	NM_133731	Prss22	6.44	4.97	6.20	0.007
A_30_P01022176	--	--	8.95	7.60	8.41	0.008
A_55_P2016166	NM_026323	Wfdc2	5.95	4.45	7.32	0.008
A_55_P2127702	NM_001253809	Racgap1	12.12	11.03	12.18	0.008
A_30_P01033613	--	--	5.13	3.53	4.57	0.008
A_30_P01018458	--	--	6.75	5.36	6.04	0.008
A_30_P01023701	--	--	9.79	8.78	9.76	0.008
A_52_P357469	NM_010237	Frk	8.58	6.94	8.87	0.008
A_55_P2104289	--	--	8.94	7.82	9.29	0.008
A_55_P2097553	NM_001033189	C77080	12.07	10.98	12.03	0.008
A_51_P241995	NM_016919	Col5a3	11.44	10.06	10.60	0.008
A_55_P2007022	NM_011925	Cd97	14.85	13.83	14.71	0.008
A_55_P2145029	NM_001033411	Gm826	7.31	5.96	7.00	0.008
A_55_P2128646	NM_020567	Gmnn	10.56	9.41	10.57	0.008
A_55_P2056654	NM_145588	Kif22	13.50	12.05	13.31	0.008
A_30_P01017632	--	--	11.48	9.92	11.44	0.008
A_51_P191649	NM_023294	Ndc80	10.10	8.59	9.86	0.008
A_51_P519791	NM_198605	Ska3	10.00	8.79	9.79	0.008
A_30_P01023785	--	--	10.17	9.11	10.17	0.009
A_66_P139052	NM_001039038	Nhlrc4	5.69	4.55	5.30	0.009

Table S1: Cluster 1						
Agilent ID	**GB Accession**	**Gene Symbol**	**siNS**	**siSix1**	**siSix4**	**pvalue**
A_55_P2075806	XM_985247	Gm8220	5.56	3.38	4.56	0.009
A_66_P111562	NM_007631	Ccnd1	16.36	14.96	16.30	0.009
A_51_P495462	NM_008078	Gad2	5.83	3.57	6.40	0.009
A_55_P1995007	NM_181416	Arhgap11a	10.17	9.14	10.15	0.009
A_55_P2026214	--	--	13.32	12.23	13.22	0.009
A_55_P2047489	NM_009790	Calm1	16.04	14.93	16.43	0.009
A_55_P2063146	--	--	13.20	11.96	13.15	0.009
A_55_P2074762	NM_010702	Lect2	6.61	5.00	7.04	0.009
A_55_P1983773	NM_001012273	Birc5	15.25	14.00	15.36	0.009
A_55_P2094964	XM_003084619	Gm7931	11.11	10.07	11.16	0.010
A_51_P247637	NM_080563	Rnf144a	7.15	5.54	6.15	0.010
A_30_P01029884	--	--	5.13	3.54	4.87	0.010
A_55_P2124791	NM_001109991	Col18a1	15.34	14.17	15.12	0.010
A_55_P1980636	NM_011497	Aurka	13.50	12.48	13.52	0.010
A_55_P2152427	NM_026507	Zwilch	12.00	10.63	12.14	0.010
A_66_P118600	NM_008480	Lama1	6.05	4.86	4.16	0.010
A_55_P2059695	NM_173437	Nav1	7.88	6.70	7.74	0.010
A_55_P2149107	NM_201364	BC055324	9.18	8.14	9.05	0.010
A_55_P2125401	NM_001024717	Gal3st3	6.02	4.84	5.30	0.010
A_55_P2115216	NM_001013816	Gm5622	6.15	3.45	5.36	0.011
A_55_P2013336	NM_010790	Melk	11.37	9.88	11.28	0.011
A_52_P139650	NM_025581	Ska1	11.04	9.27	10.72	0.011
A_55_P2026779	NR_073362	1700091H14Rik	6.72	4.53	5.73	0.011
A_55_P2252251	NR_034155	Olfr1372-ps1	9.13	8.13	9.39	0.011
A_52_P622244	NM_176921	6030419C18Rik	9.36	8.09	9.09	0.011
A_55_P2160168	NM_011164	Prl	7.82	6.46	8.57	0.011
A_30_P01026687	--	--	7.28	5.98	6.75	0.011
A_51_P481221	NM_019517	Bace2	6.29	4.39	7.26	0.011
A_55_P2007273	NM_011132	Pole	12.67	11.52	12.42	0.011
A_55_P2005838	NM_029835	Ticrr	10.34	8.83	10.21	0.011
A_51_P324814	NM_010664	Krt18	10.55	9.27	11.89	0.012
A_52_P154101	NM_001033954	Calca	6.98	5.78	6.08	0.012
A_51_P366138	NM_008587	Mertk	8.14	6.42	9.00	0.012
A_52_P235347	NM_020013	Fgf21	9.69	7.75	9.11	0.012
A_66_P120125	NM_053078	Nrep	12.49	10.98	11.72	0.012
A_55_P2046509	NM_153319	Amot	12.01	10.96	12.34	0.012
A_65_P17827	NM_027429	Cenpl	9.32	8.21	9.12	0.012
A_55_P2048588	NM_007659	Cdk1	12.76	11.56	12.29	0.012
A_55_P2229098	NR_046029	Gm20758	6.69	5.61	5.80	0.012

Table S1: Cluster 1						
Agilent ID	**GB Accession**	**Gene Symbol**	**siNS**	**siSix1**	**siSix4**	**pvalue**
A_30_P01018123	--	--	5.59	3.78	5.40	0.012
A_30_P01027827	--	--	10.25	9.22	10.45	0.012
A_30_P01030483	--	--	8.76	7.76	8.42	0.013
A_51_P351363	NR_000040	Tyms-ps	12.26	11.03	12.06	0.013
A_30_P01019195	--	--	5.99	4.98	5.78	0.013
A_55_P2081116	NM_001081120	Fam89a	6.31	5.06	5.21	0.013
A_51_P146560	NM_018857	Msln	14.56	13.21	14.86	0.013
A_55_P2162136	NM_016957	Hmgn2	13.97	12.95	13.94	0.013
A_52_P245277	NM_009267	Spt1	4.74	3.00	4.35	0.013
A_55_P2101757	NM_183089	Dscc1	9.38	8.21	9.41	0.013
A_66_P125209	NM_134471	Kif2c	8.90	7.34	8.90	0.013
A_30_P01017915	--	--	8.70	7.44	8.27	0.014
A_52_P211223	NM_175384	Cdca2	10.18	8.52	9.99	0.014
A_55_P2064984	NM_145924	Cenpi	10.59	9.43	10.48	0.014
A_55_P2131048	--	--	4.80	3.56	4.81	0.014
A_55_P2017120	XM_003945537	--	5.49	3.72	4.51	0.014
A_51_P490509	NM_009773	Bub1b	11.08	9.53	10.99	0.014
A_55_P1969276	NM_020259	Hhip	10.11	8.94	10.29	0.014
A_51_P455932	NM_007974	F2rl1	5.57	4.38	6.99	0.015
A_51_P292073	NM_026897	Haghl	12.85	11.69	12.69	0.015
A_55_P2170454	NM_008182	Gsta2	8.78	6.93	8.53	0.015
A_30_P01027398	--	--	9.17	7.72	8.54	0.015
A_55_P1953087	NM_008563	Mcm3	14.17	13.16	14.05	0.015
A_55_P1967201	NM_177652	Ryr3	6.34	5.27	5.69	0.015
A_55_P2035400	NM_023663	Ripk4	5.17	4.12	6.02	0.015
A_66_P130541	NM_011634	Traip	7.92	6.42	7.68	0.015
A_65_P15295	--	--	4.71	3.21	4.40	0.015
A_52_P473953	NM_133710	Ctdspl	8.54	7.19	8.46	0.015
A_55_P1996941	NM_026785	Ube2c	13.20	12.00	12.99	0.015
A_51_P363556	NM_198127	Abi2	9.56	8.34	9.76	0.016
A_52_P84901	NM_133891	Slc44a1	10.53	9.26	10.09	0.016
A_55_P1958097	NM_023119	Eno1	17.70	16.56	17.31	0.016
A_55_P2046003	XM_984613	Gm8165	5.56	3.76	4.58	0.016
A_55_P2133220	NM_001013377	Arhgef39	9.53	8.02	9.20	0.016
A_52_P28806	NM_008021	Foxm1	10.96	9.73	10.74	0.016
A_51_P155142	NM_026560	Cdca8	13.96	12.74	13.90	0.016
A_51_P303749	NM_178683	Depdc1b	9.61	7.88	9.61	0.016
A_55_P2133255	NM_019499	Mad2l1	12.69	11.55	12.74	0.016
A_55_P2286243	AK038689	Srrm4os	5.81	3.76	4.43	0.017

Table S1: Cluster 1						
Agilent ID	**GB Accession**	**Gene Symbol**	**siNS**	**siSix1**	**siSix4**	**pvalue**
A_51_P429308	NM_001081324	Neto2	7.19	6.03	6.89	0.017
A_51_P496540	NM_012009	Sh2d1b1	6.78	5.57	7.65	0.017
A_66_P132695	NM_001200025	1700015F17Rik	5.32	4.31	5.43	0.017
A_52_P487362	NM_028980	Ppp4r4	6.47	5.22	6.45	0.017
A_55_P2004896	--	--	6.63	4.35	5.85	0.017
A_55_P2017116	--	--	5.29	3.43	5.28	0.017
A_51_P254805	NM_008446	Kif4	10.22	8.86	10.15	0.017
A_52_P377537	NM_010250	Gabra1	6.66	5.37	7.02	0.017
A_52_P418489	NM_023476	Tinagl1	8.43	7.13	8.48	0.017
A_51_P501018	NM_010892	Nek2	10.42	8.96	10.31	0.017
A_51_P469053	NM_172510	Mfsd4	9.18	8.05	8.86	0.018
A_55_P2059352	NM_001109991	Col18a1	15.87	14.67	15.76	0.018
A_52_P330214	NM_016925	Fanca	11.31	10.10	11.24	0.018
A_52_P513123	NM_177372	Dna2	8.13	7.03	7.45	0.018
A_52_P30989	NM_028222	Cdkn3	9.43	8.30	9.44	0.018
A_55_P1965812	--	--	5.28	3.86	4.80	0.018
A_30_P01024322	--	--	10.09	8.55	9.45	0.018
A_55_P1997141	NM_008652	Mybl2	12.48	11.30	12.54	0.018
A_65_P20799	NM_001198571	Abi2	7.81	6.60	8.03	0.018
A_66_P133404	NM_026515	2810417H13Rik	9.92	8.22	9.61	0.018
A_55_P2059046	NM_172287	Spire2	6.42	5.39	5.95	0.018
A_30_P01029324	--	--	7.43	6.19	7.23	0.019
A_51_P179578	NM_010262	Gbx2	5.65	4.02	4.39	0.019
A_30_P01033624	--	--	6.43	5.40	5.81	0.019
A_55_P2099139	XM_984157	Gm8127	5.95	4.31	5.32	0.019
A_52_P26299	NM_178675	Slc35f1	10.51	9.37	10.84	0.019
A_55_P1988310	NM_153504	Rnf183	7.98	6.15	7.10	0.019
A_30_P01024363	--	--	5.43	4.04	5.69	0.019
A_55_P1991688	NM_009013	Rad51ap1	11.84	10.63	11.63	0.019
A_55_P2309100	NM_024291	Ky	5.44	3.14	4.13	0.019
A_52_P399584	NM_181589	Ckap2l	10.04	8.45	9.79	0.019
A_55_P1954698	XR_105111	--	6.49	5.46	6.35	0.019
A_55_P2020458	--	--	12.60	11.32	12.44	0.020
A_30_P01023847	--	--	8.24	7.13	8.31	0.020
A_51_P506961	NM_020293	Cldn9	8.29	7.26	7.94	0.020
A_55_P2057459	NM_145532	Mall	5.55	3.31	5.70	0.020
A_55_P2130408	XM_003946044	LOC101056010	8.32	7.13	8.35	0.020
A_30_P01023027	--	--	9.69	8.54	9.47	0.020
A_30_P01028759	--	--	5.23	3.90	5.32	0.020

Table S1: Cluster 1						
Agilent ID	**GB Accession**	**Gene Symbol**	**siNS**	**siSix1**	**siSix4**	**pvalue**
A_52_P304947	NM_028131	Cenpn	9.17	8.13	8.73	0.020
A_52_P322474	AK033210	--	8.17	6.98	7.79	0.020
A_55_P2056496	NM_009387	Tk1	13.53	11.98	13.02	0.020
A_55_P2113310	--	--	7.98	6.81	7.97	0.020
A_52_P520466	NM_197959	Kif18b	9.82	8.40	9.62	0.021
A_55_P2056473	NM_026282	Spc24	11.30	10.25	11.28	0.021
A_30_P01027041	--	--	6.67	5.65	6.25	0.021
A_55_P2024595	NM_001033436	Atxn7l1	7.31	6.23	6.88	0.021
A_51_P501656	NM_212445	Kdelc2	8.03	6.92	8.11	0.021
A_52_P27020	NM_199007	Sgol2	8.67	7.10	8.72	0.021
A_55_P1978122	NM_001159581	Mutyh	9.26	8.19	9.32	0.021
A_55_P1991718	NM_013552	Hmmr	11.91	10.80	11.88	0.021
A_52_P75348	NM_027411	Spdl1	8.35	7.19	8.40	0.021
A_66_P131979	NM_011799	Cdc6	9.73	8.29	9.63	0.021
A_55_P2081615	NM_001164081	Timeless	9.11	7.87	8.76	0.021
A_55_P2064038	--	--	10.29	9.13	10.05	0.022
A_30_P01031710	--	--	6.21	4.73	5.91	0.022
A_66_P116362	AK033758	Gm3428	6.85	5.76	6.12	0.022
A_55_P1953567	XM_003945535	LOC101056136	6.82	4.89	5.65	0.022
A_55_P2086659	NM_009015	Rad54l	9.70	8.45	9.45	0.022
A_55_P2065671	NM_172301	Ccnb1	13.48	12.30	13.51	0.022
A_55_P2086143	NM_018887	Cyp39a1	9.29	8.06	9.52	0.022
A_30_P01022821	--	--	9.95	8.53	9.30	0.023
A_51_P356931	NM_011015	Orc1	7.85	6.83	7.59	0.023
A_55_P2137049	NM_001004174	AA467197	11.89	10.88	12.45	0.023
A_30_P01023120	--	--	5.93	4.70	5.97	0.023
A_52_P420466	NM_175660	Hist1h2ab	15.69	14.69	15.84	0.023
A_52_P658437	NM_001014976	Espl1	10.49	8.88	10.14	0.023
A_51_P125135	NM_026410	Cdca5	12.38	10.96	12.39	0.024
A_51_P440743	NM_009886	Celsr1	5.83	3.73	3.88	0.024
A_52_P114962	NM_183289	Tcerg1l	5.66	3.79	3.92	0.024
A_55_P2100209	NM_134471	Kif2c	9.25	7.75	9.22	0.024
A_30_P01020205	--	--	10.12	9.08	9.82	0.024
A_55_P2106150	NM_021790	Cenpk	11.66	10.47	11.59	0.024
A_51_P324934	AK088142	Mcm3	13.59	12.53	13.36	0.024
A_55_P1982325	NM_022565	Ndst4	6.72	3.95	6.84	0.024
A_51_P105709	NM_027182	Trip13	12.28	11.25	12.43	0.025
A_55_P1958537	NM_001043355	Map6	13.05	11.79	13.01	0.025
A_51_P451151	NM_026785	Ube2c	13.49	12.27	13.28	0.025

Table S1: Cluster 1						
Agilent ID	**GB Accession**	**Gene Symbol**	**siNS**	**siSix1**	**siSix4**	**pvalue**
A_55_P2103796	NM_181416	Arhgap11a	10.06	8.99	9.53	0.025
A_55_P2103706	--	--	12.63	11.44	12.76	0.025
A_51_P393958	NM_025995	Fbxo5	12.42	11.10	12.34	0.025
A_55_P2014665	NM_001253809	Racgap1	11.35	10.16	11.37	0.025
A_51_P230098	NM_023209	Pbk	11.23	9.73	10.88	0.025
A_55_P2067971	NM_027640	Prss54	5.37	4.10	5.01	0.025
A_30_P01031741	--	--	5.25	3.79	4.49	0.025
A_30_P01021634	--	--	4.73	3.70	4.29	0.025
A_55_P1979659	NM_198654	Nsl1	5.98	4.65	5.75	0.025
A_30_P01024160	--	--	6.18	4.62	6.04	0.026
A_51_P208680	NM_145409	Chtf18	11.79	10.72	11.63	0.026
A_55_P2094963	--	--	10.62	9.39	10.32	0.026
A_55_P2117614	NM_028075	Tnfrsf13c	6.66	4.13	5.20	0.026
A_30_P01030893	--	--	6.95	5.58	6.43	0.026
A_55_P2102065	NM_001122660	Gm10639	9.85	8.08	9.70	0.026
A_66_P134542	NM_028390	Anln	13.68	12.48	13.47	0.026
A_30_P01017882	--	--	9.13	7.54	8.43	0.027
A_52_P64763	NM_177331	Gen1	8.70	7.23	8.41	0.027
A_55_P2170681	NM_026560	Cdca8	11.14	9.95	11.06	0.027
A_52_P95294	NM_183289	Tcerg1l	8.16	5.88	6.11	0.027
A_30_P01029458	--	--	5.38	4.28	5.90	0.027
A_55_P1988228	NM_009791	Aspm	10.75	9.40	10.95	0.027
A_55_P2040743	NM_026507	Zwilch	10.91	9.72	11.01	0.027
A_52_P529570	NM_198654	Nsl1	10.83	9.36	10.74	0.028
A_30_P01021589	--	--	6.46	4.53	4.70	0.028
A_55_P1979126	NM_009446	Tuba3a	5.04	3.86	3.91	0.028
A_55_P2070331	AK146072	5830416P10Rik	8.42	6.66	8.35	0.028
A_51_P347154	NM_010084	Adam18	5.53	4.25	4.78	0.028
A_55_P1979103	NM_175528	E330009J07Rik	5.82	4.68	5.33	0.028
A_66_P133993	XM_286185	Gm5093	13.99	12.27	13.65	0.029
A_51_P237668	NM_009749	Bex2	7.76	5.93	7.34	0.029
A_52_P306357	BC042707	Prok1	7.72	6.07	7.14	0.029
A_30_P01030372	--	--	4.88	3.57	3.41	0.029
A_30_P01028303	--	--	15.78	14.78	15.66	0.029
A_52_P476075	NM_175554	Clspn	8.63	7.31	8.63	0.029
A_51_P231549	NM_153761	Mill2	5.07	3.86	5.32	0.029
A_30_P01021663	--	--	5.94	3.62	5.41	0.029
A_55_P2028288	NM_001039038	Nhlrc4	10.17	8.79	10.42	0.030
A_55_P2176185	NM_001142746	Pcdh15	5.34	3.85	5.77	0.030

Table S1: Cluster 1						
Agilent ID	**GB Accession**	**Gene Symbol**	**siNS**	**siSix1**	**siSix4**	**pvalue**
A_55_P2143376	--	--	7.73	5.79	7.44	0.030
A_51_P487999	NM_028232	Sgol1	11.89	10.68	12.04	0.030
A_30_P01022863	--	--	4.54	3.12	4.45	0.030
A_30_P01031372	--	--	4.52	2.88	4.39	0.030
A_55_P2109633	NM_009331	Tcf7	5.19	3.79	5.12	0.031
A_55_P1953353	NM_001039155	Triobp	6.63	5.56	6.48	0.031
A_51_P302139	NM_025979	Mastl	8.86	7.45	8.90	0.032
A_51_P286665	NM_011249	Rbl1	9.92	8.91	9.96	0.032
A_52_P649561	NM_175256	Heg1	5.67	4.29	5.51	0.032
A_66_P106275	AY007717	Mutyh	7.80	6.55	7.78	0.032
A_52_P195018	NM_139206	Arap3	9.25	7.96	8.89	0.033
A_52_P376169	NM_177139	Lypd6	8.48	7.41	8.14	0.033
A_52_P110534	NM_009445	Ttk	8.10	6.48	8.15	0.033
A_51_P120717	NM_010721	Lmnb1	12.40	11.00	11.71	0.033
A_55_P2058942	NM_026316	Aldh3b1	11.31	10.27	11.53	0.033
A_55_P2128181	--	--	11.11	10.10	11.14	0.034
A_51_P254045	NM_011634	Traip	10.94	9.61	11.03	0.034
A_52_P318073	--	--	11.10	9.85	11.07	0.034
A_51_P239984	NM_012012	Exo1	11.95	10.72	12.03	0.034
A_55_P1983769	NM_001012273	Birc5	11.61	10.37	11.47	0.034
A_51_P123134	NM_146235	Ercc6l	9.39	8.10	9.17	0.034
A_51_P204402	NM_011369	Shcbp1	11.74	10.62	12.10	0.034
A_55_P1972040	NM_001285833	Nox4	7.32	6.15	7.50	0.034
A_55_P1988246	--	--	11.19	9.92	10.47	0.034
A_55_P2414619	AK085239	B130021B11Rik	7.85	6.76	8.49	0.035
A_30_P01028973	--	--	6.96	5.64	6.15	0.035
A_55_P2313658	BG066537	--	7.47	6.19	7.38	0.035
A_55_P2028491	NM_016957	Hmgn2	12.27	11.12	12.24	0.035
A_30_P01030592	--	--	8.49	7.46	7.74	0.036
A_51_P148105	NM_011234	Rad51	11.74	10.43	11.53	0.036
A_55_P2024391	--	--	10.05	8.35	9.56	0.036
A_55_P2077263	NM_021790	Cenpk	10.87	9.77	10.73	0.037
A_55_P2383128	AK135532	6820445E23Rik	5.53	4.53	5.67	0.037
A_55_P2397869	BX520338	AI428406	5.18	4.16	5.06	0.037
A_51_P163261	--	--	10.03	8.72	10.02	0.037
A_65_P07627	NM_007826	Dach1	8.29	7.19	7.52	0.037
A_51_P117226	AK046533	Zdhhc2	8.28	6.72	8.12	0.037
A_55_P2129925	NM_008652	Mybl2	10.85	9.68	10.88	0.038
A_30_P01020518	--	--	8.91	7.37	8.82	0.038

Table S1: Cluster 1						
Agilent ID	**GB Accession**	**Gene Symbol**	**siNS**	**siSix1**	**siSix4**	**pvalue**
A_30_P01021179	--	--	8.97	7.95	8.66	0.038
A_55_P2037643	--	--	5.73	4.42	5.07	0.038
A_55_P2139878	--	--	9.66	8.40	9.68	0.038
A_52_P633714	NM_030159	Troap	8.20	7.01	8.13	0.038
A_52_P102559	NM_172644	Dars2	10.29	9.26	10.30	0.038
A_55_P1993365	--	--	9.50	8.50	9.39	0.038
A_55_P2111745	NM_001013362	Npcd	6.29	4.93	5.54	0.038
A_52_P655265	NM_175265	Bora	8.88	7.76	8.82	0.039
A_55_P2052361	NM_001011790	Olfr1382	5.25	4.00	5.12	0.039
A_55_P1953920	NM_181407	Me3	8.62	7.15	8.43	0.039
A_55_P2056493	--	Tk1	10.91	9.76	10.78	0.039
A_55_P2108012	NM_001160262	Fam78b	8.84	7.68	8.43	0.039
A_30_P01021786	--	--	5.62	4.55	4.58	0.039
A_51_P429335	NM_019429	Prss16	6.44	5.34	7.33	0.039
A_52_P556099	NM_001042653	Oip5	8.93	7.79	8.97	0.039
A_55_P1986247	NM_008051	Fut1	5.12	4.09	4.12	0.039
A_52_P148212	NM_172578	Mis18bp1	8.65	6.90	8.86	0.039
A_52_P411003	NM_144553	Dlgap5	8.66	7.29	8.72	0.039
A_55_P2068673	NM_025285	Stmn2	9.75	6.92	9.85	0.040
A_55_P1974984	BC054084	--	12.65	11.47	12.56	0.040
A_30_P01031848	--	--	10.05	9.04	9.09	0.040
A_51_P467268	NM_008547	Mak	5.56	4.42	5.84	0.040
A_55_P2020911	NM_025949	Rps6ka6	9.60	8.38	9.72	0.040
A_55_P2032946	NM_001243092	Gm3776	9.41	7.74	9.33	0.040
A_30_P01024765	--	--	6.89	5.37	6.21	0.040
A_30_P01028766	--	--	9.43	7.75	9.35	0.041
A_52_P672689	NM_007568	Btc	6.14	4.89	5.54	0.041
A_52_P139413	NM_001100462	Tmem221	7.30	5.23	4.87	0.041
A_55_P2032905	--	--	5.95	4.93	5.12	0.041
A_30_P01018791	--	--	8.29	7.08	8.13	0.041
A_55_P1983768	NM_009689	Birc5	12.55	11.19	12.33	0.041
A_65_P20433	NM_029249	Parpbp	9.00	7.72	9.09	0.041
A_55_P2111478	NM_029977	Polq	9.06	7.61	8.90	0.042
A_55_P2058962	NM_027290	Mcm10	11.86	10.61	11.81	0.042
A_30_P01018054	--	--	5.55	4.20	5.90	0.043
A_55_P2082653	NM_177747	Zfp711	6.80	5.45	6.10	0.043
A_55_P1975155	NM_001161767	Galnt6	8.34	6.39	6.87	0.043
A_55_P2016652	NM_007659	Cdk1	9.42	7.87	9.21	0.044
A_55_P1971094	NM_007957	Esx1	7.18	5.57	5.53	0.044

Table S1: Cluster 1						
Agilent ID	**GB Accession**	**Gene Symbol**	**siNS**	**siSix1**	**siSix4**	**pvalue**
A_51_P113003	NM_031863	Cenpq	9.96	8.91	10.07	0.044
A_51_P463087	NM_178269	Cenpm	8.00	6.80	7.95	0.044
A_30_P01030570	--	--	7.04	5.15	6.40	0.044
A_30_P01024983	--	--	7.16	5.91	7.19	0.045
A_51_P424810	NM_133762	Ncapg2	10.27	9.24	10.39	0.045
A_52_P213207	NM_027667	Arhgap19	5.26	3.51	4.70	0.045
A_30_P01020056	--	--	8.64	7.59	8.35	0.046
A_51_P123676	NM_177340	Synpo	6.88	5.60	5.64	0.046
A_55_P2042743	NM_008132	Glrp1	8.49	7.34	8.61	0.046
A_55_P2114776	NM_015764	Greb1	10.81	9.75	10.52	0.047
A_30_P01027000	--	--	7.16	5.83	6.64	0.047
A_51_P422497	NM_134216	Vmn1r206	5.46	4.24	4.85	0.047
A_30_P01030807	--	--	7.28	5.66	7.52	0.047
A_51_P388298	NM_025962	Mmachc	10.98	9.93	10.82	0.047
A_55_P1953919	NM_181407	Me3	9.40	7.98	9.08	0.048
A_30_P01018415	--	--	5.14	3.22	4.29	0.048
A_30_P01020366	--	--	5.09	3.90	4.50	0.049
A_55_P2050439	NM_144553	Dlgap5	9.67	8.30	9.61	0.049

Table S2: Probe list of Cluster #2

Probes categorized into Cluster #2 are listed in the following table. Agilent probe ID, Genebank accession number, gene symbol, the average log2 expression values are shown. The probes are sorted by pvalue comparing siNS with siSix1. Probes with no gene symbol are denoted with --.

Table S2: Cluster 2						
Agilent ID	**GB Accession**	**Gene Symbol**	**siNS**	**siSix1**	**siSix4**	**pvalue**
A_55_P1973906	NM_021897	Trp53inp1	8.83	10.53	9.06	0.000
A_52_P144263	NM_020296	Rbms1	10.84	11.84	11.41	0.000
A_55_P2269394	AK085021	BB116930	5.99	7.03	6.25	0.000
A_51_P215896	NM_029805	Tsc22d4	6.48	8.59	6.07	0.000
A_55_P1956267	NM_018804	Syt11	9.96	12.21	9.60	0.000
A_51_P379750	NM_021508	Myoz1	6.85	7.94	7.02	0.000
A_51_P392705	NM_009531	Xpc	9.46	10.59	10.19	0.000
A_51_P461031	NM_172416	Ostm1	10.94	11.96	11.55	0.000
A_55_P2179448	--	--	9.77	11.99	9.49	0.000
A_66_P120949	NM_011235	Rad51d	7.59	8.97	8.45	0.000
A_55_P1995195	NM_008037	Fosl2	10.74	12.47	11.55	0.000
A_52_P628590	NM_027514	Pvr	11.52	12.94	11.27	0.000
A_55_P2154416	NM_030558	Car15	7.48	9.00	7.46	0.000
A_55_P1975065	NM_001033430	Jhdm1d	5.86	7.15	6.07	0.000
A_55_P2031302	NM_001033159	Zfp597	6.83	8.07	7.20	0.000
A_55_P1972719	NM_013872	Pmm1	10.05	11.32	10.21	0.000
A_51_P158638	AK002723	Ggnbp1	7.11	8.12	7.26	0.000
A_55_P2308283	NR_045686	Gm16062	9.66	11.04	10.05	0.000
A_66_P122551	NM_011770	Ikzf2	6.07	7.33	6.56	0.000
A_55_P2088615	NM_011812	Fbln5	8.52	10.99	8.61	0.000
A_51_P227962	NM_029297	Dynlrb2	5.82	7.52	7.09	0.000
A_51_P229990	NM_029494	Rab30	5.25	6.57	5.61	0.000
A_52_P541270	NM_177687	Crebl2	7.11	9.09	7.37	0.000
A_55_P2057881	AK159765	9130011E15Rik	5.84	7.26	5.28	0.000
A_52_P142208	NM_023423	Akirin1	12.07	13.26	13.08	0.000
A_51_P235801	NM_007564	Zfp36l1	10.49	12.12	10.77	0.000
A_55_P1981241	NM_019518	Grasp	10.47	11.77	10.98	0.000
A_51_P244531	AK147342	--	9.97	11.12	10.28	0.000
A_52_P612137	NM_009822	Runx1t1	5.49	8.08	5.45	0.000
A_55_P2045891	NM_175937	Cpeb2	5.75	7.26	5.99	0.000
A_51_P324838	NM_025276	Evpl	7.59	8.70	7.86	0.000
A_55_P2109382	NM_009630	Adora2a	7.26	9.31	7.33	0.000
A_55_P2096422	NM_008381	Inhbb	10.83	12.94	10.94	0.000
A_55_P2100928	NM_008963	Ptgds	6.21	7.70	6.65	0.000
A_55_P1992040	NM_001201341	Msi2	5.19	7.23	5.32	0.000

Table S2: Cluster 2						
Agilent ID	**GB Accession**	**Gene Symbol**	**siNS**	**siSix1**	**siSix4**	**pvalue**
A_55_P2185840	NM_010924	Nnmt	8.71	10.15	9.16	0.000
A_55_P2174935	NM_001081235	Mn1	7.04	9.26	6.30	0.000
A_55_P2152014	--	--	6.72	8.15	6.61	0.000
A_66_P116860	NR_033624	5031434O11Rik	4.20	6.08	3.74	0.000
A_30_P01019010	--	--	12.81	13.88	13.09	0.000
A_51_P497317	NM_146008	Tcp11l2	7.85	9.18	8.45	0.000
A_55_P2152936	NM_199024	Nol4	6.91	8.70	6.82	0.000
A_51_P165087	NM_011427	Snai1	10.45	11.80	10.65	0.000
A_55_P2117400	AK032173	Cacng7	10.01	11.43	9.92	0.000
A_55_P2074836	NM_001202445	Mapk8ip1	11.57	13.08	11.44	0.000
A_51_P363642	NM_138581	1700088E04Rik	6.81	8.20	7.51	0.000
A_55_P1978336	NM_001163572	Tmem170b	6.39	7.92	7.19	0.000
A_30_P01026276	--	--	6.27	7.43	6.79	0.000
A_51_P169693	NM_198095	Bst2	10.16	11.53	10.66	0.000
A_55_P1959305	NM_178446	Rbm47	6.89	8.60	7.96	0.000
A_55_P2123199	NM_023423	Akirin1	10.33	11.63	11.57	0.000
A_55_P2136813	AK171768	--	8.31	9.71	8.43	0.000
A_55_P2015363	NM_023143	C1ra	4.41	6.10	4.88	0.000
A_51_P481238	NM_027293	Dopey2	11.43	12.53	11.68	0.000
A_52_P39418	NM_028181	Ccpg1	6.79	7.90	6.70	0.000
A_55_P1972720	NM_013872	Pmm1	13.62	14.89	13.87	0.000
A_30_P01020301	--	--	6.03	7.92	6.06	0.000
A_55_P1962149	NM_019536	Dnah10	3.61	7.55	4.53	0.000
A_55_P2086677	AK082185	Snrk	5.27	6.55	5.63	0.000
A_55_P2143095	--	--	7.51	8.83	7.39	0.000
A_51_P371051	NM_028608	Glipr1	8.41	10.43	8.03	0.000
A_51_P405167	NM_001025577	Maf	7.97	10.09	8.89	0.000
A_55_P1961715	NM_080637	Nme5	5.52	7.48	6.25	0.000
A_30_P01027805	--	--	4.97	7.19	5.15	0.000
A_66_P115580	AK076360	1700038P13Rik	5.16	7.81	5.73	0.000
A_55_P2089520	NM_009925	Col10a1	6.41	9.63	5.30	0.000
A_30_P01018124	--	--	5.92	8.26	5.90	0.000
A_55_P1967659	NM_030717	Lactb	9.44	10.48	10.03	0.000
A_51_P484526	NM_011915	Wif1	3.23	7.04	3.18	0.000
A_55_P2007699	NM_028016	Nanog	8.50	9.66	8.75	0.000
A_66_P126842	NM_001004178	AA415398	6.69	8.17	6.98	0.000
A_30_P01030707	--	--	4.62	5.66	4.96	0.000
A_55_P2130970	NM_001163576	Parp10	9.37	11.02	9.14	0.000
A_55_P2111459	NM_011706	Trpv2	7.97	9.36	8.04	0.000

Table S2: Cluster 2						
Agilent ID	**GB Accession**	**Gene Symbol**	**siNS**	**siSix1**	**siSix4**	**pvalue**
A_52_P489295	NM_009621	Adamts1	8.81	10.81	9.23	0.000
A_66_P132832	NM_001033208	Myzap	4.29	5.77	4.07	0.000
A_55_P1974612	NM_001112731	C030039L03Rik	7.24	8.29	6.85	0.000
A_55_P1967391	AK013005	Antxr1	6.45	7.99	6.71	0.000
A_55_P2423228	AK089957	AI464196	6.97	8.34	7.66	0.000
A_55_P2154027	NM_008968	Ptgis	12.90	14.54	13.12	0.000
A_55_P2334112	NR_027388	1700096K18Rik	4.96	6.15	5.68	0.000
A_55_P2077027	NM_001163465	Rhpn1	5.92	7.11	6.55	0.000
A_66_P110490	NM_030229	Polr3h	10.16	11.22	11.32	0.000
A_51_P438967	NM_053110	Gpnmb	11.67	13.30	11.78	0.000
A_55_P2083824	AK007003	1700085B13Rik	6.39	7.80	6.34	0.000
A_30_P01030815	--	--	6.54	7.56	6.98	0.000
A_55_P2005783	NM_027835	Ifih1	7.27	9.05	6.85	0.000
A_66_P116252	NM_130447	Dusp16	10.27	11.28	10.61	0.000
A_55_P2117853	NM_001042577	Lhx9	3.79	5.20	4.07	0.000
A_51_P491916	NM_028478	Rassf6	3.97	5.88	3.85	0.000
A_52_P533250	AK006671	--	5.09	6.40	5.12	0.000
A_55_P2061273	NM_011538	Tbx6	4.14	6.83	5.04	0.000
A_55_P2035519	NM_010628	Kif9	3.23	5.03	4.37	0.000
A_51_P345367	NM_010724	Psmb8	7.20	9.16	6.91	0.000
A_51_P435922	NM_029338	Rsph9	9.90	11.94	10.89	0.000
A_51_P343356	NM_026158	Isoc2b	9.01	10.14	9.44	0.000
A_30_P01020606	--	--	7.47	8.71	7.66	0.000
A_66_P128997	NM_178087	Pml	10.01	11.23	10.18	0.000
A_55_P1979341	NM_007806	Cyba	11.72	13.00	12.32	0.000
A_30_P01032994	--	--	8.19	9.42	8.30	0.000
A_52_P435118	NM_146258	Stard13	7.22	8.27	7.19	0.000
A_55_P2087205	AK020648	9530077C14Rik	6.70	7.94	6.42	0.000
A_51_P111612	NM_001042592	Arrdc4	5.11	6.85	6.05	0.000
A_51_P131800	NM_007806	Cyba	9.07	10.20	9.40	0.000
A_52_P494686	NM_177645	Kansl1l	8.30	9.41	8.60	0.000
A_55_P2116968	U58109	Neb	9.31	10.68	9.08	0.000
A_51_P166339	NM_009635	Avil	3.79	5.55	3.41	0.000
A_30_P01021398	--	--	7.05	8.07	6.99	0.000
A_51_P181922	XM_978251	Yjefn3	7.95	9.39	7.84	0.000
A_55_P2213828	NR_038025	4933412E12Rik	8.63	9.76	8.94	0.000
A_55_P2100968	NM_001160386	Dnah7b	6.70	8.08	7.46	0.000
A_52_P474902	NM_028518	Col20a1	4.45	6.62	4.78	0.001
A_55_P2078123	NM_013646	Rora	6.67	8.32	6.31	0.001

Table S2: Cluster 2						
Agilent ID	**GB Accession**	**Gene Symbol**	**siNS**	**siSix1**	**siSix4**	**pvalue**
A_66_P119045	XR_107832	--	8.31	9.49	8.43	0.001
A_51_P270733	NM_009303	Syngr1	7.23	8.83	7.79	0.001
A_51_P487298	NM_139307	Vasn	11.33	12.49	11.67	0.001
A_55_P2091751	--	--	8.63	9.92	8.97	0.001
A_51_P284426	NM_030137	Cstad	8.55	10.60	7.80	0.001
A_55_P1978601	NM_001177389	4933403O08Rik	5.12	6.96	5.55	0.001
A_55_P1953301	NM_146126	Sord	9.34	10.52	9.79	0.001
A_55_P2085333	NM_173401	Fbxo44	5.36	6.62	5.51	0.001
A_66_P115389	BB558042	--	11.05	12.23	11.60	0.001
A_55_P2015520	NM_133942	Plekha1	11.27	12.40	11.68	0.001
A_55_P2023391	NM_001013756	Grhl3	6.81	8.87	6.59	0.001
A_55_P2419961	NM_019933	Ptpn4	5.62	7.02	6.07	0.001
A_51_P259975	NM_023113	Aspa	6.66	8.06	7.35	0.001
A_55_P2029581	--	--	8.35	9.84	8.78	0.001
A_66_P135651	NM_023709	Capn9	5.58	6.73	5.42	0.001
A_55_P2079928	NM_201362	Ccdc68	5.01	6.21	6.06	0.001
A_30_P01032638	--	--	10.79	11.86	10.91	0.001
A_51_P203955	NM_010260	Gbp2	6.27	7.84	5.85	0.001
A_51_P350817	NM_009922	Cnn1	6.34	10.01	6.35	0.001
A_51_P183213	NM_025506	Riiad1	5.97	7.03	6.81	0.001
A_52_P131548	NM_010590	Ajuba	10.89	12.15	11.34	0.001
A_52_P87839	NM_013657	Sema3c	5.39	7.61	5.49	0.001
A_51_P173100	NM_145925	Pttg1ip	12.32	13.54	13.39	0.001
A_52_P597461	NM_011386	Skil	9.23	10.26	9.54	0.001
A_52_P220810	NM_144551	Trib2	7.23	8.60	7.31	0.001
A_30_P01024217	--	--	3.55	5.52	2.71	0.001
A_51_P117581	NM_022021	Cables1	6.84	8.40	7.67	0.001
A_52_P526396	NM_178628	Atl1	5.63	7.14	5.90	0.001
A_55_P2301312	NM_146254	Wdr78	8.12	9.76	8.72	0.001
A_55_P2057681	NM_029441	Cdyl2	8.81	9.90	8.96	0.001
A_51_P239654	NM_010444	Nr4a1	11.05	12.44	12.00	0.001
A_52_P413515	NM_011770	Ikzf2	5.90	6.99	6.36	0.001
A_55_P2001903	NR_024069	Smim4	12.42	13.58	12.47	0.001
A_55_P2077558	NM_011435	Sod3	5.95	7.87	5.95	0.001
A_55_P2075294	--	--	7.21	8.48	6.75	0.001
A_55_P2174203	NM_144862	Lims2	8.50	10.52	8.42	0.001
A_52_P324754	NM_026916	Nupr1l	6.80	7.84	6.83	0.001
A_55_P2162727	NM_183000	Asic3	5.81	7.18	5.90	0.001
A_55_P2186180	NM_026209	Saysd1	5.11	6.25	5.01	0.001

Table S2: Cluster 2						
Agilent ID	**GB Accession**	**Gene Symbol**	**siNS**	**siSix1**	**siSix4**	**pvalue**
A_55_P2119927	CB193388	--	6.03	7.87	7.03	0.001
A_55_P2199717	NR_077223	9330102E08Rik	7.89	8.89	7.94	0.001
A_51_P425071	NM_030888	C1qtnf3	10.16	11.94	9.01	0.001
A_66_P120603	NM_032000	Trps1	8.96	10.05	9.18	0.001
A_51_P384318	NM_023143	C1ra	4.11	6.18	4.47	0.001
A_55_P2182452	NM_177371	Tnfsf15	6.58	7.79	6.48	0.001
A_55_P2066116	NM_033601	Bcl3	10.91	11.94	11.33	0.001
A_55_P2085974	NM_010512	Igf1	4.84	7.88	6.64	0.001
A_30_P01026788	--	--	7.28	8.67	7.31	0.001
A_66_P100586	AK042039	--	4.46	5.91	4.76	0.001
A_51_P175580	NM_021897	Trp53inp1	11.73	13.53	12.05	0.001
A_52_P254174	NM_008173	Nr3c1	7.03	8.54	7.43	0.001
A_55_P2041961	NM_007553	Bmp2	6.32	8.38	6.96	0.001
A_52_P123944	NM_029730	Mospd2	7.38	8.45	7.77	0.001
A_55_P2013751	NM_207228	Tsga10	4.95	6.19	4.91	0.001
A_30_P01026151	--	--	3.65	5.89	4.13	0.001
A_30_P01022603	--	--	4.70	6.29	4.78	0.001
A_52_P600946	NM_026681	Ccdc88c	4.17	5.24	4.08	0.001
A_51_P220806	NM_008110	Gdf9	7.60	9.01	7.64	0.001
A_52_P637812	NM_178695	Prrg4	9.48	10.53	10.38	0.001
A_55_P2021146	NM_145132	Mchr1	3.84	6.68	3.55	0.001
A_52_P376360	NM_019971	Pdgfc	10.51	11.94	10.58	0.001
A_51_P290074	NM_021272	Fabp7	8.54	9.95	9.09	0.001
A_30_P01021929	--	--	12.19	13.31	12.24	0.001
A_30_P01030784	--	--	9.33	10.65	9.62	0.001
A_51_P237575	NM_023423	Akirin1	12.68	13.69	13.92	0.001
A_52_P46085	NM_080638	Mvp	10.51	11.53	10.72	0.001
A_30_P01018472	--	--	6.99	8.13	7.10	0.001
A_30_P01025844	--	--	7.13	8.89	6.73	0.001
A_52_P153291	NM_145700	Ackr4	3.40	5.90	4.10	0.001
A_55_P2031631	NM_010512	Igf1	7.18	10.40	7.65	0.001
A_51_P165504	NM_007855	Twist2	8.77	9.93	8.53	0.001
A_52_P33831	NM_027164	Lrrc27	4.85	6.33	5.45	0.001
A_30_P01020812	--	--	7.63	8.82	7.61	0.001
A_55_P2032079	NM_016974	Dbp	9.80	10.99	10.04	0.001
A_55_P2085984	NM_010512	Igf1	6.89	10.24	7.53	0.001
A_30_P01018499	--	--	6.92	7.96	7.38	0.001
A_66_P100165	NM_009250	Serpini1	4.08	5.91	4.50	0.001
A_55_P1999641	NM_177863	Frem1	3.99	7.61	4.75	0.001

Table S2: Cluster 2						
Agilent ID	**GB Accession**	**Gene Symbol**	**siNS**	**siSix1**	**siSix4**	**pvalue**
A_30_P01023348	--	--	8.92	9.97	9.07	0.001
A_30_P01023371	--	--	4.89	6.47	4.09	0.001
A_52_P618379	NM_028756	Slc35a5	5.21	6.27	5.84	0.001
A_55_P1961567	NM_026875	Ypel3	11.63	12.69	11.92	0.001
A_66_P105074	NM_032003	Enpp5	6.82	8.40	7.11	0.001
A_52_P239536	NM_181595	Ppp1r9a	8.69	9.82	8.44	0.001
A_51_P112355	NM_018738	Igtp	8.44	10.23	8.83	0.001
A_55_P2093849	NM_199024	Nol4	5.50	6.55	5.34	0.001
A_51_P227165	NM_025865	2310030G06Rik	7.95	9.03	7.78	0.001
A_55_P2029106	NM_138313	Bmf	6.84	8.60	7.28	0.001
A_30_P01031064	--	--	4.82	6.00	5.71	0.001
A_55_P2107667	NM_010135	Enah	8.41	9.43	8.53	0.002
A_55_P2394308	NM_008046	Fst	10.72	13.02	11.04	0.002
A_55_P2180934	XR_140622	Gm8273	7.74	8.91	7.82	0.002
A_30_P01026564	--	--	6.33	7.92	5.74	0.002
A_55_P2022793	NM_011643	Trpc1	5.01	6.14	5.42	0.002
A_55_P2037428	NM_026713	Mogat1	4.13	5.85	3.37	0.002
A_55_P2054350	NM_173401	Fbxo44	7.64	8.88	8.14	0.002
A_55_P1982420	NM_001033192	C78339	10.82	11.84	10.87	0.002
A_30_P01033655	--	--	3.61	4.92	4.66	0.002
A_52_P28960	NM_013526	Gdf6	6.88	8.80	8.35	0.002
A_55_P1957245	--	--	11.49	12.62	11.66	0.002
A_52_P622230	NR_045822	Gm4890	6.18	7.25	5.76	0.002
A_55_P1954196	NM_153155	C1ql3	4.99	7.08	5.78	0.002
A_51_P171616	NM_009518	Wnt10a	5.71	8.24	6.96	0.002
A_52_P159490	NM_181595	Ppp1r9a	4.10	5.75	4.48	0.002
A_52_P282500	NM_001039472	Kif21b	8.31	9.68	8.88	0.002
A_30_P01030685	--	--	5.50	6.63	6.04	0.002
A_52_P156452	NM_007717	Cmah	6.74	7.82	6.79	0.002
A_52_P257502	NM_010517	Igfbp4	8.06	9.76	7.99	0.002
A_66_P101427	AK009512	2310026L22Rik	4.61	5.84	4.05	0.002
A_52_P302544	NM_199473	Col8a2	3.52	6.44	5.50	0.002
A_30_P01019086	--	--	9.81	11.09	9.39	0.002
A_52_P220163	NR_073359	5830454E08Rik	6.37	7.44	6.10	0.002
A_30_P01026443	--	--	7.12	8.26	7.26	0.002
A_30_P01033043	--	--	9.14	10.18	9.10	0.002
A_51_P174081	NM_146073	Zdhhc14	6.80	8.01	6.83	0.002
A_51_P376238	NM_009776	Serping1	6.07	8.44	6.60	0.002
A_30_P01019643	--	--	9.37	10.39	9.23	0.002

Table S2: Cluster 2						
Agilent ID	**GB Accession**	**Gene Symbol**	**siNS**	**siSix1**	**siSix4**	**pvalue**
A_30_P01027831	--	--	8.53	9.69	8.88	0.002
A_55_P1957053	NM_001167879	Garem1	7.45	9.27	7.52	0.002
A_51_P306789	NR_015543	2810055G20Rik	6.84	8.00	7.23	0.002
A_55_P2015994	NM_013518	Fgf9	8.04	10.39	7.71	0.002
A_55_P2109257	NM_028995	Nipal3	6.85	8.13	7.67	0.002
A_51_P312121	NM_011723	Xdh	7.74	9.19	7.67	0.002
A_51_P512783	NM_025476	Rmdn1	10.47	11.57	10.42	0.002
A_52_P561161	NM_177192	Dennd5b	5.72	7.01	5.83	0.002
A_55_P1972842	NM_008453	Klf3	12.04	13.06	12.37	0.002
A_55_P2011092	NM_001033442	Gm1604b	3.69	5.20	3.74	0.002
A_51_P387123	NM_011854	Oasl2	6.37	7.89	5.10	0.002
A_55_P1969058	NM_001122889	Epha7	7.28	8.29	7.76	0.002
A_51_P148069	NM_001134829	Lpgat1	12.30	13.52	12.79	0.002
A_55_P2093704	NM_008579	Meig1	4.07	5.88	5.35	0.002
A_55_P2003828	NR_073370	4930451G09Rik	4.53	5.68	5.81	0.002
A_55_P2024463	NM_198100	Tbkbp1	4.91	5.98	5.03	0.002
A_30_P01017815	--	--	4.62	5.99	4.26	0.002
A_30_P01024457	--	--	7.48	8.62	7.74	0.002
A_55_P2161400	NM_001012322	Sctr	9.02	10.50	8.41	0.002
A_51_P345649	NM_011058	Pdgfra	6.74	8.33	6.53	0.002
A_30_P01030050	--	--	5.44	6.54	6.34	0.002
A_55_P1968235	NM_016858	Rab33b	10.29	11.47	10.22	0.002
A_55_P1998957	NM_033541	Oas1c	5.72	6.80	6.50	0.002
A_30_P01028637	--	--	9.09	10.25	9.20	0.003
A_55_P2019483	NM_001195006	Ndrg4	12.26	13.36	12.80	0.003
A_55_P2127258	NM_172708	Dok7	9.97	11.07	10.01	0.003
A_30_P01033272	--	--	4.96	6.04	5.67	0.003
A_30_P01030338	--	--	9.84	10.92	9.99	0.003
A_52_P454295	NM_011652	Ttn	11.86	12.97	11.03	0.003
A_55_P2010871	NM_001008231	Daam2	7.64	9.88	7.64	0.003
A_51_P137184	NM_029608	Fam209	4.82	6.07	4.89	0.003
A_55_P2118866	NM_001284519	Cmah	6.51	7.57	6.44	0.003
A_52_P248343	NM_153789	Mylip	4.93	6.19	5.30	0.003
A_55_P2220937	NM_027715	Otud1	6.85	7.96	7.38	0.003
A_55_P2024993	NM_010459	Hoxb4	7.32	8.74	8.02	0.003
A_55_P1970164	NM_013876	Rnf11	11.81	12.91	12.12	0.003
A_55_P2043382	NM_001252532	Llgl2	6.24	7.34	7.04	0.003
A_52_P522255	NM_011097	Pitx1	7.44	9.03	7.24	0.003

Table S2: Cluster 2						
Agilent ID	**GB Accession**	**Gene Symbol**	**siNS**	**siSix1**	**siSix4**	**pvalue**
A_30_P01031353	--	--	3.60	4.85	4.93	0.003
A_30_P01032845	--	--	4.69	6.14	5.40	0.003
A_52_P252953	NM_053144	Pcdhb19	3.56	5.06	4.45	0.003
A_30_P01029275	--	--	5.15	6.19	5.48	0.003
A_55_P2111533	NM_001081053	Itga10	7.74	9.22	8.18	0.003
A_51_P391716	NM_013848	Ermap	6.38	7.79	5.26	0.003
A_55_P1966833	NM_001037713	Xaf1	7.20	9.02	6.82	0.003
A_55_P2050226	AY072938	Ackr4	4.80	7.02	6.03	0.003
A_52_P604735	AK089994	Fbxl2	5.06	6.87	6.46	0.003
A_55_P1958220	NM_177687	Crebl2	5.11	6.48	4.99	0.003
A_52_P543079	NM_001081131	Dhtkd1	5.88	6.96	6.65	0.003
A_51_P470328	NM_001042614	Sepp1	9.30	10.50	9.54	0.003
A_55_P1981949	NM_175174	Klhl5	10.52	11.54	10.82	0.003
A_55_P2190426	NM_011377	Sim2	8.38	9.73	8.95	0.003
A_55_P1961034	NM_001161608	Gm13272	9.91	10.93	10.03	0.003
A_30_P01028374	--	--	10.18	11.32	10.70	0.003
A_55_P1962675	NM_001033430	Jhdm1d	5.83	7.13	5.66	0.003
A_55_P1978646	AK044481	Wasf3	5.03	6.64	5.88	0.003
A_55_P1992019	NM_001083119	Ptpru	6.39	7.60	6.22	0.003
A_30_P01019173	--	--	10.83	11.96	11.15	0.003
A_52_P569375	NM_010203	Fgf5	7.97	9.18	7.99	0.003
A_30_P01019594	--	--	9.85	11.06	10.06	0.003
A_55_P2003438	NM_010264	Nr6a1	5.16	6.40	6.07	0.003
A_52_P560848	NM_029198	4930538K18Rik	3.90	5.59	2.42	0.003
A_55_P2066862	NM_027602	Nsun7	4.10	6.36	4.66	0.003
A_52_P1026777	NM_001033141	Ecscr	4.84	6.33	4.56	0.003
A_51_P169516	NM_001085501	Ppp1r3d	8.36	9.82	8.97	0.003
A_55_P2148688	--	Nipal3	6.46	7.69	7.28	0.003
A_55_P2016462	NM_021274	Cxcl10	6.29	9.38	5.79	0.003
A_55_P2097913	NM_001081053	Itga10	7.69	9.20	8.17	0.003
A_66_P111090	NM_001012322	Sctr	9.06	10.58	8.47	0.003
A_52_P563340	NR_024069	Smim4	12.40	13.48	12.47	0.004
A_55_P2153031	NM_011652	Ttn	10.29	11.37	9.76	0.004
A_52_P449259	NM_029570	Atp11b	5.34	6.47	5.05	0.004
A_51_P254425	NM_009644	Ahrr	7.55	8.77	8.08	0.004
A_30_P01021129	--	--	10.20	11.29	10.71	0.004
A_55_P1997225	NM_001033263	Agap2	5.64	7.71	4.96	0.004
A_30_P01025339	--	--	10.13	11.30	10.72	0.004
A_30_P01026224	--	--	6.51	7.60	6.59	0.004
A_51_P175567	NM_001190466	Dact1	6.31	7.86	5.71	0.004

Table S2: Cluster 2						
Agilent ID	**GB Accession**	**Gene Symbol**	**siNS**	**siSix1**	**siSix4**	**pvalue**
A_55_P2033376	NM_001163145	1810041L15Rik	9.24	11.31	7.81	0.004
A_51_P268094	NM_009255	Serpine2	11.39	12.39	11.69	0.004
A_66_P113662	NM_175285	Tmem62	9.33	10.46	9.88	0.004
A_52_P486718	NM_001085421	Tspyl5	4.50	5.85	4.78	0.004
A_30_P01019023	--	--	4.63	6.21	4.12	0.004
A_30_P01022594	--	--	10.92	12.03	10.90	0.004
A_55_P2005585	NM_032000	Trps1	9.25	10.27	9.55	0.004
A_66_P115161	NM_001204983	Cep85l	7.05	8.19	6.95	0.004
A_30_P01018769	--	--	6.45	7.52	6.69	0.004
A_30_P01029305	--	--	10.23	11.37	10.88	0.004
A_55_P2057118	AY540040	Mid1	4.77	6.19	5.24	0.004
A_51_P272876	NM_001160378	Fam46a	6.47	8.00	6.97	0.004
A_30_P01024294	--	--	4.67	5.87	5.43	0.004
A_55_P2183015	NM_011026	P2rx4	11.14	12.29	11.73	0.004
A_55_P2135526	NM_010371	Gzmc	4.76	6.06	7.24	0.004
A_52_P364232	NM_011083	Pik3c2a	8.46	9.62	9.38	0.004
A_30_P01030378	--	--	8.66	9.76	8.25	0.004
A_30_P01028906	--	--	4.09	5.42	4.33	0.004
A_55_P1952182	NM_001104573	Vmn2r111	8.03	9.10	8.24	0.004
A_30_P01026167	--	--	9.45	10.54	9.77	0.004
A_55_P2361647	NR_030700	4831440E17Rik	5.73	6.89	5.23	0.004
A_55_P2086741	--	Fam3a	5.53	6.61	5.51	0.004
A_55_P2068233	NM_001005748	Phactr1	5.58	6.66	5.30	0.005
A_55_P2319468	NR_015553	9430076C15Rik	6.10	7.14	6.48	0.005
A_30_P01027194	--	--	5.92	7.39	6.24	0.005
A_55_P2009217	NR_004415	Rnu3b1	11.29	12.30	11.27	0.005
A_55_P2075661	AK030799	--	7.33	9.04	7.28	0.005
A_51_P359800	NM_009131	Clec11a	5.82	6.94	5.28	0.005
A_30_P01026806	--	--	6.45	7.62	7.19	0.005
A_51_P198694	NM_144909	Gckr	3.83	5.73	3.95	0.005
A_55_P2155216	NM_001024851	Ankrd34a	8.84	10.08	9.29	0.005
A_30_P01024279	--	--	3.73	5.17	4.24	0.005
A_51_P111962	NM_001141922	Bean1	8.64	9.74	7.77	0.005
A_55_P2093705	NM_008579	Meig1	4.93	6.97	6.23	0.005
A_55_P2169775	--	--	5.49	6.89	5.71	0.005
A_52_P638459	NM_013653	Ccl5	8.01	10.37	7.39	0.005
A_55_P1998816	XM_003945593	LOC101056249	5.74	7.04	5.80	0.005
A_52_P393314	NM_011027	P2rx7	8.54	9.79	9.28	0.005
A_30_P01022977	--	--	9.24	10.45	8.82	0.005

Table S2: Cluster 2						
Agilent ID	**GB Accession**	**Gene Symbol**	**siNS**	**siSix1**	**siSix4**	**pvalue**
A_55_P2116689	NM_001285952	1700024P16Rik	4.50	6.07	4.62	0.005
A_52_P262219	NM_010234	Fos	8.00	9.51	8.58	0.005
A_65_P15245	NM_001077406	Nrp2	7.85	8.98	6.89	0.005
A_51_P257762	NM_020005	Kat2b	5.64	6.94	6.26	0.005
A_52_P730743	AK046703	--	5.01	6.68	4.90	0.005
A_55_P2022524	NM_001277116	Rbpj	8.37	9.61	8.96	0.005
A_30_P01026160	--	--	7.93	9.33	8.38	0.005
A_51_P248865	NM_010225	Foxf2	9.04	10.21	9.49	0.005
A_52_P656699	NM_013456	Actn3	13.13	14.63	11.93	0.005
A_51_P374726	NM_008987	Ptx3	5.39	7.46	5.66	0.005
A_55_P2132781	NM_009197	Slc16a2	5.93	7.86	6.52	0.005
A_55_P1959560	NR_040469	5031425E22Rik	6.10	7.22	6.38	0.005
A_55_P2104988	NM_009597	Asic1	5.91	7.11	7.40	0.005
A_55_P2287910	NM_027491	Rragd	7.21	8.42	7.47	0.005
A_55_P1961640	NM_001081198	Tmem182	6.69	8.58	5.82	0.006
A_51_P404463	NM_024283	1500015O10Rik	3.99	6.06	4.02	0.006
A_52_P771446	NR_045780	1110035M17Rik	5.90	7.49	5.43	0.006
A_55_P2164524	NM_001033813	Zfp872	4.32	5.40	4.76	0.006
A_51_P428754	NM_008168	Grik5	8.21	9.66	8.72	0.006
A_30_P01024134	--	--	6.46	7.69	6.27	0.006
A_55_P1963508	NM_001004148	Slc13a5	5.87	7.75	6.65	0.006
A_30_P01028037	--	--	5.78	7.01	5.45	0.006
A_55_P1960768	NM_001163569	Kif9	3.99	5.52	5.53	0.006
A_55_P2025820	AK036896	Plcb4	7.52	8.72	8.04	0.006
A_30_P01028139	--	--	6.16	7.26	6.23	0.006
A_30_P01022216	--	--	5.57	6.66	5.73	0.006
A_55_P1974243	NM_138942	Dbh	8.67	10.05	7.18	0.006
A_52_P193194	NM_001001321	Slc35d2	6.77	7.95	7.41	0.006
A_55_P1962305	NM_139198	Plac8	7.20	8.40	8.21	0.006
A_51_P425401	NM_175214	Kif27	3.30	5.37	4.06	0.006
A_30_P01033385	--	--	4.57	5.76	4.29	0.006
A_30_P01020880	--	--	5.73	6.98	5.95	0.006
A_55_P1984253	KC860259	--	5.55	6.84	5.57	0.006
A_30_P01027135	--	--	10.22	11.31	10.76	0.006
A_55_P2059931	NM_001163577	Prom1	5.24	6.28	5.71	0.006
A_30_P01025385	--	--	4.83	6.47	4.79	0.006
A_55_P2015485	NM_027972	Ccdc19	5.11	6.42	6.64	0.006
A_30_P01021244	--	--	4.05	5.22	4.40	0.006
A_55_P2062573	NM_001204134	C1qtnf3	12.78	13.94	11.61	0.007

Table S2: Cluster 2						
Agilent ID	**GB Accession**	**Gene Symbol**	**siNS**	**siSix1**	**siSix4**	**pvalue**
A_52_P474089	NM_007603	Capn6	6.33	8.08	7.17	0.007
A_30_P01025874	--	--	11.26	12.81	11.52	0.007
A_51_P167660	NR_027971	2610204G22Rik	4.93	5.95	4.93	0.007
A_30_P01019463	--	--	4.86	6.37	5.06	0.007
A_30_P01028855	--	--	4.41	7.52	5.74	0.007
A_66_P125948	AK170726	Cass4	4.29	5.41	4.55	0.007
A_55_P2269626	AK051229	D130019J16Rik	5.72	7.58	6.43	0.007
A_30_P01027295	--	--	3.72	5.34	4.13	0.007
A_51_P214470	NM_173744	Tdrp	4.86	6.20	5.88	0.007
A_51_P160913	NM_008209	Mr1	5.21	6.61	6.26	0.007
A_55_P1977498	NM_008311	Htr2b	8.02	9.73	8.04	0.007
A_30_P01030480	--	--	6.09	7.10	6.04	0.007
A_51_P150722	NM_010748	Lyst	4.64	5.97	5.02	0.007
A_52_P246698	NM_053090	Fam126a	5.49	6.82	6.16	0.007
A_55_P1984168	NM_007609	Casp4	5.01	7.13	5.63	0.007
A_55_P2125252	AK137555	Celf2	3.43	5.40	4.41	0.007
A_30_P01018924	--	--	4.69	5.76	4.36	0.007
A_55_P2067563	--	--	9.45	10.51	9.52	0.007
A_55_P2143025	NM_013657	Sema3c	8.75	10.73	9.07	0.008
A_51_P161021	NM_008332	Ifit2	7.29	8.30	7.60	0.008
A_55_P2121456	NM_177632	Fam43a	6.42	7.63	6.30	0.008
A_30_P01019112	--	--	8.10	9.53	8.32	0.008
A_30_P01030970	--	--	6.58	7.70	6.96	0.008
A_55_P1982127	NM_001277293	Grip1	7.39	8.53	7.75	0.008
A_52_P463977	NM_197986	Tmem140	9.78	11.16	9.68	0.008
A_55_P2000027	NM_183284	Spink2	6.22	7.54	5.78	0.008
A_55_P1961335	NM_007802	Ctsk	9.20	10.81	8.81	0.008
A_30_P01026069	--	--	12.58	13.94	12.94	0.008
A_51_P249793	NM_175118	Dusp28	9.37	10.42	9.69	0.008
A_55_P1977431	NM_001284508	Cck	11.64	14.56	11.61	0.008
A_55_P2022569	NM_001195049	Pak3	8.83	10.27	9.04	0.008
A_30_P01024659	--	--	4.21	5.58	4.98	0.008
A_55_P2023542	NM_007719	Ccr7	6.46	7.77	6.32	0.008
A_55_P1954955	NM_001199632	Fbxl13	4.93	6.08	4.67	0.008
A_52_P218379	NM_001097621	Kif26a	3.37	5.48	4.63	0.008
A_30_P01021648	--	--	4.72	6.45	4.38	0.008
A_51_P279038	NM_008904	Ppargc1a	9.92	11.12	9.85	0.008
A_51_P321743	AK161240	Slc4a3	7.42	8.47	6.88	0.009
A_55_P2133007	NM_001136056	Cntfr	5.80	7.20	6.22	0.009

Table S2: Cluster 2						
Agilent ID	**GB Accession**	**Gene Symbol**	**siNS**	**siSix1**	**siSix4**	**pvalue**
A_55_P1969392	NM_026594	Rpl39l	6.80	8.04	6.56	0.009
A_55_P2031721	NM_008718	Npas1	3.59	5.64	3.65	0.009
A_51_P417720	NM_176922	Itga11	5.67	7.34	5.61	0.009
A_30_P01024706	--	--	3.65	5.44	4.20	0.009
A_30_P01031936	--	--	7.48	9.05	7.25	0.009
A_55_P2160750	NM_198711	Col25a1	7.52	10.21	7.62	0.009
A_52_P373666	NM_001081217	Zfp174	4.32	5.86	5.44	0.009
A_55_P2116160	NM_146178	Ccdc106	5.41	6.42	5.36	0.009
A_52_P111031	NM_001013753	Pcdh17	8.24	9.90	8.99	0.009
A_52_P454183	NM_177068	Olfml2b	9.76	11.04	9.13	0.009
A_30_P01019094	--	--	4.68	5.86	5.49	0.009
A_51_P359570	NM_010501	Ifit3	5.27	7.04	5.21	0.009
A_52_P354744	NM_011401	Slc2a3	6.69	8.72	6.64	0.009
A_55_P2183597	NM_198664	Tbc1d2	10.86	12.00	11.30	0.009
A_30_P01030359	--	--	5.76	7.01	4.31	0.009
A_55_P1987409	NM_173444	Nbeal1	7.83	9.19	8.35	0.009
A_51_P334942	NM_013467	Aldh1a1	7.34	9.13	7.49	0.009
A_55_P2012146	NM_145820	Veph1	3.71	5.05	3.87	0.009
A_51_P241843	NM_178388	Tmem202	6.35	7.76	6.64	0.009
A_55_P2026982	NM_173744	Tdrp	8.22	9.41	8.91	0.009
A_55_P2235931	AK142841	D930026N18Rik	5.54	7.19	4.78	0.009
A_52_P329185	NM_013875	Pde7b	2.67	5.09	4.73	0.010
A_30_P01018721	--	--	11.40	12.47	11.77	0.010
A_52_P253044	NM_030725	Syt13	11.34	12.72	11.86	0.010
A_30_P01020209	--	--	6.74	7.77	6.79	0.010
A_55_P2016601	NM_028628	Lce1l	4.47	5.76	4.85	0.010
A_55_P2021014	NM_207278	Tigd4	5.46	6.60	5.80	0.010
A_52_P228551	NM_201367	Gpr176	9.57	11.06	9.78	0.010
A_55_P1971313	AK156978	--	5.40	6.49	5.46	0.010
A_55_P2032318	AK019690	4930522L14Rik	7.28	8.32	7.61	0.010
A_55_P2061170	NM_198664	Tbc1d2	10.31	11.47	10.66	0.010
A_55_P2035932	NM_008008	Fgf7	8.76	10.50	9.84	0.010
A_55_P2112937	NM_146578	Olfr1033	6.21	7.26	5.99	0.010
A_30_P01020899	--	--	6.22	7.57	6.51	0.011
A_55_P2361652	XR_168559	LOC101056045	5.96	7.61	6.94	0.011
A_30_P01020935	--	--	14.04	15.14	14.12	0.011
A_55_P2004142	NR_030688	Gm6402	4.51	5.74	4.63	0.011
A_55_P2124441	NM_001285936	Zdbf2	5.54	7.43	5.63	0.011
A_51_P282144	NM_011780	Adam23	6.90	8.32	6.68	0.011

Table S2: Cluster 2						
Agilent ID	**GB Accession**	**Gene Symbol**	**siNS**	**siSix1**	**siSix4**	**pvalue**
A_55_P2071236	NM_009701	Aqp5	10.85	12.37	12.49	0.011
A_55_P2102936	NM_001033225	Pnrc1	10.77	11.85	11.01	0.011
A_55_P2355330	NM_001040632	C1qtnf5	7.34	8.43	7.16	0.011
A_30_P01020973	--	--	6.19	7.63	5.87	0.012
A_30_P01033044	--	--	3.14	5.71	4.15	0.012
A_55_P1984881	NM_001285952	1700024P16Rik	4.49	5.98	4.81	0.012
A_55_P2062936	NM_013855	Abca3	10.51	11.83	10.76	0.012
A_55_P2097665	NM_001039515	Arl4a	8.94	9.98	8.57	0.012
A_30_P01022208	--	--	6.93	8.33	7.31	0.012
A_51_P383001	NM_008584	Meox2	5.07	6.76	4.18	0.012
A_30_P01032527	--	--	10.39	11.80	10.70	0.012
A_30_P01033186	--	--	4.33	5.79	4.94	0.012
A_51_P213725	NM_001285936	Zdbf2	7.43	8.94	7.23	0.012
A_52_P71105	NM_133210	Sertad3	9.87	10.89	10.51	0.012
A_30_P01029794	--	--	3.86	5.05	4.67	0.012
A_30_P01032339	--	--	4.41	6.07	4.73	0.013
A_30_P01031404	--	--	5.06	6.19	4.86	0.013
A_55_P1987694	NM_011211	Ptprd	7.99	9.27	8.44	0.013
A_30_P01029545	--	--	3.96	5.46	3.97	0.013
A_55_P1959303	NM_178446	Rbm47	3.41	5.48	4.97	0.013
A_55_P1966102	NM_080637	Nme5	8.56	9.78	9.10	0.013
A_55_P1970105	NM_013589	Ltbp2	10.53	12.16	11.02	0.013
A_66_P114768	NM_001109661	Bach2	4.83	6.63	5.06	0.013
A_55_P1994927	NM_144538	Rab3il1	10.07	11.44	10.33	0.013
A_55_P2177899	NM_001190466	Dact1	6.32	7.57	4.94	0.013
A_51_P309920	NM_001001309	Itga8	4.35	6.43	3.95	0.013
A_51_P319460	NM_011019	Osmr	8.01	9.63	8.45	0.013
A_52_P106766	NM_177352	Gk5	4.24	5.47	5.35	0.013
A_52_P229924	NM_175013	Pgm5	6.17	8.00	5.94	0.013
A_51_P249930	NM_146236	Tceal1	8.22	9.32	9.44	0.013
A_52_P305949	NM_010806	Mllt4	6.02	7.34	6.38	0.013
A_55_P1958394	NM_178804	Slit2	8.00	9.42	8.02	0.013
A_30_P01032808	--	--	4.56	5.72	4.76	0.014
A_55_P2001553	NM_020043	Igdcc4	11.28	12.49	11.82	0.014
A_51_P248666	NM_021893	Cd274	3.96	5.96	4.02	0.014
A_55_P1962747	NM_207105	H2-Ab1	5.86	7.28	6.34	0.014
A_55_P2154252	NM_013529	Gfpt2	6.83	8.68	6.70	0.014
A_30_P01031385	--	--	13.30	14.66	13.47	0.014
A_55_P2132024	NM_001282006	Tekt1	5.61	6.89	5.39	0.014

Table S2: Cluster 2						
Agilent ID	**GB Accession**	**Gene Symbol**	**siNS**	**siSix1**	**siSix4**	**pvalue**
A_52_P356698	NM_013665	Shox2	3.99	5.10	3.21	0.014
A_55_P1972872	NM_001005858	I830012O16Rik	3.43	5.97	4.67	0.014
A_51_P513032	NM_032000	Trps1	9.22	10.33	9.55	0.014
A_30_P01024553	--	--	6.01	7.15	6.24	0.015
A_30_P01030419	--	--	7.48	8.48	6.90	0.015
A_55_P1964902	XR_168453	Gm3014	9.55	10.98	9.97	0.015
A_55_P2111302	NM_007752	Cp	5.41	7.25	6.13	0.015
A_66_P131433	--	--	5.75	7.08	5.72	0.015
A_30_P01023011	--	--	3.91	5.42	3.77	0.015
A_55_P1992889	NM_009776	Serping1	7.23	9.09	7.65	0.015
A_30_P01029886	--	--	6.80	8.02	7.20	0.015
A_30_P01030776	--	--	7.22	8.24	7.49	0.015
A_52_P492081	NM_130447	Dusp16	5.66	6.74	5.64	0.015
A_30_P01025791	--	--	5.61	6.62	5.79	0.016
A_55_P1985950	NM_133213	Xpnpep2	4.20	6.41	6.05	0.016
A_51_P436594	NM_027948	1700003E16Rik	5.21	6.35	5.85	0.016
A_52_P382048	NM_001039198	Zfhx2	5.55	6.65	5.57	0.016
A_55_P2114863	NM_001166251	Mgll	5.90	7.18	4.80	0.016
A_55_P2135220	--	--	8.74	9.80	8.10	0.016
A_30_P01032637	--	--	4.67	6.00	4.14	0.016
A_55_P2054967	AK082406	Lrrc49	3.42	5.18	4.46	0.016
A_51_P240253	NM_019662	Rrad	8.08	9.74	8.31	0.017
A_51_P157042	NM_010217	Ctgf	12.26	14.13	12.50	0.017
A_55_P2074591	NM_001110218	Ppm1h	6.97	8.15	6.96	0.017
A_55_P2419021	NR_102319	9330188P03Rik	4.03	5.09	4.29	0.017
A_55_P2179964	XM_355019	Prickle4	3.86	5.69	4.16	0.017
A_55_P2056926	NM_198625	Mtss1l	10.10	11.57	10.20	0.017
A_55_P1964573	NM_152801	Arhgef6	10.07	11.49	10.25	0.017
A_55_P1996963	NM_001114098	Soga2	9.99	11.12	10.03	0.017
A_51_P348665	NM_016894	Ramp1	9.18	10.29	9.40	0.017
A_55_P2057051	XR_106099	--	6.45	7.76	6.89	0.017
A_55_P2089219	--	--	13.53	15.00	15.28	0.017
A_55_P2024461	NM_198100	Tbkbp1	9.06	10.28	9.21	0.017
A_30_P01024223	--	--	4.08	5.30	3.91	0.018
A_30_P01024958	--	--	3.63	4.80	4.44	0.018
A_55_P2052016	NM_030209	Crispld2	4.34	5.56	4.50	0.018
A_51_P511315	NM_011193	Pstpip1	7.53	8.95	6.42	0.018
A_55_P1970825	--	--	6.50	8.32	6.40	0.018
A_65_P08507	NM_001177600	Adam23	3.79	4.84	4.38	0.018

Table S2: Cluster 2						
Agilent ID	**GB Accession**	**Gene Symbol**	**siNS**	**siSix1**	**siSix4**	**pvalue**
A_55_P1971483	NM_172679	4932438A13Rik	6.30	7.48	6.67	0.018
A_30_P01023790	--	--	4.59	5.72	4.97	0.019
A_30_P01030196	--	--	6.27	7.41	5.29	0.019
A_30_P01025026	--	--	4.83	5.98	5.45	0.019
A_55_P2002578	NM_010145	Ephx1	13.23	14.32	13.98	0.019
A_55_P1970826	NM_011782	Adamts5	5.97	8.11	5.66	0.019
A_55_P2006747	NM_028657	Mfsd12	4.67	5.69	4.22	0.019
A_51_P511015	NM_010246	Fzd9	8.84	10.47	8.32	0.019
A_30_P01019537	--	--	6.98	8.48	6.39	0.019
A_30_P01018430	--	--	3.56	5.59	3.46	0.020
A_30_P01023778	--	--	3.37	4.68	4.93	0.020
A_55_P2063316	NM_001166251	Mgll	7.51	8.77	7.00	0.020
A_55_P2350720	--	--	5.56	6.68	5.73	0.020
A_51_P501844	NM_175475	Cyp26b1	9.72	11.07	11.38	0.020
A_55_P2143885	NM_001081006	Etl4	9.06	10.07	9.49	0.020
A_51_P397437	NM_183103	Prss46	6.44	7.77	3.46	0.020
A_66_P105689	NM_030684	Trim34a	4.99	6.53	5.34	0.020
A_30_P01028870	--	--	5.26	6.31	5.75	0.020
A_55_P2029558	NM_007420	Adrb2	7.32	8.66	7.53	0.020
A_52_P554650	NM_010372	Gzmd	9.14	10.46	10.63	0.021
A_55_P1960238	NM_172659	Slc2a6	9.96	11.07	9.35	0.021
A_52_P72587	NM_008859	Prkcq	4.03	5.71	3.71	0.021
A_55_P2021704	BC089320	Enpp5	6.42	7.74	7.66	0.021
A_52_P577208	NM_178672	Scfd2	4.99	6.37	5.26	0.021
A_55_P2103698	NM_015783	Isg15	9.51	11.28	9.31	0.021
A_30_P01031758	--	--	3.74	5.58	4.50	0.021
A_51_P174275	NM_027866	Colec11	4.54	5.85	5.23	0.021
A_52_P330289	NM_001024617	Inpp4b	8.15	9.38	8.46	0.022
A_30_P01029534	--	--	5.85	6.90	6.12	0.022
A_55_P2096545	NM_001099331	R3hdml	10.21	11.24	9.89	0.022
A_30_P01020515	--	--	4.89	6.42	5.33	0.022
A_51_P394814	NM_022814	Svep1	7.73	8.76	7.79	0.022
A_55_P2081105	NM_001204910	AI607873	6.55	7.87	5.94	0.022
A_55_P1965416	NM_015731	Atp9a	12.00	14.33	12.42	0.022
A_52_P585124	NM_009911	Cxcr4	9.17	10.35	9.36	0.022
A_55_P1992079	NM_011213	Ptprf	9.93	11.08	10.16	0.022
A_52_P460957	NM_013498	Crem	10.14	11.27	10.16	0.023
A_55_P2375194	XR_140553	P2rx3	5.83	6.89	6.08	0.023
A_55_P2051914	NM_001167872	Zfp568	12.02	13.18	11.34	0.023

Table S2: Cluster 2						
Agilent ID	**GB Accession**	**Gene Symbol**	**siNS**	**siSix1**	**siSix4**	**pvalue**
A_52_P154026	NM_001005426	Zcwpw1	5.27	6.48	5.53	0.023
A_52_P401484	NM_010564	Inha	9.38	10.68	8.98	0.023
A_51_P204252	NM_172497	Efhb	2.89	4.63	5.11	0.023
A_55_P2121729	--	--	3.37	5.14	3.76	0.023
A_55_P2435563	NM_001177630	Etl4	8.04	9.31	8.66	0.023
A_51_P200667	NM_053155	Clmn	4.05	5.18	3.77	0.024
A_55_P1970033	NM_011065	Per1	10.77	11.79	11.18	0.024
A_30_P01021884	--	--	5.91	6.99	4.96	0.024
A_55_P1990121	NM_009701	Aqp5	12.68	14.13	14.57	0.024
A_52_P574945	AK048993	1500026H17Rik	5.72	7.54	6.00	0.024
A_55_P2023727	NM_001001980	Limch1	7.85	9.76	7.05	0.024
A_51_P181865	NM_028053	Tmem38b	7.34	8.60	7.15	0.024
A_55_P1954555	BY718677	--	7.22	8.34	7.28	0.024
A_30_P01023367	--	--	3.90	5.40	3.77	0.025
A_51_P511236	NM_001077495	Pik3r1	8.14	9.46	8.89	0.025
A_52_P605517	NM_001005748	Phactr1	5.36	6.45	4.94	0.025
A_51_P278653	NM_023396	Rprm	6.42	7.89	6.35	0.025
A_55_P2099840	AK159631	--	3.17	4.62	4.22	0.025
A_52_P633489	NM_026161	C1qtnf4	6.09	7.19	6.00	0.025
A_65_P17602	NM_175013	Pgm5	8.25	9.87	6.90	0.025
A_52_P661587	NM_001025576	Ccdc141	7.11	8.22	6.84	0.025
A_30_P01017854	--	--	4.03	6.07	3.61	0.025
A_55_P1962334	NM_001042503	Trim71	6.80	8.63	7.02	0.026
A_55_P2029687	NM_010442	Hmox1	10.68	11.79	11.20	0.026
A_30_P01020043	--	--	4.27	5.56	3.88	0.026
A_30_P01024535	--	--	5.56	6.66	5.98	0.026
A_55_P2023732	NM_001001980	Limch1	8.53	10.77	7.88	0.026
A_30_P01025738	--	--	5.56	6.83	6.10	0.026
A_66_P139387	NM_011169	Prlr	4.41	5.82	4.08	0.026
A_51_P385351	NM_145394	Slc44a3	4.10	5.64	3.76	0.027
A_55_P1962429	AK151738	Maf	4.94	5.97	5.31	0.027
A_30_P01030146	--	--	4.24	5.62	4.64	0.027
A_51_P153053	NM_020561	Smpdl3a	8.62	9.66	9.55	0.027
A_55_P1987414	NM_173444	Nbeal1	4.19	5.35	4.55	0.027
A_55_P2014780	NM_001039122	Defb25	9.95	11.00	10.00	0.027
A_55_P1956918	NM_011782	Adamts5	4.75	6.88	5.55	0.027
A_30_P01018341	--	--	5.13	6.15	5.40	0.028
A_55_P2139261	AV575454	--	4.36	5.51	5.45	0.028
A_55_P2022211	NM_026162	Plxdc2	13.59	14.85	14.40	0.028

Table S2: Cluster 2						
Agilent ID	**GB Accession**	**Gene Symbol**	**siNS**	**siSix1**	**siSix4**	**pvalue**
A_51_P202801	NM_019875	Abcb9	9.59	10.80	9.70	0.028
A_30_P01023410	--	--	3.60	5.30	4.14	0.028
A_51_P451052	NM_175013	Pgm5	11.18	12.68	10.11	0.028
A_55_P2424042	NM_028004	Ttn	9.73	11.16	8.57	0.028
A_55_P2045642	NM_019675	Stmn4	7.92	10.02	7.09	0.029
A_55_P2213823	--	--	4.38	5.52	4.65	0.029
A_51_P438619	NM_175407	Sobp	7.77	9.16	8.14	0.029
A_66_P114784	NM_013737	Pla2g7	5.90	7.32	5.84	0.029
A_51_P363749	NM_016851	Irf6	6.02	7.21	5.08	0.029
A_55_P2172852	NM_025760	Ptplad2	5.15	6.23	5.80	0.030
A_66_P101251	AK014818	Chmp3	7.41	8.46	7.25	0.030
A_52_P62121	NM_010338	Gpr37	7.08	9.65	6.27	0.030
A_51_P326685	NM_176920	Lrtm1	6.16	7.42	6.91	0.030
A_55_P1999331	--	--	3.85	5.01	3.78	0.030
A_66_P101942	XR_168557	Gm9706	7.43	8.96	6.93	0.031
A_55_P2256158	AK043779	--	3.79	4.94	5.12	0.031
A_30_P01033111	--	--	4.82	7.57	5.90	0.031
A_51_P325281	NM_001204910	AI607873	3.74	6.18	4.02	0.031
A_55_P2121106	NM_001282088	Tomt	4.94	6.07	5.56	0.032
A_51_P183051	NM_133995	Upb1	5.19	6.32	6.42	0.032
A_52_P223809	NM_030150	Dhx58	4.54	5.74	4.56	0.032
A_55_P2149337	NM_145155	Wasf3	4.10	5.38	4.01	0.032
A_55_P2057050	XR_106099	--	6.86	8.06	7.30	0.032
A_55_P1954693	NM_009311	Tac1	2.89	4.99	5.08	0.032
A_55_P1960857	NM_001205219	Sorbs2	5.71	6.74	5.86	0.032
A_55_P1971647	NM_028705	Herc3	5.53	6.61	4.31	0.033
A_55_P1984886	NM_011827	Hcst	4.68	5.69	4.73	0.033
A_55_P2245904	AK020539	9530003O04Rik	6.27	7.40	6.59	0.033
A_51_P423578	NM_011408	Slfn2	4.80	5.91	4.61	0.033
A_55_P2151956	--	--	6.20	7.93	5.94	0.033
A_52_P167382	NM_021793	Tmem8	6.06	7.08	6.68	0.033
A_55_P1995647	NM_001162957	Rsph4a	3.42	5.06	4.13	0.033
A_51_P194249	NM_019675	Stmn4	7.75	10.13	6.52	0.033
A_51_P272283	NM_181588	Cmbl	6.18	7.20	6.82	0.033
A_51_P419117	NM_134050	Rab15	10.18	11.44	9.85	0.034
A_52_P220879	NM_009373	Tgm2	5.81	7.13	6.20	0.034
A_51_P295085	NM_008760	Ogn	10.18	12.52	10.78	0.034
A_55_P2188862	CX239135	C030034E14Rik	3.71	4.98	4.15	0.034
A_51_P463428	NM_178149	Pik3ip1	8.17	9.24	7.65	0.034

Table S2: Cluster 2						
Agilent ID	**GB Accession**	**Gene Symbol**	**siNS**	**siSix1**	**siSix4**	**pvalue**
A_30_P01025008	--	--	5.18	6.56	5.09	0.035
A_51_P461877	NM_011581	Thbs2	9.48	10.49	9.72	0.035
A_55_P1981276	AK131772	Gm2582	4.30	5.64	4.56	0.035
A_55_P2126615	AK035945	Nav3	3.78	5.25	3.63	0.035
A_30_P01019369	--	--	6.51	7.65	6.65	0.036
A_30_P01033617	--	--	3.50	5.18	5.06	0.036
A_55_P2044242	NM_001004148	Slc13a5	6.62	8.21	7.34	0.036
A_30_P01022297	--	--	7.15	8.18	7.24	0.036
A_55_P2065294	AK148881	Scn3a	4.70	6.52	4.98	0.036
A_55_P2137611	NM_019440	Irgm2	7.72	9.10	8.29	0.037
A_55_P2318934	AK004627	1200007C13Rik	4.11	5.17	5.18	0.037
A_55_P2204804	NM_001111053	Dclk1	12.51	13.87	11.83	0.037
A_55_P2114697	NM_008103	Gcm1	13.15	14.41	13.80	0.037
A_55_P1969414	NM_027089	Eqtn	3.47	5.12	4.10	0.037
A_51_P270426	NM_020596	Egr4	5.10	6.14	4.50	0.038
A_51_P276452	NM_178646	Tigd5	4.05	5.37	4.30	0.039
A_55_P2210213	AK028644	4732423E21Rik	10.12	11.37	10.75	0.039
A_55_P2412319	NR_045403	A830052D11Rik	7.56	8.85	7.87	0.039
A_51_P427828	AK009836	Mlip	3.17	5.36	3.61	0.040
A_51_P410681	NM_018826	Irx5	5.71	7.01	5.41	0.040
A_30_P01022936	--	--	5.74	7.15	6.45	0.041
A_51_P454008	NM_008489	Lbp	4.16	5.34	4.21	0.041
A_51_P430900	NM_013642	Dusp1	10.72	11.81	11.05	0.041
A_55_P2178678	NM_033321	P2rx5	10.42	11.52	10.28	0.043
A_55_P2368710	AK082316	C230037E05Rik	6.51	7.75	6.44	0.043
A_55_P2017982	NM_001170669	Pde8b	3.84	5.63	4.83	0.043
A_30_P01024091	--	--	5.80	7.07	6.10	0.044
A_30_P01027994	--	--	5.01	6.12	5.69	0.045
A_65_P04847	NM_028572	Vgll3	7.09	8.24	7.81	0.045
A_55_P2037702	NR_027829	Gm10638	8.55	10.00	8.83	0.045
A_51_P212782	NM_008361	Il1b	7.26	8.49	6.16	0.045
A_55_P1991253	AK132276	Zfp407	3.67	5.03	4.62	0.045
A_51_P344249	NM_009685	Apbb1	8.54	9.67	8.16	0.046
A_51_P514712	NM_001039530	Parp14	6.31	7.97	6.04	0.046
A_51_P171107	NM_026239	Tmem35	10.84	11.91	10.83	0.046
A_55_P2025655	CB248850	--	5.88	6.90	6.59	0.046
A_30_P01018142	--	--	8.56	9.91	8.30	0.046
A_55_P2029682	NM_172887	Fry	7.66	8.67	7.47	0.047
A_55_P2133776	NM_178247	Dppa1	3.61	5.05	4.16	0.047

Table S2: Cluster 2						
Agilent ID	**GB Accession**	**Gene Symbol**	**siNS**	**siSix1**	**siSix4**	**pvalue**
A_55_P2081318	AK039035	Gnas	8.36	9.82	7.60	0.047
A_55_P2028847	--	--	13.39	14.64	14.08	0.048
A_30_P01030185	--	--	4.64	5.66	4.78	0.048
A_55_P2069022	NM_178791	Vstm4	4.22	5.47	4.29	0.048
A_55_P2144391	--	--	11.58	12.60	11.62	0.049
A_30_P01032535	--	--	5.74	7.00	5.70	0.049
A_30_P01026892	--	--	5.12	6.16	5.39	0.050

Table S3: GSEA Results from the Control vs. Six1 siRNA.

The entire gene expression data set was analyzed by GSEA using the Molecular Signature Database version 4.0, comparing expression values from the siControl treatment with the siSix1. The number of genes within a gene set as well as the Normalized Enrichment Score (NES) is indicated. The corresponding p-values (Nominal p-value), the False Discovery Rate (FDR) and Familywise Error Rate (FWER) are also provided. Only gene sets with an FDR < 0.05 are shown. A positive enrichment score indicates genes are expressed at higher levels in the control vs. the Six1 knock-down; a negative enrichment score indicates genes are expressed at higher levels in the Six1 knock-down vs. the control.

Table S3: GSEA					
Gene Set	**SIZE**	**NES**	**Nominal p-value**	**FDR**	**FWER**
CELL_CYCLE_PROCESS	183	2.2279716	0.000	0.001	0.001
RNA_SPLICING	89	2.1138647	0.000	0.003	0.007
M_PHASE	107	2.083702	0.000	0.003	0.009
DNA_DEPENDENT_DNA_REPLICATION	53	2.082301	0.000	0.002	0.009
M_PHASE_OF_MITOTIC_CELL_CYCLE	82	2.0174916	0.000	0.005	0.023
CELL_CYCLE_PHASE	160	2.0161216	0.000	0.004	0.023
MITOSIS	79	1.940973	0.000	0.010	0.069
MRNA_PROCESSING_GO_0006397	71	1.9353639	0.000	0.010	0.075
MITOTIC_CELL_CYCLE	147	1.9272268	0.000	0.010	0.085
DNA_REPAIR	121	1.9057558	0.000	0.011	0.112
DNA_RECOMBINATION	40	1.9048032	0.000	0.010	0.113
COFACTOR_BIOSYNTHETIC_PROCESS	20	1.8995593	0.000	0.010	0.124
CELL_DIVISION	20	1.8797736	0.002	0.012	0.152
RNA_PROCESSING	165	1.8717711	0.000	0.012	0.164
CYTOKINESIS	18	1.8708483	0.002	0.012	0.165
DNA_REPLICATION	97	1.8585466	0.000	0.013	0.191
CELL_CYCLE_GO_0007049	291	1.8561487	0.000	0.012	0.193
NEGATIVE_REGULATION_OF_DNA_METABOLIC_PROCESS	18	1.8318833	0.002	0.016	0.256
MITOTIC_SISTER_CHROMATID_SEGREGATION	15	1.8086917	0.000	0.020	0.320
MICROTUBULE_CYTOSKELETON_ORGANIZATION_AND_BIOGENESIS	34	1.8071084	0.000	0.019	0.325
MRNA_METABOLIC_PROCESS	81	1.7957827	0.000	0.021	0.363
SISTER_CHROMATID_SEGREGATION	16	1.7923009	0.000	0.021	0.374
RNA_SPLICINGVIA_TRANSESTERIFICATION_REACTIONS	34	1.7749228	0.006	0.025	0.450
DOUBLE_STRAND_BREAK_REPAIR	23	1.7663597	0.002	0.027	0.484
INTERPHASE	64	1.7614937	0.002	0.027	0.498
HETEROCYCLE_METABOLIC_PROCESS	21	1.7500498	0.014	0.029	0.539
REGULATION_OF_DNA_REPLICATION	20	1.7263771	0.011	0.036	0.633

Table S3: GSEA

Gene Set	SIZE	NES	Nominal p-value	FDR	FWER
MICROTUBULE_ORGANIZING_CENTER_ORGANIZATION_AND_BIOGENESIS	16	1.719018	0.008	0.038	0.664
RESPONSE_TO_DNA_DAMAGE_STIMULUS	155	1.7165325	0.000	0.038	0.672
INTERPHASE_OF_MITOTIC_CELL_CYCLE	58	1.7081631	0.000	0.039	0.694
DNA_METABOLIC_PROCESS	241	1.7034076	0.000	0.040	0.712
SPLICEOSOME_ASSEMBLY	21	1.701444	0.007	0.039	0.718
MICROTUBULE_BASED_PROCESS	75	1.7012092	0.000	0.038	0.719
SULFUR_METABOLIC_PROCESS	30	1.6895124	0.010	0.041	0.761
RESPONSE_TO_ENDOGENOUS_STIMULUS	185	1.6815947	0.000	0.044	0.796
REGULATION_OF_MITOSIS	40	1.6753728	0.010	0.045	0.811
CENTROSOME_ORGANIZATION_AND_BIOGENESIS	15	1.6750803	0.012	0.044	0.811

Table S4: Cluster #1 Gene Ontology

Gene ontology was performed on Cluster #1. The results are shown in the following table. FDR B&H corresponds to the Benjamini-Hochberg false discovery rate. Gene hits corresponds to the number of genes from Cluster #1 found in the GO category.

Table S4: Cluster 1 GO

GO ID	GO Term	FDR B&H	Gene Hits	Genes in List
GO:0008283	cell proliferation	3.04E-04	76	1887
GO:0048584	positive regulation of response to stimulus	3.04E-04	67	1584
GO:0042127	regulation of cell proliferation	3.41E-04	62	1439
GO:0006952	defense response	6.93E-04	63	1515
GO:2000026	regulation of multicellular organismal development	1.66E-03	60	1469
GO:0045444	fat cell differentiation	1.66E-03	16	182
GO:0009967	positive regulation of signal transduction	1.66E-03	49	1118
GO:0023056	positive regulation of signaling	1.66E-03	51	1188
GO:0043067	regulation of programmed cell death	1.66E-03	57	1392
GO:0006954	inflammatory response	1.66E-03	32	599
GO:0010647	positive regulation of cell communication	1.68E-03	51	1196
GO:0048646	anatomical structure formation involved in morphogenesis	1.88E-03	45	1009
GO:0042981	regulation of apoptotic process	1.88E-03	56	1376
GO:0009891	positive regulation of biosynthetic process	2.72E-03	61	1578
GO:0031328	positive regulation of cellular biosynthetic process	2.72E-03	60	1547
GO:0008284	positive regulation of cell proliferation	2.72E-03	38	816
GO:0051094	positive regulation of developmental process	2.72E-03	41	911
GO:1902531	regulation of intracellular signal transduction	2.72E-03	59	1518
GO:1903034	regulation of response to wounding	2.72E-03	23	379
GO:0051240	positive regulation of multicellular organismal process	2.72E-03	33	665
GO:0010959	regulation of metal ion transport	3.04E-03	19	279
GO:0009628	response to abiotic stimulus	3.33E-03	44	1025
GO:0010941	regulation of cell death	3.33E-03	57	1466
GO:0001816	cytokine production	3.61E-03	30	590
GO:0012501	programmed cell death	3.73E-03	67	1832
GO:0080134	regulation of response to stress	3.73E-03	43	1005
GO:0007610	behavior	3.73E-03	33	687
GO:0050793	regulation of developmental process	3.73E-03	69	1912
GO:0006915	apoptotic process	3.73E-03	66	1806
GO:0051924	regulation of calcium ion transport	3.73E-03	15	193
GO:0022610	biological adhesion	3.76E-03	45	1077
GO:0046903	secretion	3.76E-03	43	1014

Table S4: Cluster 1 GO				
GO ID	GO Term	FDR B&H	Gene Hits	Genes in List
GO:0050727	regulation of inflammatory response	3.76E-03	18	268
GO:0070838	divalent metal ion transport	3.76E-03	22	373
GO:0009719	response to endogenous stimulus	3.76E-03	55	1424
GO:0010557	positive regulation of macromolecule biosynthetic process	4.60E-03	55	1436
GO:2000021	regulation of ion homeostasis	4.61E-03	14	177
GO:0044057	regulation of system process	4.61E-03	24	438
GO:0014805	smooth muscle adaptation	4.61E-03	3	4
GO:0006816	calcium ion transport	4.61E-03	21	355
GO:0010243	response to organonitrogen compound	4.61E-03	35	771
GO:1902533	positive regulation of intracellular signal transduction	4.61E-03	34	740
GO:0007155	cell adhesion	4.63E-03	44	1067
GO:0014065	phosphatidylinositol 3-kinase signaling	5.02E-03	10	96
GO:0072511	divalent inorganic cation transport	5.20E-03	22	388
GO:0042325	regulation of phosphorylation	5.41E-03	49	1248
GO:0032101	regulation of response to external stimulus	5.84E-03	30	628
GO:0009611	response to wounding	5.96E-03	49	1255
GO:0034109	homotypic cell-cell adhesion	6.25E-03	8	63
GO:0009306	protein secretion	6.36E-03	16	236
GO:0048015	phosphatidylinositol-mediated signaling	6.72E-03	15	213
GO:0043270	positive regulation of ion transport	6.72E-03	14	189
GO:0048017	inositol lipid-mediated signaling	6.92E-03	15	214
GO:0007204	positive regulation of cytosolic calcium ion concentration	7.38E-03	16	241
GO:0060401	cytosolic calcium ion transport	7.38E-03	11	124
GO:0006928	movement of cell or subcellular component	7.38E-03	61	1703
GO:0014074	response to purine-containing compound	7.38E-03	12	146
GO:1901698	response to nitrogen compound	7.47E-03	36	836
GO:0001817	regulation of cytokine production	7.58E-03	26	523
GO:1901700	response to oxygen-containing compound	7.58E-03	50	1314
GO:0048511	rhythmic process	7.78E-03	17	270
GO:0035456	response to interferon-beta	8.74E-03	5	23
GO:0046683	response to organophosphorus	8.74E-03	11	128
GO:0051241	negative regulation of multicellular organismal process	9.40E-03	22	414
GO:0009409	response to cold	9.57E-03	6	37
GO:0071310	cellular response to organic substance	9.57E-03	64	1840
GO:0001558	regulation of cell growth	9.57E-03	20	359
GO:0045595	regulation of cell differentiation	9.57E-03	52	1405

Table S4: Cluster 1 GO				
GO ID	GO Term	FDR B&H	Gene Hits	Genes in List
GO:0051928	positive regulation of calcium ion transport	9.57E-03	9	89
GO:0008585	female gonad development	9.83E-03	10	110
GO:0032940	secretion by cell	9.83E-03	37	891
GO:0022414	reproductive process	9.83E-03	48	1269
GO:0016049	cell growth	9.83E-03	23	449
GO:0030036	actin cytoskeleton organization	9.83E-03	25	509
GO:0051173	positive regulation of nitrogen compound metabolic process	9.83E-03	54	1484
GO:0007167	enzyme linked receptor protein signaling pathway	9.83E-03	41	1028
GO:0030030	cell projection organization	9.83E-03	46	1201
GO:1901701	cellular response to oxygen-containing compound	1.02E-02	35	829
GO:0071495	cellular response to endogenous stimulus	1.12E-02	40	1002
GO:0032846	positive regulation of homeostatic process	1.16E-02	9	93
GO:0051480	cytosolic calcium ion homeostasis	1.26E-02	16	261
GO:0098542	defense response to other organism	1.26E-02	21	401
GO:0050673	epithelial cell proliferation	1.26E-02	18	316
GO:0040007	growth	1.30E-02	38	944
GO:0050795	regulation of behavior	1.31E-02	13	186
GO:0051050	positive regulation of transport	1.34E-02	31	714
GO:0048585	negative regulation of response to stimulus	1.35E-02	43	1120
GO:0010628	positive regulation of gene expression	1.35E-02	49	1332
GO:0050714	positive regulation of protein secretion	1.39E-02	10	118
GO:0045087	innate immune response	1.39E-02	36	883
GO:0044060	regulation of endocrine process	1.40E-02	6	42
GO:0030029	actin filament-based process	1.40E-02	27	592
GO:0009887	organ morphogenesis	1.40E-02	37	920
GO:0008406	gonad development	1.40E-02	15	241
GO:0008015	blood circulation	1.40E-02	22	439
GO:0048514	blood vessel morphogenesis	1.40E-02	24	500
GO:0040011	locomotion	1.40E-02	54	1522
GO:0043065	positive regulation of apoptotic process	1.40E-02	22	440
GO:0009612	response to mechanical stimulus	1.40E-02	13	191
GO:0001525	angiogenesis	1.40E-02	21	411
GO:0002675	positive regulation of acute inflammatory response	1.40E-02	5	28
GO:0001944	vasculature development	1.40E-02	27	595
GO:0003013	circulatory system process	1.40E-02	22	441
GO:0040008	regulation of growth	1.40E-02	28	627

Table S4: Cluster 1 GO				
GO ID	GO Term	FDR B&H	Gene Hits	Genes in List
GO:0007548	sex differentiation	1.40E-02	17	297
GO:0032844	regulation of homeostatic process	1.42E-02	19	354
GO:0034097	response to cytokine	1.44E-02	28	629
GO:0070098	chemokine-mediated signaling pathway	1.56E-02	6	44
GO:0048660	regulation of smooth muscle cell proliferation	1.56E-02	9	101
GO:0035587	purinergic receptor signaling pathway	1.56E-02	5	29
GO:0060402	calcium ion transport into cytosol	1.56E-02	10	123
GO:0043068	positive regulation of programmed cell death	1.56E-02	22	447
GO:0048729	tissue morphogenesis	1.61E-02	26	572
GO:0060986	endocrine hormone secretion	1.68E-02	6	45
GO:0090030	regulation of steroid hormone biosynthetic process	1.68E-02	4	17
GO:0045597	positive regulation of cell differentiation	1.68E-02	29	671
GO:0031399	regulation of protein modification process	1.68E-02	47	1290
GO:0009892	negative regulation of metabolic process	1.68E-02	63	1880
GO:0010942	positive regulation of cell death	1.68E-02	23	482
GO:0048661	positive regulation of smooth muscle cell proliferation	1.68E-02	7	63
GO:0045893	positive regulation of transcription, DNA-templated	1.71E-02	45	1221
GO:0051128	regulation of cellular component organization	1.71E-02	59	1733
GO:0048659	smooth muscle cell proliferation	1.74E-02	9	104
GO:0055074	calcium ion homeostasis	1.75E-02	19	365
GO:0023057	negative regulation of signaling	1.75E-02	38	979
GO:0031032	actomyosin structure organization	1.75E-02	7	64
GO:0046660	female sex differentiation	1.75E-02	10	127
GO:0046545	development of primary female sexual characteristics	1.75E-02	10	127
GO:0007517	muscle organ development	1.80E-02	19	368
GO:0007185	transmembrane receptor protein tyrosine phosphatase signaling pathway	1.80E-02	3	8
GO:0014049	positive regulation of glutamate secretion	1.80E-02	3	8
GO:0010524	positive regulation of calcium ion transport into cytosol	1.80E-02	6	47
GO:0032611	interleukin-1 beta production	1.80E-02	6	47
GO:0045935	positive regulation of nucleobase-containing compound metabolic process	1.80E-02	51	1448
GO:0050679	positive regulation of epithelial cell proliferation	1.80E-02	11	152
GO:0010906	regulation of glucose metabolic process	1.80E-02	9	106
GO:0014048	regulation of glutamate secretion	1.80E-02	4	18

Table S4: Cluster 1 GO				
GO ID	GO Term	FDR B&H	Gene Hits	Genes in List
GO:0048608	reproductive structure development	1.80E-02	22	459
GO:0010522	regulation of calcium ion transport into cytosol	1.80E-02	8	85
GO:0006955	immune response	1.88E-02	50	1416
GO:0045687	positive regulation of glial cell differentiation	1.92E-02	5	32
GO:0000165	MAPK cascade	1.92E-02	28	653
GO:0019221	cytokine-mediated signaling pathway	1.92E-02	20	402
GO:0045944	positive regulation of transcription from RNA polymerase II promoter	1.92E-02	36	922
GO:0001501	skeletal system development	1.92E-02	22	463
GO:0061458	reproductive system development	1.92E-02	22	463
GO:0009888	tissue development	1.98E-02	60	1794
GO:0071345	cellular response to cytokine stimulus	1.99E-02	24	527
GO:0035590	purinergic nucleotide receptor signaling pathway	2.06E-02	4	19
GO:0031324	negative regulation of cellular metabolic process	2.06E-02	58	1723
GO:0031347	regulation of defense response	2.11E-02	25	562
GO:0014070	response to organic cyclic compound	2.11E-02	31	759
GO:0009266	response to temperature stimulus	2.11E-02	10	133
GO:0009968	negative regulation of signal transduction	2.11E-02	36	930
GO:0023014	signal transduction by protein phosphorylation	2.11E-02	29	693
GO:0002252	immune effector process	2.13E-02	27	628
GO:0050729	positive regulation of inflammatory response	2.16E-02	8	89
GO:0014896	muscle hypertrophy	2.16E-02	6	50
GO:0032386	regulation of intracellular transport	2.17E-02	20	409
GO:0003006	developmental process involved in reproduction	2.19E-02	28	663
GO:1902532	negative regulation of intracellular signal transduction	2.19E-02	18	350
GO:0001568	blood vessel development	2.19E-02	25	566
GO:0048771	tissue remodeling	2.19E-02	11	159
GO:0048755	branching morphogenesis of a nerve	2.20E-02	3	9
GO:0032892	positive regulation of organic acid transport	2.24E-02	5	34
GO:0060341	regulation of cellular localization	2.25E-02	37	972
GO:0006874	cellular calcium ion homeostasis	2.25E-02	18	352
GO:0008285	negative regulation of cell proliferation	2.28E-02	27	634
GO:0043901	negative regulation of multi-organism process	2.30E-02	9	113
GO:0036293	response to decreased oxygen levels	2.30E-02	15	267
GO:0019216	regulation of lipid metabolic process	2.30E-02	15	267

Table S4: Cluster 1 GO				
GO ID	GO Term	FDR B&H	Gene Hits	Genes in List
GO:0006357	regulation of transcription from RNA polymerase II promoter	2.33E-02	55	1629
GO:0051047	positive regulation of secretion	2.35E-02	17	325
GO:1902680	positive regulation of RNA biosynthetic process	2.36E-02	45	1262
GO:0030198	extracellular matrix organization	2.38E-02	19	385
GO:0071622	regulation of granulocyte chemotaxis	2.40E-02	5	35
GO:0043062	extracellular structure organization	2.42E-02	19	386
GO:0016337	single organismal cell-cell adhesion	2.44E-02	17	327
GO:0072507	divalent inorganic cation homeostasis	2.46E-02	19	387
GO:0010648	negative regulation of cell communication	2.46E-02	37	981
GO:0008306	associative learning	2.51E-02	7	72
GO:1901863	positive regulation of muscle tissue development	2.52E-02	4	21
GO:0001932	regulation of protein phosphorylation	2.54E-02	38	1019
GO:0032612	interleukin-1 production	2.54E-02	6	53
GO:0045137	development of primary sexual characteristics	2.56E-02	15	272
GO:0070527	platelet aggregation	2.59E-02	5	36
GO:0032504	multicellular organism reproduction	2.61E-02	32	813
GO:0030334	regulation of cell migration	2.61E-02	24	547
GO:0042107	cytokine metabolic process	2.80E-02	9	118
GO:0048732	gland development	2.80E-02	20	424
GO:0002688	regulation of leukocyte chemotaxis	2.80E-02	7	74
GO:0042832	defense response to protozoan	2.87E-02	4	22
GO:0022602	ovulation cycle process	2.90E-02	8	96
GO:0014066	regulation of phosphatidylinositol 3-kinase signaling	2.98E-02	7	75
GO:0051254	positive regulation of RNA metabolic process	2.98E-02	45	1284
GO:0050769	positive regulation of neurogenesis	3.00E-02	11	169
GO:0032268	regulation of cellular protein metabolic process	3.02E-02	54	1620
GO:1901861	regulation of muscle tissue development	3.02E-02	9	120
GO:0030001	metal ion transport	3.02E-02	31	789
GO:0071357	cellular response to type I interferon	3.08E-02	7	76
GO:0060337	type I interferon signaling pathway	3.08E-02	7	76
GO:0007423	sensory organ development	3.08E-02	23	525
GO:0048878	chemical homeostasis	3.08E-02	35	931
GO:0070162	adiponectin secretion	3.08E-02	2	3
GO:0042091	interleukin-10 biosynthetic process	3.08E-02	2	3
GO:0070163	regulation of adiponectin secretion	3.08E-02	2	3

Table S4: Cluster 1 GO				
GO ID	GO Term	FDR B&H	Gene Hits	Genes in List
GO:0045074	regulation of interleukin-10 biosynthetic process	3.08E-02	2	3
GO:0072503	cellular divalent inorganic cation homeostasis	3.08E-02	18	369
GO:0009615	response to virus	3.11E-02	16	310
GO:0070482	response to oxygen levels	3.11E-02	15	281
GO:0043207	response to external biotic stimulus	3.11E-02	29	726
GO:0051707	response to other organism	3.11E-02	29	726
GO:0050715	positive regulation of cytokine secretion	3.11E-02	7	77
GO:0034340	response to type I interferon	3.11E-02	7	77
GO:0051049	regulation of transport	3.11E-02	51	1517
GO:0022407	regulation of cell-cell adhesion	3.11E-02	8	99
GO:0048505	regulation of timing of cell differentiation	3.11E-02	3	11
GO:1900744	regulation of p38MAPK cascade	3.11E-02	3	11
GO:0007171	activation of transmembrane receptor protein tyrosine kinase activity	3.11E-02	3	11
GO:0048711	positive regulation of astrocyte differentiation	3.11E-02	3	11
GO:0043551	regulation of phosphatidylinositol 3-kinase activity	3.16E-02	5	39
GO:0048525	negative regulation of viral process	3.28E-02	7	78
GO:0060537	muscle tissue development	3.33E-02	18	374
GO:0022603	regulation of anatomical structure morphogenesis	3.34E-02	30	766
GO:0098602	single organism cell adhesion	3.34E-02	18	375
GO:0001503	ossification	3.34E-02	18	375
GO:0033002	muscle cell proliferation	3.34E-02	10	149
GO:0031960	response to corticosteroid	3.34E-02	10	149
GO:0090022	regulation of neutrophil chemotaxis	3.34E-02	4	24
GO:0034110	regulation of homotypic cell-cell adhesion	3.34E-02	4	24
GO:0045926	negative regulation of growth	3.34E-02	13	229
GO:0042698	ovulation cycle	3.34E-02	8	101
GO:0030522	intracellular receptor signaling pathway	3.34E-02	15	286
GO:0001659	temperature homeostasis	3.35E-02	5	40
GO:0031348	negative regulation of defense response	3.39E-02	9	125
GO:0042035	regulation of cytokine biosynthetic process	3.50E-02	8	102
GO:0071417	cellular response to organonitrogen compound	3.51E-02	21	472
GO:0010605	negative regulation of macromolecule metabolic process	3.51E-02	56	1721
GO:0051781	positive regulation of cell division	3.52E-02	7	80
GO:0032870	cellular response to hormone stimulus	3.52E-02	23	537
GO:0055082	cellular chemical homeostasis	3.58E-02	25	604

Table S4: Cluster 1 GO				
GO ID	GO Term	FDR B&H	Gene Hits	Genes in List
GO:0003341	cilium movement	3.58E-02	5	41
GO:0045071	negative regulation of viral genome replication	3.58E-02	5	41
GO:0043549	regulation of kinase activity	3.58E-02	30	775
GO:0002028	regulation of sodium ion transport	3.58E-02	6	60
GO:0001553	luteinization	3.58E-02	3	12
GO:0043116	negative regulation of vascular permeability	3.58E-02	3	12
GO:0040034	regulation of development, heterochronic	3.58E-02	3	12
GO:0038066	p38MAPK cascade	3.58E-02	3	12
GO:0040012	regulation of locomotion	3.58E-02	26	639
GO:1902622	regulation of neutrophil migration	3.58E-02	4	25
GO:0001562	response to protozoan	3.58E-02	4	25
GO:0046885	regulation of hormone biosynthetic process	3.58E-02	4	25
GO:0043269	regulation of ion transport	3.66E-02	24	574
GO:0051674	localization of cell	3.70E-02	41	1170
GO:0048870	cell motility	3.70E-02	41	1170
GO:0051338	regulation of transferase activity	3.70E-02	33	883
GO:0001666	response to hypoxia	3.70E-02	14	263
GO:0002690	positive regulation of leukocyte chemotaxis	3.74E-02	6	61
GO:0050810	regulation of steroid biosynthetic process	3.74E-02	6	61
GO:0045600	positive regulation of fat cell differentiation	3.74E-02	5	42
GO:0010675	regulation of cellular carbohydrate metabolic process	3.74E-02	10	154
GO:0001819	positive regulation of cytokine production	3.74E-02	15	293
GO:1901699	cellular response to nitrogen compound	3.74E-02	22	511
GO:0043408	regulation of MAPK cascade	3.74E-02	24	577
GO:0048598	embryonic morphogenesis	3.74E-02	24	577
GO:0002682	regulation of immune system process	3.88E-02	42	1212
GO:2000145	regulation of cell motility	3.89E-02	24	579
GO:0048468	cell development	3.89E-02	62	1970
GO:0033198	response to ATP	3.89E-02	4	26
GO:0002824	positive regulation of adaptive immune response based on somatic recombination of immune receptors built from immunoglobulin superfamily domains	3.91E-02	6	62
GO:0050920	regulation of chemotaxis	4.04E-02	9	131
GO:0071456	cellular response to hypoxia	4.10E-02	8	107
GO:0022008	neurogenesis	4.13E-02	48	1441
GO:0090330	regulation of platelet aggregation	4.16E-02	3	13
GO:0032308	positive regulation of prostaglandin secretion	4.16E-02	3	13

Table S4: Cluster 1 GO				
GO ID	GO Term	FDR B&H	Gene Hits	Genes in List
GO:0016477	cell migration	4.17E-02	38	1073
GO:0051607	defense response to virus	4.24E-02	12	212
GO:0032731	positive regulation of interleukin-1 beta production	4.35E-02	4	27
GO:0048609	multicellular organismal reproductive process	4.41E-02	30	792
GO:0036294	cellular response to decreased oxygen levels	4.45E-02	8	109
GO:2000637	positive regulation of gene silencing by miRNA	4.45E-02	2	4
GO:0060148	positive regulation of posttranscriptional gene silencing	4.45E-02	2	4
GO:0030003	cellular cation homeostasis	4.47E-02	21	489
GO:0044092	negative regulation of molecular function	4.54E-02	35	972
GO:0051222	positive regulation of protein transport	4.54E-02	13	243
GO:0009607	response to biotic stimulus	4.54E-02	29	760
GO:0006875	cellular metal ion homeostasis	4.56E-02	20	458
GO:1903036	positive regulation of response to wounding	4.59E-02	8	110
GO:0043550	regulation of lipid kinase activity	4.59E-02	5	45
GO:0006109	regulation of carbohydrate metabolic process	4.65E-02	10	161
GO:0019218	regulation of steroid metabolic process	4.66E-02	7	87
GO:0061061	muscle structure development	4.66E-02	23	558
GO:0010562	positive regulation of phosphorus metabolic process	4.67E-02	33	904
GO:0045937	positive regulation of phosphate metabolic process	4.67E-02	33	904
GO:0042036	negative regulation of cytokine biosynthetic process	4.68E-02	4	28
GO:0044262	cellular carbohydrate metabolic process	4.68E-02	15	304
GO:0072358	cardiovascular system development	4.68E-02	33	905
GO:0072359	circulatory system development	4.68E-02	33	905
GO:0009890	negative regulation of biosynthetic process	4.68E-02	42	1233
GO:0048839	inner ear development	4.68E-02	11	189
GO:0055065	metal ion homeostasis	4.68E-02	22	527
GO:0042711	maternal behavior	4.68E-02	3	14
GO:0032306	regulation of prostaglandin secretion	4.68E-02	3	14
GO:0046541	saliva secretion	4.68E-02	3	14
GO:0032310	prostaglandin secretion	4.68E-02	3	14
GO:0044744	protein targeting to nucleus	4.68E-02	13	246
GO:1902593	single-organism nuclear import	4.68E-02	13	246
GO:0006606	protein import into nucleus	4.68E-02	13	246
GO:0050886	endocrine process	4.69E-02	7	88
GO:0014015	positive regulation of gliogenesis	4.72E-02	5	46

Table S4: Cluster 1 GO				
GO ID	GO Term	FDR B&H	Gene Hits	Genes in List
GO:0007015	actin filament organization	4.74E-02	14	276
GO:0051384	response to glucocorticoid	4.98E-02	9	138

Table S5: Oligonucleotide sequences used for RT-PCR, siRNA, and cloning.

Table S5: Oligonucleotides		
Name	**Sequence**	**Application**
Six1_RT_Forward	TTTTACGCAAGAGCAAGTGG	RT-PCR
Six1_RT_Reverse	CTCTCGTTCTTGTGCAGGTG	RT-PCR
Six4_RT_Forward	CGAGACCCAGTCCAAAAGC	RT-PCR
Six4_RT_Reverse	GCTAGAGAGGCTGAGGTTGG	RT-PCR
Ccnd1_RT_Forward	CGGATGAGAACAAGCAGACC	RT-PCR
Ccnd1_RT_Reverse	GCAGGAGAGGAAGTTGTTGG	RT-PCR
Rps26_RT_Forward	GCCATCCATAGCAAGGTTGT	RT-PCR
Rps26_RT_Reverse	GCCTCTTTACATGGGCTTTG	RT-PCR
Rplp0_RT_Forward	CTGCACTCTCGCTTTCTGG	RT-PCR
Rplp0_RT_Reverse	ACTCAGTCTCCACAGACAATGC	RT-PCR
Tbp_RT_Forward	TCATGGACCAGAACAACAGC	RT-PCR
Tbp_RT_Reverse	GCTGTGGAGTAAGTCCTGTGC	RT-PCR
Ccnb1_RT_Forward	CATGCTGGACTACGACATGG	RT-PCR
Ccnb1_RT_Reverse	GGTGCTGCATAACAGGAAGC	RT-PCR
Foxm1_RT_Forward	ACCAATATCCAGTGGCTTGG	RT-PCR
Foxm1_RT_Reverse	AGGGCTCCTCAACCTTAACC	RT-PCR
Ccna2_RT_Forward	TTCACTCATTGCTGGAGCTG	RT-PCR
Ccna2_RT_Reverse	TCCAGTCTGTTGTGCCAATG	RT-PCR
Cdk1_RT_Forward	ACGTCAAGAACCTGGACGAG	RT-PCR
Cdk1_RT_Reverse	CAAAGTACGGGTGCTTCAGG	RT-PCR
Mybl2_RT_Forward	GAATGCCCTGGAGAAGTACG	RT-PCR
Mybl2_RT_Reverse	GCCTCATGTCATCCTCAATG	RT-PCR
Plk1_RT_Forward	GCAGGAAACCTCTCAAAGTCC	RT-PCR
Plk1_RT_Reverse	CACTCAATGGCCTCATTTGTC	RT-PCR

Table S5: Oligonucleotides		
Name	**Sequence**	**Application**
Akt3_RT_Forward	AAATTCCCCCGAACACTCTC	RT-PCR
Akt3_RT_Reverse	ATGCCTCATGATTTCTTTTGC	RT-PCR
Ski_RT_Forward	GGACGACGTGAAGGAGAAG	RT-PCR
Ski_RT_Reverse	GACACTGCAGGGGACCAG	RT-PCR
Snai2_RT_Forward	CATTGCCTTGTGTCTGCAAG	RT-PCR
Snai2_RT_Reverse	CAGTGAGGGCAAGAGAAAGG	RT-PCR
Igf2bp2_RT_Forward	GCCAGACGAGAATGAGGAAG	RT-PCR
Igf2bp2_RT_Reverse	GGGTATCTCTGCTCCTGCTG	RT-PCR
Myc_RT_Forward	TAGTGCTGCATGAGGAGACAC	RT-PCR
Myc_RT_Reverse	GGTTTGCCTCTTCTCCACAG	RT-PCR
Hoxd10_ChIP_Forward	GAGAAATCGGACTCACCTTCC	ChIP-PCR
Hoxd10_ChIP_Reverse	CACATACCCAGGCAGAACG	ChIP-PCR
Ccnd1_ChIP_Forward	ACCACTAGAGGTCGCACTGAC	ChIP-PCR
Ccnd1_ChIP_Reverse	GCCTACAGCCCTGTTACCTG	ChIP-PCR
Myc_ChIP_Forward	GTCAGAAGAGCCTGCAGATG	ChIP-PCR
Myc_ChIP_Reverse	CAGGAAGACGGCTACTTCTCC	ChIP-PCR
Six1-A	GCGAGGAGACCAGCUACUGCUUUAA	siRNA
Six1-B	ACUCCUCCUCCAACAAGCAGAAUCA	siRNA
Six1-C	GCAACUUCCGCGAGCUCUACAAGAU	siRNA
Six4-A	GCAAGUACUUCACCUGUCUUCCUUA	siRNA
Six4-B	UAAGGAAGACAGGUGAAGUACUUGC	siRNA
Six4-C	GGGACACAAUGGAGUUAUCCUUAAU	siRNA
Six4-D	AUUAAGGAUAACUCCAUUGUGUCCC	siRNA
Ccnd1_Bam_F	GATGACGGATCCGCCAACATGGAACACCAGCTCCTGTGC	Cloning
Ccnd1HaTga+E+X_R	GATGACTCTAGAGAATTCTCAAGCGTAATCTGGAACATCGTATGGGTAGATGTCCACATCTCGCACGTC	Cloning
Six1optBamKoz_F	GACGACGAGCTCGGATCCGTTTAGTGAACCGTCAGAAGCCACCATGAG	Cloning
Six1optXbaSalHa_R	ATGACTCTAGAGTCGACTCAAGCGTAATCTGGAACATCGTATGGGTAGGAACCCAAATC	Cloning

Table S6: List of antibodies used and dilutions

Antibody	Dilution	Source or Product Number	Manufacturer
Six1	1:500	Purified from immunized rabbits	Open Biosystems
Six4	1:1000	Purified from immunized rabbits	Open Biosystems
Btubulin	1:1000	Hybridoma Cells Clone 9E7	DSHB
MHC	1:1	Hybridoma Cells Clone MF20	DHSB
Ccnd1	1:500	DCS-6	Santa Cruz
Myod	1:1000	5.8A	Santa Cruz
Ki67	1:100	SP6	Abcam
Pax7	1:100	Pax7	DSHB